Technical University of Munich
TUM School of Medicine and Health

Vascular characterization of proliferative lesions in murine liver

Margaret Tulessin

Complete reprint of the dissertation approved by the TUM School of Medicine and Health of the Technical University of Munich for the award of the Doktorin der Medizin (Dr. med.).

Chair: Prof. Dr. Lars Mägdefessel

Examiners:

1. Prof. Dr. Carolin Mogler
2. Priv.-Doz. Dr. Ursula Ehmer
3. Prof. Dr. Silvia Ribback

The dissertation was submitted to the Technical University of Munich on 16 May 2023 and accepted by the TUM School of Medicine and Health on 20 December 2023.

TABLE OF CONTENTS

1 ABSTRACT (ENGLISH)

Nowadays one the most common cancers in the world is hepatocellular carcinoma (HCC). It is a highly vascularized tumor with a strong dependence on angiogenesis. The vascular remodeling is strongly required for further tumor progression. Thus, hepatocellular carcinoma attracts a vast majority of researchers, who are interested in understanding the tumor progression. In the studies of hepatocarcinogenesis, rodent models are frequently used to explore the pathophysiology and progression of hepatocellular carcinoma. However, there are only a few studies were done on hepatocarcinogenesis and on its angiogenetic properties in rodent liver models. Here my study shows, the presence of vascular remodeling in the pre-neoplastic and neoplastic lesions in rodent models.

In this study, I comprehensively characterized the pre-neoplastic foci of cellular alteration (FCA) and cancerous lesion (HCC) by using tissue-based techniques and computer assisted analysis to get a better understanding if vascular remodeling appears in rodent models and how. Different immunohistochemistry markers were used including such as CD31, Collagen IV, α-SMA, Desmin, VEGF164, Ki-67 and LYVE1; and RNA *in-situ* hybridization (VEGF-A). Additionally, computational image analysis was used to evaluate parameters including microvessel density, vessel size, pericyte coverage, including intratumoral vessel distribution and architecture. Software programs that were used for computational analysis: Aperio ImageScope and Definiens.

I found that FCA lesions have higher microvessel density and a larger amount of smaller immature vessels. On the contrary, HCC lesions have larger vessels with a lower number of vessels, and a higher degree of vessel maturation. In conclusion, I have validated the presence of vascular remodeling in the early stages of experimental hepatocarcinogenesis. I anticipate that this detailed characterization could be used as a solid basis for further angiogenesis studies in these models.

2 ZUSAMMENFASSUNG (DEUTSCH)

Das hepatozelluläre Karzinom (HCC) ist eine der häufigsten Krebsarten weltweit. Es handelt sich um einen stark vaskularisierten Tumor, dessen Wachstum auch in Abhängigkeit pathologischer Gefäßneubildung (Angiogenese) erfolgt. Der Gefäßumbau ist für die weitere Tumorprogression von entscheidender Bedeutung und daher ein intensiv beforschtes Gebiet. Zur Untersuchung der Hepatokarzinogenese bzw. Pathopysiologie und Progression des HCC werden meist Nagetiermodelle verwendet. Interessanterweise gibt es bislang nur wenige spezifische Untersuchungen zum Ablauf der Angiogenese während der Hepatokarzinogenese in den Nagern.

In der vorliegenden Studie wird der Gefäßumbau in präneoplastischen und neoplastischen Läsionen in einem Nagetiermodell untersucht. Präneoplastische Foci mit zellulären Veränderungen (FCA) und das HCC wurden mit Hilfe gewebebasierter Techniken und computergestützter Analyse detailliert untersucht, um ein besseres Verständnis dafür zu erlangen, ob und wie Gefäßumbau in Nagetiermodellen auftritt und ob Nagetiermodelle für die Untersuchungen angiogenetischer Prozesse geeignet sein können.
Immunhistochemische Gefäßmarker (CD31, Kollagen IV, Glattmuskelaktin (α-SMA), Desmin, vaskulärer endothelialer Wachstumsfaktor (VEGF164), Proliferationsmarker Ki-67 und LYVE1), sowie eine RNA-in-situ-Hybridisierung (VEGF-A) wurden angewandt. Mittels computergestützter Bildanalyse (Aperio ImageScope, Definiens) wurden Parameter wie Mikrogefäßdichte, Gefäßgröße, Vorkommen von Perizyten sowie intratumorale Gefäßverteilung und -architektur umfassend analysiert.

Resultierend zeigte sich, dass FCA-Läsionen eine höhere Mikrogefäßdichte und eine größere Anzahl kleinerer unreifer Gefäße aufweisen. Im Gegensatz dazu haben HCC-Läsionen größere Gefäßdurchmesser bei geringerer Anzahl von Gefäßen, was auf einen höheren Grad der Gefäßreifung hinweist.

Zusammenfassend zeigte sich, dass Gefäßumbau in den frühen Stadien der experimentellen Hepatokarzinogenese auch im Nagermodell eine wichtige Rolle spielt. Diese detaillierte Charakterisierung kann als solide Grundlage für weitere Angiogenesestudien in diesen Modellen dienen.

3 ABBREVIATIONS

A

ABP 4-Aminobiphenyl

ADH Alcohol dehydrogenase

Adk Adenosine kinase

APC Adenomatous polyposis coli

C

CAF Cancer-associated fibroblasts

CDD Choline deficient diet

CEP Comparative Experimental Pathology

CS Cigarette smoking

CTNNB1 Catenin beta 1 gene

CYP2E1 Cytochrome p450 2E1

D

DEN N-nitrosodiethylamine

DN Dysplastic nodule

dsDNA Double-stranded DNA

E

ECM Extracellular matrix

EMT Epithelial mesenchymal transition

F

FCA Foci of alteration

FFPE Fixed paraffin-embedded

FGF Fibroblast growth factor

G

GEMM Genetically engineered mice models

GLOBOCAN Global Cancer Observatory

GMNT Glycine N-methyltransferase

H

H&E hematoxylin and eosin

HBV Hepatitis B virus

HCC Hepatocellular carcinoma

HCV Hepatitis C virus

HFA Hollow fibre assays

HGDN High-grade dysplastic nodules

HIF Hypoxia- inducible factor

HSC Hepatic stellate cells

I

IGF Insulin-like growth factor

INHAND International Harmonization of Nomenclature and Diagnostic Criteria

K

KRAS Kirsten rat sarcoma virus

L

LCC Large cell change

LGDN Low-grade dysplastic nodules

M

MAPK Mitogen-activated protein kinases

MSCS Maternal inhalation of mainstream cigarette smoking

MVD Microvessel density

mRNA Messenger RNA

N

NAFLD Nonalcoholic fatty liver disease

NASH Nonalcoholic steatohepatitis

Nfia Nuclear factor IA

P

PDGF Platelet derived growth factors

PIGF Placental growth factor

PTEN Phosphatase and tensine homolog

R

RB Retinoblastoma

ROS Reactive oxygen species

S

SCC Small cell change

SMA Smooth muscle actin

ssRNA Single-stranded RNA

T

TERT Telomerase reverse transcriptase

TGF Transforming growth factor alpha

TNF-α Tumor necrosis factor alpha

TME Tumor microenvironment

V

VEGF Vascular-endothelial growth factor

W

WHO World health organization

4 INTRODUCTION

4.1 BACKGROUND INFORMATION ON HEPATOCELLULAR CARCINOMA AND EPIDEMIOLOGY.

Primary liver tumors, with hepatocellular carcinoma being the most common type, are a significant health concern worldwide [1-6]. According to Global Cancer Observatory (GLOBOCAN) reports from 2020, liver tumors rank sixth in incidence rate among all cancers and third in mortality rate globally (Figure 1, Figure 2) [1]. Alarmingly, it is predicted that the number of cases of liver cancer will exceed one million within next 20 years [7, 8]. The distribution of liver cancer within continents in GLOBOCAN 2020 shows that Asian countries (e.g., Mongolia, Thailand, Cambodia, Egypt) have the highest number of new cases and mortality rates, with some specific countries having particularly high rates [1]. In comparison, Italy, the Russian Federation, France, and Germany are leading European countries with higher rates of liver cancer (Figure 3) [9]. Although breast, prostate, and colorectal cancers are currently the leading causes of cancer-related deaths, it is suspected that pancreatic and liver cancers will surpass them in number by 2030 [10]. Given these trends, it is crucial to continue researching and developing effective treatments and prevention strategies HCC.

There are several predisposing factors resulting in the formation of HCC, such as viral etiologies, cirrhosis, alcohol abuse, tobacco use, obesity, metabolic diseases, aflatoxins and certain inherited diseases [11-19]. One of the global health burdens are acute and chronic viral infections of Hepatitis B and C, which cause liver cirrhosis, end-stage liver disease and HCC [20-22].

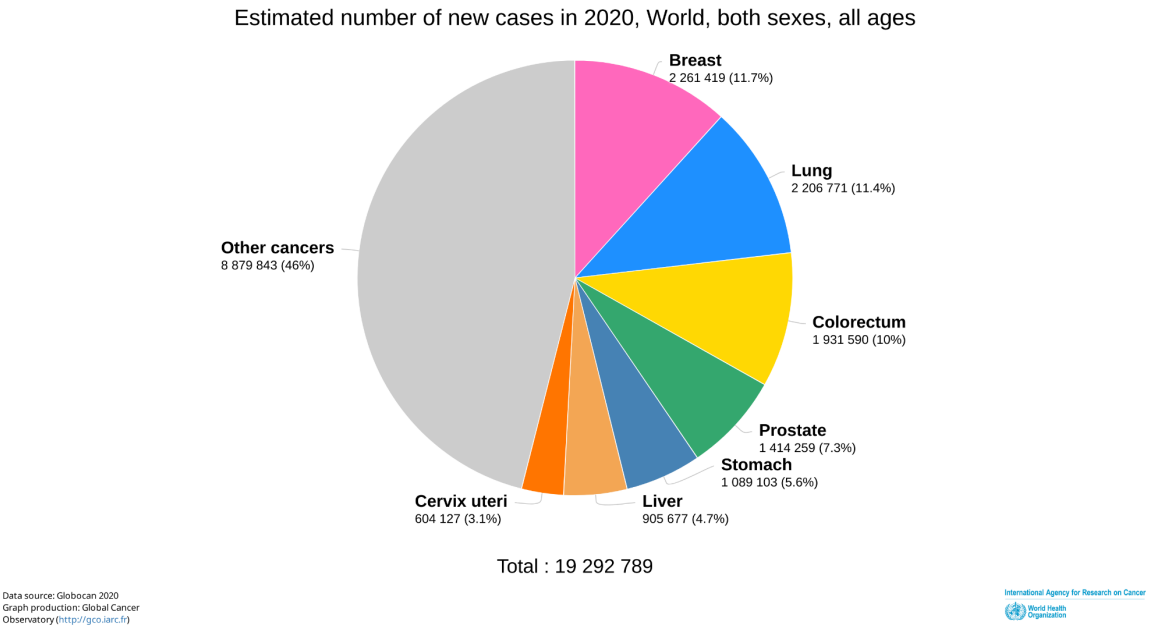

Figure 1. Estimated number of new cases in 2020, World, both sexes, all ages (Incidence Rate of cancers) (Figure taken from GLOBOCAN 2020 [23]).

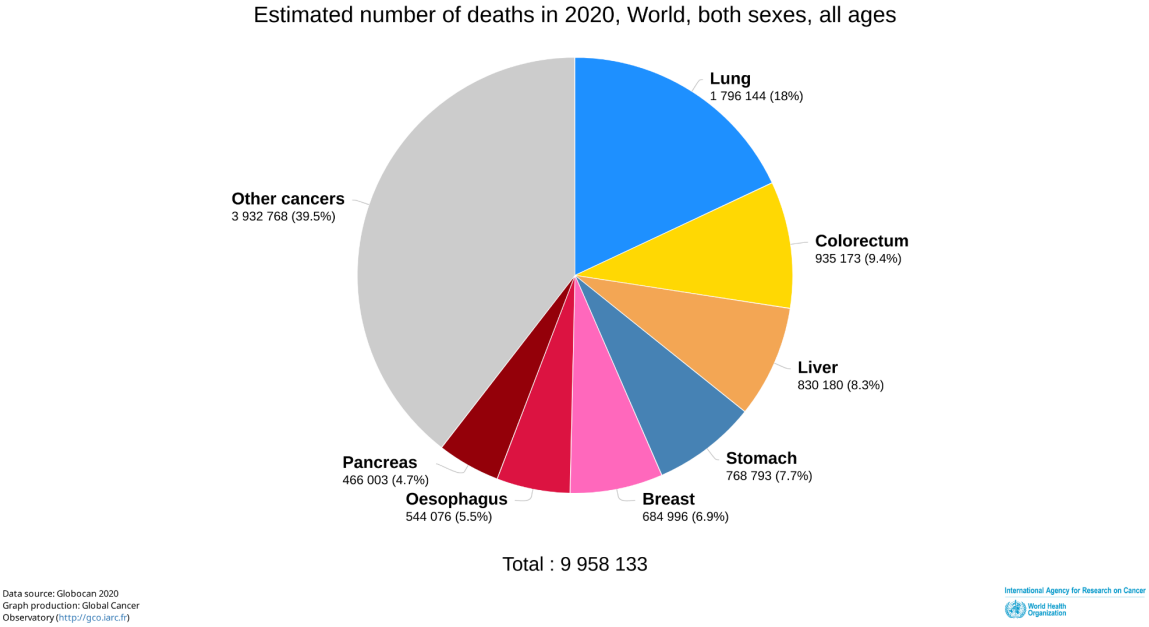

Figure 2. Estimated number of deaths in 2020, World, both sexes, all ages (Mortality Rate of cancers) (Figure taken from GLOBOCAN 2020 [24]).

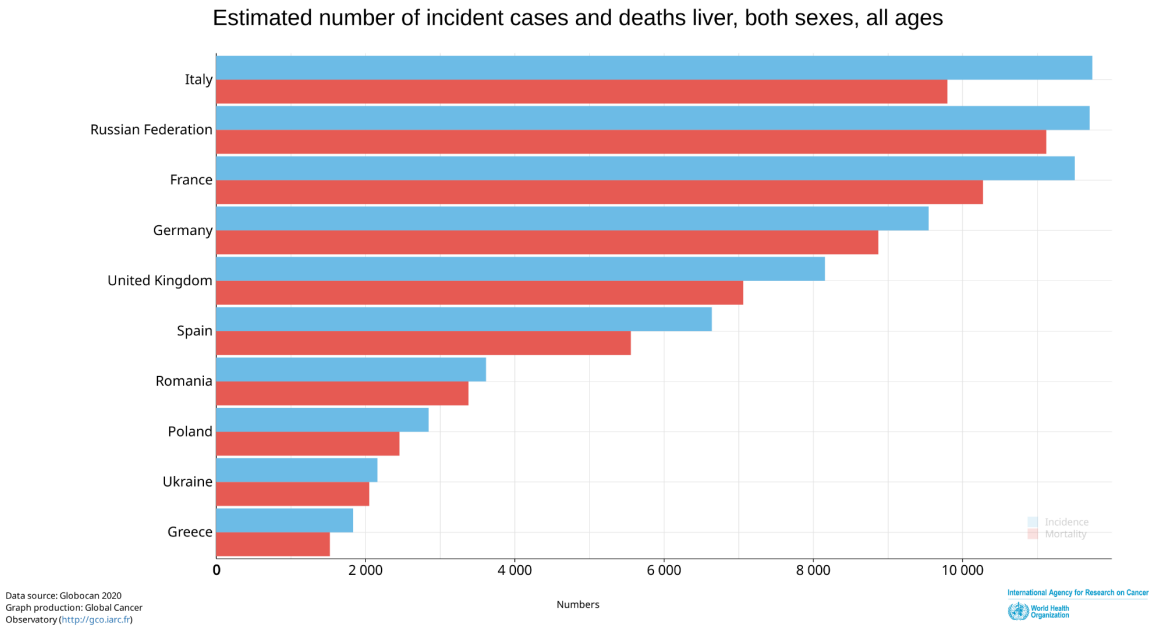

Figure 3. Estimated number of incident cases and deaths liver, both sexes, all ages (Incidence and Mortality) (Figure taken from GLOBOCAN 2020 [9]).

4.1.1 VIRAL HEPATITIS

Viral hepatitis is a major public health problem worldwide, chronic infection with hepatitis B virus (HBV) or hepatitis C virus (HCV) is the leading cause of development and progression of [1, 25]. The estimated by World Health Organization (WHO) number of patients with chronic Hepatitis B infection (2019) is around 296 million, with 1.5 million new infections each year [26]. Yearly around 1.5 million are newly affected by HCV [27-30]. In the 2019 WHO survey, more than 250.000 people died from complication of HCV [27] and approximately 820.000 deaths from HBV complications [26], mostly due to cirrhosis or HCC , indicating that it is a global burden [25, 31-33].

- **Hepatitis B virus (HBV):** is a dsDNA virus of Hepadnavirus family group, and one of the common predisposing factors causing HCC, due its property to cause chronic hepatitis and risk of developing end-stage liver disease [20, 34-37].

The main pathogenetic pathway of HBV is through integration to the hosts genome, which is also involved in several tumors promoting signaling pathways, resulting in the development of HCC. HBV DNA acts through direct or indirect pathways, causing genomic instability and insertion into the hosts genome [38-44]. In the most recent studies genes that are frequently are altered: *TERT*, *MLL4*, *CCNE1*, *NTRK2*, *IRAK2*, *p42MAPK1* and tumor suppressor genes (*TP53*, *RB1*, *CDNK2A* and *TP73*) [45-48]. Chronic HBV infection causes liver damage with necroinflammation and later resulting in HCC [43, 49, 50], in some studies the chronically infected patients with HBV may still develop HCC independent of having cirrhosis [51, 52]. Since HBV has its own subtypes, some of the genotypes have higher risk factors developing HCC [51, 53-55] . The exact role of action of the viral genotypes in the HCC formation remain not fully understood or known, it is still a highly debatable topic [43]. Although, currently there are some studies on genotypes of HBV, but there is still a need for more studies, which will focus on exploration of the epidemiological factors, the variants contribution in the HCC development and the treatment options [43].

- **Hepatitis D virus (HDV):** is an RNA virus it requires presence of HBV surface proteins in order to replicate and be infective [7, 56-60]. HDV infection may result in severe outcomes such as fulminant hepatitis, progression to chronic hepatitis, cirrhosis and HCC [58, 61-63]. HDV alone does not integrate into the host genome, since it lacks abilities to do it without HBV, therefore it is highly unlikely that HDV has properties of direct oncogenic mechanism [60]. Several studies have postulated that the risk of HCC is much higher in the cases of HBV/HDV coinfection, compared to HBV infection alone [7, 60].

- **Hepatitis C virus (HCV)**: is a ssRNA virus from a family of Flaviviridae, it causes acute and chronic hepatitis, resulting in the inflammation of liver [56]. Common serious complications of HCV are liver cirrhosis and further progression to HCC [36, 57, 64]. HCV similar to HBV has its own viral genotypes, distribution of them is varied in the world, most common ones are genotype 1, 2 and 3 [33]. However, the HCV does not integrate into human genome, if the host cannot fully clear the viral load it results in the HCC due to chronic inflammation [32, 56, 65].

  In addition to HCV genotypes, there are other viral factors that contribute to the development of HCC, such as HCV core protein and other non-structural/structural

proteins [57]. HCV core protein is known to play a significant role in liver tumorigenesis by interfering with the functions of proto-oncogenes and tumor-suppressor proteins, such as *TP53, p73* and *RB* [57, 64-68]. Moreover, HCV protein has been found to downregulate the expression of cyclin-dependent kinase inhibitors p21/WAF, regulate the epithelial-mesenchymal transition (EMT) through *Wnt/β-catenin* signaling, and upregulate *TERT* gene activity, which contributes to liver carcinogenesis [66, 69, 70]. Furthermore, HCV accelerates fibrosis progression by directly inducing profibrogenic factors in infected hepatocytes without causing severe inflammatory responses [71].

Another worrying infection is the coinfection of HBV and HCV, which is relatively common occurrence that significantly increases the risk of developing HCC [56, 72-74]. The coinfection progresses rapidly, and individuals are at greater risk of developing cirrhosis and HCC due to the synergistic effect of the two viruses on liver cell damage and inflammation, which leads to an increased risk of mutations [75-77].

4.1.2 ALCOHOL RELATED LIVER DAMAGE

Alcohol consumption is one of the other contributing factors that can cause liver damage and increase the risk of liver cancer [7, 18, 78, 79]. It increases the risk of liver cancer, it is considered as a linear dose dependent relationship of alcohol use, cirrhosis and HCC [79-81]. Chronic alcohol consumption considered as one of common causes and risk factors for HCC in developed countries [82]. Especially on of the highest alcohol consumption is in the world is European region, leading countries in alcohol consumption per capita are Lithuania, Estonia and on 9th place is Germany [78, 83]. In the Danish study by Ganne-Carrie et al., they were comparing the HCC incidence rate in patients with alcoholic cirrhosis, so patients with alcoholic cirrhosis exhibit high incidence rate of HCC (2.9%) and other small cancers [84]. In addition, having other contributing risk factors for the HCC development together with the chronic alcohol consumption, increases the risk of having liver cancer [79, 85, 86].

The pathophysiology of alcohol consumption resulting in alcoholic steatohepatitis, it is characterized by the accumulation of fat in the liver (steatosis) along with inflammation and cell damage, and liver cancer involves multiple mechanisms [87, 88]. Alcohol firstly gets metabolized in the hepatocytes by alcohol dehydrogenase (ADH) enzyme and cytochrome p450 2E1 (CYP2E1) into acetaldehyde [88], which is also considered as carcinogenic agent in

animals [89-92]. Then forming formation of reactive oxygen species (ROS) and activating hepatic stellate cells (HSC) [88, 93], increasing the production of type I collagen and resulting in fibrosis [94, 95]. Moreover, acetaldehyde induces inflammation, which can result in the activation of immune cells and release of pro-inflammatory cytokines, leading to further liver injury and cell death [80, 96]. Later on, it increases oxidative stress and forms of ROS, it can also bind to DNA and result in cell damage and hepatocarcinogenesis [88, 97]. There are additional studies that have shown that patients have increased risk of liver failure if they have with alcohol consumption has other metabolic diseases, such as viral hepatitis, obesity, diabetes or hemochromatosis [98-103].

In summary, the accumulation of fat, inflammation, oxidative stress, increased levels of acetaldehyde, and impaired DNA repair mechanisms can all contribute to the development of alcoholic steatohepatitis and increase the risk of liver cancer in heavy drinkers.

4.1.3 NAFLD AND NASH

Non-alcoholic Fatty Liver Disease (NAFLD) is a condition where fat accumulates in the liver cells in the absence of alcohol consumption, causing liver damage [104]. It is a common type of liver disease and can range from simple fatty liver (steatosis) to more severe conditions such as non-alcoholic steatohepatitis (NASH) and cirrhosis [105-107]. The incidence of NAFLD is rapidly increasing in burden, due to growing incidence of obesity, diabetes and other metabolic diseases [18, 108-113]. Nowadays due to rising prevalence of obesity and metabolic diseases, such as diabetes, in adults and children the prevalence of NAFLD is also increasing [114]. Thus, becoming all together frequent risk factors for HCC, especially considered as the fastest growing etiology in the Western countries [7, 107, 111].

Nonalcoholic steatohepatitis (NASH) is a liver disease that is characterized by fat accumulation in the liver along with inflammation and fibrosis [115]. The exact cause of NASH is not well understood, but it is thought to be related to a strong combination of factors including obesity and diabetes mellitus [116, 117]. In the study of U.S. Veterans Affairs health system Mittal et al., have found that patients with HCC and NAFLD or metabolic syndromes had five times higher risk of developing HCC without exhibiting cirrhosis, compared to HCV-related HCC [118]. Similarly, in the cohort study of Huang et al. in Taiwanese population, patients with diabetes have higher risk of developing HCC [119]. Elevated insulin levels and insulin

resistance lead to increased inflammation, cellular proliferation, inhibition of apoptosis and resulting in mutation forming tumor [64, 120].

The pathophysiology of NASH involves several key mechanisms: insulin resistance is often associated NASH, which leads to an increase in fatty acid production and decreased ability of the liver to remove fat, resulting in the accumulation of fat in the liver [104]. Consequently, the accumulation of fat in the liver can trigger an inflammatory response, leading to the activation of immune cells and the release of pro-inflammatory cytokines [121-123]. Also, the accumulation of fat in the liver can also lead to an increase in oxidative stress, which can cause cell damage and contributes to liver inflammation [124]. NASH can lead to changes in cellular signaling pathways, which can impair the ability of the liver to repair and regenerate, leading to the development of fibrosis and cirrhosis [64].

4.2 OTHER RISK FACTORS RELATED TO HEPATOCELLULAR CARCINOMA (AFLATOXINS, SMOKING).

Cigarette smoking (CS) is one of the preventable carcinogenic elements that cause different types of cancer, including liver cancer [125-129]. The trace element of cigarette smoke 4-Aminobiphenyl (ABP) is considered as bladder and liver carcinogen in rodents, which acts as DNA adduct [130-133]. In the study of Petrick et al., they compared former and current smokers and the risk of those patients to develop HCC, the risk was found to be in dose dependent and intensity dependent manner [125]. In one of the interesting researches, which was done on mice (C57BL/6), have found in mice that maternal inhalation of mainstream CS (MSCS) increases the severity and progression of NASH in offspring mice [134].

Aflatoxin is considered as a potent carcinogen and an occupational hazard [135, 136] It is a toxin that is produced by species of genus Aspergillus (fungi), found in grains, agricultural crops, textile field [130, 135]. Chronic administration of aflatoxin in rats, showed a linear association with liver tumorigenesis, it has high carcinogenic potency resulting in tumor formation [133]. The pathogenic mechanism of aflatoxin, is by forming DNA-adducts and activating tumor suppressor genes and resulting in mutations of p53, thus contributing towards HCC formation [137-139].

The visual description and summary of histopathological progression and molecular changes of HCC is described in the Figure 4 [140].

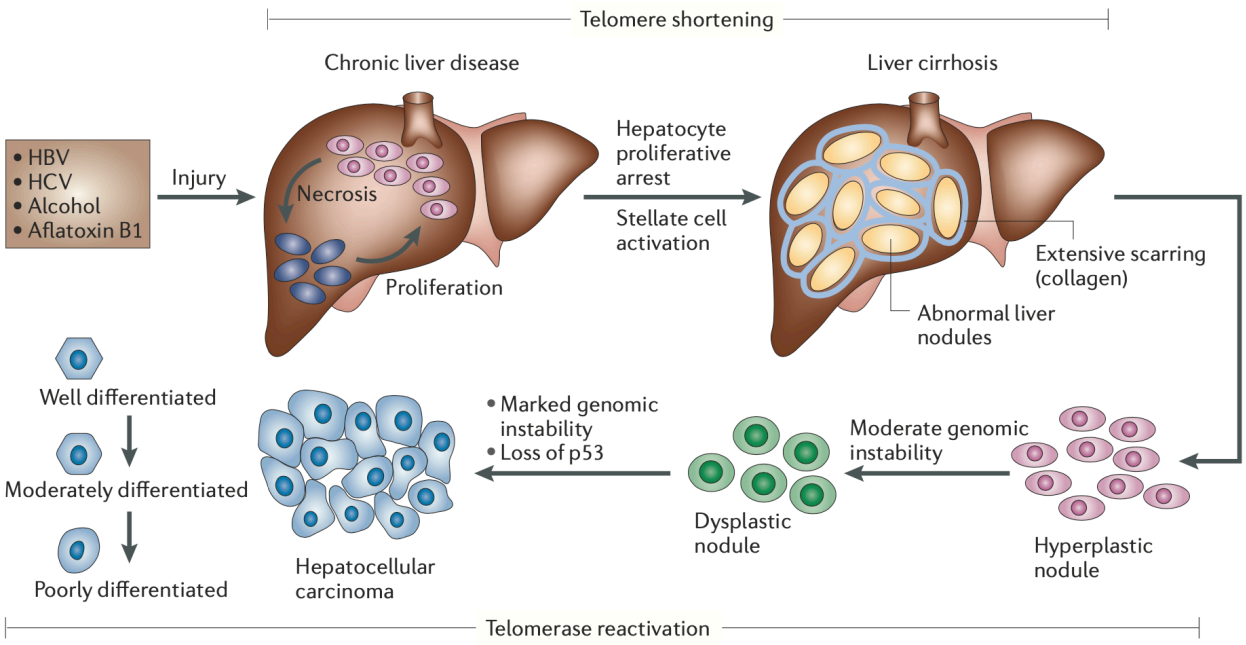

Figure 4. Histopathological progression and molecular features of HCC. (Unchanged figure taken from Farazi et al. Hepatocellular carcinoma pathogenesis: from genes to environment. Nature Reviews Cancer, Volume 6, 2006 (https://doi.org/10.1038/nrc1934)). Reproduced with permission from Springer Nature. [140].

4.3 PATHOGENESIS AND ANGIOGENESIS OF HEPATOCELLULAR CARCINOMA.

The pathogenesis of hepatocellular carcinoma (HCC) is a complex and multistep process involving the interplay of genetic and epigenetic changes in liver cells leading to uncontrolled cell proliferation and liver tumor formation [7, 141-143]. The whole process depends on the risk factors for HCC include chronic infection with HBV, HCV, alcohol consumption, NAFLD, smoking, aflatoxin exposure and other factors [7, 19, 140]. These risk factors affect liver differently, causing chronic liver injury and inflammation, furthermore resulting in gene mutations, that are involved in cell proliferation, apoptosis, and DNA repair [7, 140]. Consequently, leading to the accumulation of genetic changes, activation of oncogenes and

inactivation of tumor suppressor genes promoting tumorigenesis [140, 144]. Moreover, other factors such as oxidative stress, epigenetic modifications, and changes in the microenvironment of the liver can also contribute to the development of HCC [145, 146]. Inflammatory cytokines and oxidative stress can cause DNA damage and promote the accumulation of genetic changes in liver cells [7, 147]. Some key common mutational drivers in HCC are *TERT*, *TP53* and *CTNNB1*, which are hardly targetable in the therapy [71, 148, 149].

Moreover, HCC is one of the most highly vascularized tumors, in which angiogenesis plays a crucial role [150]. Angiogenesis, the process of forming new blood vessels, is necessary for the growth and metastasis of tumors, as it provides the necessary blood supply for tumor cells to receive oxygen and nutrients [151-153]. Since the angiogenesis in the HCC strongly associated with the disease progression, thus is a potential therapeutic target [154-157]. In HCC, angiogenesis is also promoted by the interaction between the tumor and the surrounding liver tissue [158, 159]. The liver has a unique microenvironment known as the "sinusoidal" network, which is composed of specialized blood vessels that provide direct access to the tumor cells [160-162]. This direct access allows HCC cells to release pro-angiogenic factors into the circulation and recruit new blood vessels to the tumor. Thus , it is a characteristic feature of the HCC, the release of the pro-angiogenic factors produced by tumor cells, vascular endothelial cells, immune cells, and surrounding tumor microenvironment (TME) [145]. Pro-angiogenic factors are a class of proteins that play a critical role in the liver angiogenesis, by supporting the growth and survival of HCC tumor cells [163-165]. These factors stimulate the proliferation and migration of endothelial cells and the formation of new blood vessels, providing the tumor with a constant source of oxygen and nutrients. In addition, they help to create a vascular network composing it of leaky and abnormal vessels, causing hypovascular regions within the tumor, which promotes hypoxia and necrosis [145, 156]. Consequently, hypoxia induces autophagy providing energy for tumor cells and its surrounding environment through catabolic breakdown of cellular elements to help promote cancer survival [145]. Vascular endothelial growth factor (VEGF) is a potent pro-angiogenic factor and a mediator in hepatocarcinogenesis and regulated by oncogenic gene mutations, hormones, and cytokines [152, 157, 159, 166-168]. Hypoxia and acidotic environment stimulate the overexpression of the VEGF, which produces leakier, structurally and functionally abnormal vessels, however also allowing tumor cells to get oxygen and other nutrients [66, 156, 169]. Furthermore, the tumor microenvironment promotes the release of other angiogenic molecules: Angiopoietins 1 and 2, and basic fibroblast growth factor (FGF), which help to form a dysfunctional vasculature in the HCC [159]. Moreover, the VEGF's impact on endothelial

cells is augmented by Angiopoietin 2, and it forms the molecules which have a negative effect on basement membrane and further expand the tumor's hypoxic environment [163]. Also, VEGF works together with other factors, in combination with basic FGF, it stimulates the angiogenesis, and with platelet-derived endothelial cell growth factor, it results in cell migration and new vessel formation [145]. The paper of Poon et al. suggests that circulating angiogenic factors may be beneficial in the evaluation of angiogenesis, especially VEGF, which could provide prognostic information (patient survival and recurrence rate) [168]. Therefore, it is targeted as angiogenesis inhibitor in several tumor treatments as Bevacizumab (rhuMAb-VEGF) is a humanized monoclonal antibody targets VEGF, therefore inhibits one of the main promoters of tumor angiogenesis [170-172].

One another important factor is chronic hepatic injury, which plays a critical role in the pathogenesis of the liver carcinogenesis, it induces fibrosis due to the deposition of the extracellular matrix (ECM), followed by poor oxygenation and hypoxia [145, 146]. Consequently, it results in the further progression of the hypoxia, which stimulates the production of the pro-angiogenic factors by stromal cells, especially of VEGF, which promotes cell proliferation [145, 146]. The high production of the ECM and their reduced turnover, results in a fibrotic environment which stimulates the tumor growth, survival and further proliferation via various type of integrin signaling.

Another groups of cells that have a significant impact on the promotion of the tumor growth, angiogenesis, inflammation and attenuating immune surveillance are cancer-associated fibroblasts (CAFs); it secretes factors and interferes in the cross-talk communication with cancer cells [144-146, 173, 174]. Thus, CAFs have a strong correlation with the tumor progressions, prognosis and staging [144, 173, 174]. In addition, reportedly CAFs stimulate the secretion of VEGF and Angiopoietin 1 or 2 [175, 176]. In addition, the angiogenic pathway in HCC is also influenced by the presence of other signaling pathways, such as the *Wnt*-signaling pathway and the insulin-like growth factor (IGF) signaling pathway [7]. Activation of these pathways can result in the over-expression of pro-angiogenic factors, further promoting angiogenesis and tumor progression.

4.4 COMPARATIVE PATHOLOGY OF LIVER LESIONS.

Rodent models are widely used to investigate hepatocarcinogenesis [177]. Especially the broad spectrum of the etiologies that predispose towards developing HCC, widely attracts researcher's attention. Thus nowadays, one of the common fields of interest amongst researchers are liver diseases and their pathologies. Among various models, genetically engineered mice are considered as new and elegant tool, however models might present with a wide of histological diagnosis and therefore usage of such models needs experienced researchers [178]. Otherwise choosing an inappropriate model, may mislead or may result in publishing wrong results [7, 177, 179, 180]. Genetically engineered mice models (GEMMs) are the most suitable models in cancer research, with wide range of benefits such as being an applicable tool to understand human diseases and their mechanism on molecular level, due to its similarity with human genome [181]. However, choosing an appropriate mice model should be done in the beginning, in order to be able to answer the specific research questions of HCC, and accordingly having a model for particular etiology [182].

4.4.1 EXPERIMENTAL LIVER MICE MODELS

1. **Chemically induced models:** common carcinogens are N-nitrosodiethylamine (DEN), choline deficient diet (CDD) and aflatoxin, they are administered through diet (food, drinking water), gas inhalation or intraperitoneal/subcutaneous injection [182].

   DEN model is frequently used in cancer studies, DEN has ability to cause oxidative stress and form reactive oxygen species (ROS) and alkylating DNA structures [183]. Thus, inducing HCC in dose dependent manner, being a good study model with a poor prognosis [184]. Another model is CDD, it is an accepted model for steatohepatitis studies with later HCC development, exhibiting ballooning of hepatocytes, fibrosis and further cirrhosis [185, 186]. Lastly, one more carcinogen is aflatoxin, which induces hepatocarcinogenesis in mice models similarly to humans, by affecting damaging DNA and forming DNA-adducts [139, 187]. In general, chemically induced models are preferred if study investigates the predisposing risk factors to develop HCC [183].

2. **Xenograft models:** there are several models such as ectopic implantation, orthotopic implantation and hollow fibre assays (HFA), which could be determined through direct implantation of tissue or inoculation or cancer liver cells from humans [183]. Those models commonly are used in pre-clinical studies, drug screenings to understand its pharmacodynamics and toxicity, as "proof-of-principle experiments" [188]. However, when a researcher chooses this model, should keep in mind the difference of cellular heterogenicity between humans and mice, which negatively affects reproducibility of findings [183].

3. **Genetically engineered mice models:** considered as the best model for human cancer studies, since it has some similarities in molecular way with humans [182, 189].

- Transgenic models expressing viral genes.

  It is used to study in specific HBV and HCV molecular mechanisms and to understand how it contributes to HCC formation [182, 190, 191]. However, one caveat is that in the mice models not all HBV genotypes cause HCC, due to "species-specific liver tropism" and differences in receptor post-binding steps [192, 193].

- Transgenic mice over-expressing oncogenes.

  Myc proteins: Transgenic-*Myc* mice are good models of poor prognosis HCC, with higher mortality genomic instability and incident rate [194]. Moreover, *Myc* protein is also involved in the mutation of *CTNNB1* gene, which plays a key role in the HCC formation [182, 194, 195].

  Beta-catenin protein: a protein which is strongly correlated with the *Wnt* signaling pathway in hepatocarcinogenesis, especially in the early HCC formation [149, 182, 183]. Mice models with the protein activation considered also as a good study models, especially if combined with other mutation such as adenomatous polyposis coli (APC) [196].

- Models over-expressing growth factors: it plays a vital role in the mediation of hepatocytes growth, which in result induces HCC. Current examples of transgenic mice models with over-expressed Epidermal growth factor (EGF) [197, 198], Transforming growth factor alpha (TGF-α) [194, 199], Fibroblast growth factor 19 (FGF19) [200].

- Creating a tumor environment: these models preferred in to study tumor microenvironment and underlying pathogenesis process of the HCC, such as injury and fibrosis. There are alpha-1 antitrypsin models [201, 202], platelet-derived growth factor (PDGF) [203], TGF-β [204, 205], Glycine N-methyltransferase (GMNT) [206, 207]. In addition, phosphatase and tensine homolog (PTEN) models, PTEN is a tumor suppressor gene, mice models with PTEN-deletion showed to have similarities with human NASH development with further progression into HCC [183, 208].

  Lastly, kirsten rat sarcoma virus (KRAS) mice models, KRAS is an oncogene that mutated in almost 30% of cancers, the molecular mechanisms of it in cancer progression is currently poorly understood [209, 210]. KRAS is strongly involved in the Mitogen-activated protein kinases (*MAPK*) pathway and with other signaling pathways, thus regulates processes such as cellular proliferation, survival, differentiation and migration [210]. Ras-oncogene activation is also considered as a frequent mutation in the hepatocarcinogenesis [211]. In the interesting study of Steiger et al, where they compared PTEN and KRAS mice models and its number of liver lesions, they have demonstrated the revealing information that KRAS models presented with higher number of malignant lesions [178]. Especially with more than 60 % of precancerous lesions (FCA) and more than 30% of HCC lesions. Pointing towards that those KRAS mutated models are actually good models to study liver disease especially precancerous lesions [178].

Moreover, other types of newly developed GEMMs are present: simple liver-specific transgenic approach that employs the SB transposase system and the hydrodynamics-based transfection method [212-214]. However, it is crucial and strongly recommended before conducting a research, scientists should define their purpose and what they are trying to achieve with their studies, thus choose the appropriate mice model accordingly (**Figure** 5) [182, 183, 215].

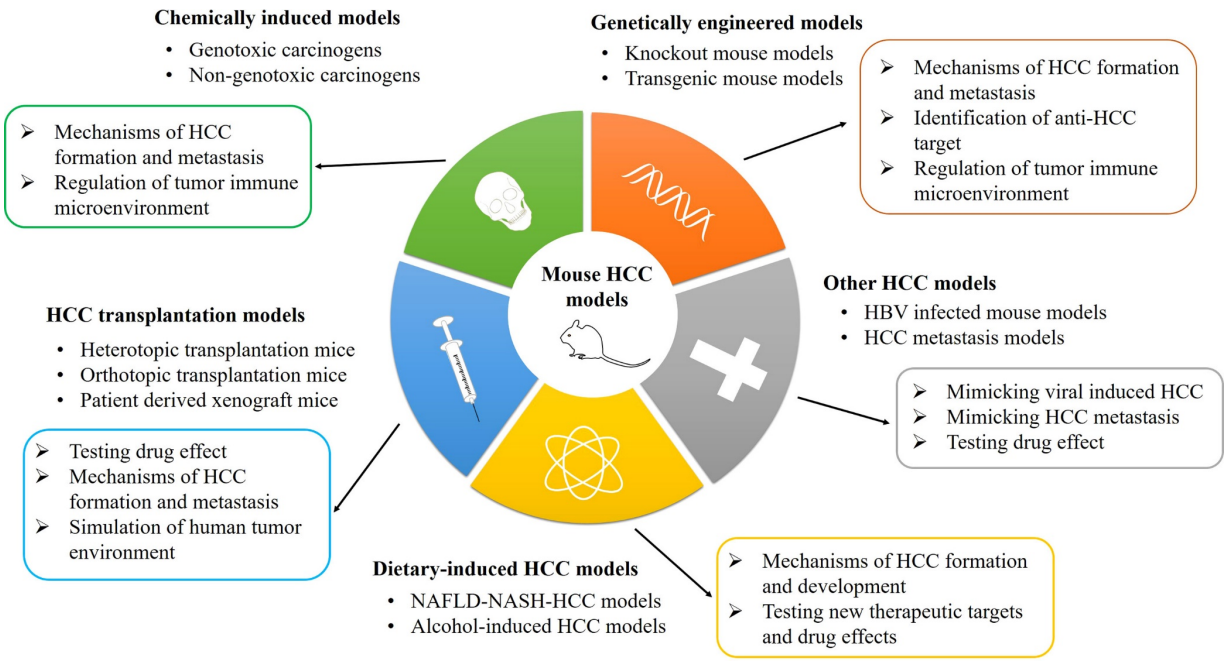

Figure 5. The classification, advancement, and application of mouse HCC models. (Unchanged figure taken from Sha Liu et al. Mouse Models of Hepatocellular Carcinoma: Classification, Advancement, and Application. Frontiers in Oncology, Volume 12, 2022; (https://doi.org/10.3389/fonc.2022.902820). Copyright owners Liu, Huang, Ru, Wang, Zhang, Chen and Chu. [215].

4.4.2 PRENEOPLASTIC AND NEOPLASTIC LESIONS

In the GEMM may present with various lesions, not all of them could be used in the comparative studies with humans. The counterpart of human liver preneoplastic lesions "dysplastic nodule" (DN) is focus of cellular alteration (FCA). The diagnostic features of FCA were described as [216, 217]: "FCA is characterized as a localized proliferation of hepatocytes phenotypically different from surrounding hepatocyte parenchyma. FCA are circular or ovoid in shape; irregular formed foci may occur; may be subclassified based on predominant cell type. The fact that 80% of the focus is composed of one morphologic cell type (basophilic, eosinophilic, etc.) or a mixed cell type. Normally no or only minimal compression of the surrounding liver tissue. Liver plates merge imperceptible with surrounding hepatic parenchyma; nevertheless, foci are sharply demarcated from the adjacent normal hepatocytes by the appearance and staining reaction of its cells. Normally absence of cellular atypia. Intracytoplasmic inclusions of various types may be present. Morphological subtypes of FCA are basophilic, eosinophilic, mixed, clear cell, amphophilic."

Already in the 90s in the study of Kolaja et al., it was already identified that DEN has direct effect on mice liver and increases the number of FCAs [218]. In the humans, the comparative counterpart of FCA lesions are dysplastic nodules, which were reviewed and described by Thoolen et al. [217]: FCAs (eosinophilic, basophilic and clear cell foci) and compared with the human counterparts of large cell change (LCC) and small cell change (SCC). "Eosinophilic and basophilic FCA in the rat and LCC and SCC in humans showed common histomorphological characteristics, which might be indicative of a mutual presumptive role in the process of hepatocarcinogenesis" [216].

The criteria for HCC diagnosis in the murine liver was described by Thoolen et al. [217]: "HCC are local infiltrating growth and/or lack of distinct demarcation, marked cellular pleomorphism may occur. Loss of normal lobular architecture, vascular invasion or metastases may be observed. Increased mitotic index possible. Hemorrhage, necrosis, and extramedullary hematopoietic foci may be present. May occur as a single morphologic type or a combination of them as in the following. Morphological subtypes of HCC are trabecular, acinar, solid, adenoid".

The pathogenesis of HCC depends on the exposure of carcinogens, could form spontaneously in some cases or due to specific genetic alterations in the mice [217]. Moreover, other studies had thoroughly described the pathophysiology of the HCC and cirrhosis, which starts with the development of the pre-cancerous DNs [219, 220]. DNs size is more than 1mm, has two types according to the degree of atypia: low-grade DN ((LGDN) appear normal or show minimal nuclear atypia, slightly increased nucleocytoplasmic ratio, has no mitotic figures) and high- grade DN ((HGDN) has cytological atypia, cytoplasmic basophilia or clear cell change, high nucleocytoplasmic ratio (crowding of nuclei), occasional mitotic figures)[219-221]. Firstly, LGDN forms, later progresses into HGDN, which later has a potential to transform into early-stage HCC and advanced HCC. Malignant transformation into HCC can originate from various cell types including mature hepatocyte and stem or progenitor cells [7, 222-224]. As a summary, the liver carcinogenesis is a multistep process with a distinct sequence of lesions: cirrhosis/low-grade dysplastic nodules → (LGDN)/high-grade dysplastic nodules → (HGDN)/early HCC/progressed HCC and advanced HCC [148, 225].

4.5 THE GAP OR MISSING KNOWLEDGE OF ANGIOGENESIS.

Angiogenesis is required for tumor tissues to obtain their nutrients, survive and metastasize, as well as form new vessels called "neovascularization"[226]. Angiogenesis is regulated by inhibiting and activating molecules, when activating molecules are upregulated and inhibiting molecules are down-regulated, the so-called "angiogenetic switch" is turned on [227-230]. There are several key regulators and factors that help promote the vascular proliferation and the formation of new blood vessels. The main angiogenetic factors are mainly VEGF, Tie2, Angiopoietin family, Hypoxia- inducible factor (HIF) - 1α, Transforming growth factor (TGF), Tumor necrosis factor alpha (TNF-α), Placental growth factor (PIGF), bFGF [158, 226, 231-233]. Mice models are commonly used to study cancer diseases; however, little is known regarding the angiogenesis of HCC in mice. The majority of studies have explored VEGF and other angiogenetic factors. One study found increased levels of VEGF and HIF-1α in DEN-induced liver fibrosis and upregulated expression of VEGF, PIGF, and HIF-1α in tumor nodules [234]. Another study of portal hypertension with cirrhosis in rats found increased mesenteric vascular density and increased VEGF expression, highlighting the importance of VEGF in angiogenesis [235]. Furthermore, they showed a positive correlation between CD31 expression and increased microvascular density with the extent of angiogenesis [235].

VEGF-A is considered to be one the potential predictive biomarkers of the HCC [236, 237], however in the study previous studies of VEGF-A, when compared with PIGF expression and its correlation with early recurrence of HCC, it was found to have a positive correlation and is a good prognostic factor of HCC compared to VEGF-A or VEGF-C [238]. In the paper by Turlin et al., their research team used VEGF as a vascular staining in hepatic microcancers [167]. VEGF plays a crucial role in the angiogenesis and vascular remodeling in the liver cancer, which correlates with the disease severity. In the large number of studies, the evaluation of the circulatory VEGF levels in the various of tumors, showed a strong association with the advanced disease progression and poor prognosis [13, 152, 153, 159, 166, 239, 240]. Additionally, Vanderborght et al. thoroughly described that there is a strong correlation of VEGF and Angiopoietin pathway, which has a significant influence on the vessel development and sprouting in the HCC [150]. In the paper of Anja Runge et al. [241], they researched and described the vasculature of HCC. In the angiogenesis of the HCC lesions, vessels need to sprout and bud for further proliferation and the expansion of the vascular network by remodeling the extracellular matrix and migrating [242, 243]. In the interesting study of

Kornek et al., they have injected mice with alcohol and thioacetamide, which later developed fibrosis and HCC faster [244]. Moreover, they have found that expression of VEGF, VEGF receptors was higher in the tumors that have fibrotic background, which accelerates further HCC development.

Current knowledge about tumor vessels undergoing the process of capillarization describes them as irregular in diameter, possessing an abnormal vascular branching pattern, tortuous properties, leaky, partially covered by pericytes, and having an incomplete basal membrane [243, 245]. The characteristics of these vessels were mainly studied through electron microscopy, which identifies difference between normal hepatic sinusoids and the vessels of HCCs [246]. Haratake et al's study revealed thickening of endothelial cells, intermediate junctions between neighboring cells, reduction or lack of fenestrations, formation of basement membranes, and paucity of sinusoidal macrophages [246]. The presence of small arterioles with smooth muscles in their walls was also found in tumor areas [246]. The study concluded that the sinusoids of HCCs lack the specifically differentiated morphology of normal sinusoids and develop characteristics of capillary and precapillary blood vessels [246]. Additionally, endothelial cells of HCC lesions have a tendency to lose their polarity, leading to stratification and protrusion into the vessel lumen [247].

5 AIMS OF THE STUDY

The aim of this study was therefore to perform a comprehensive characterization and comparison of the vasculature in mouse models used for hepatocarcinogenesis studies. This was a follow study of Steiger et al., Cancers 2020, since in this study it was found that one mouse model (with KRAS mutation) presented with a very high number of neoplastic lesions, especially FCA (67%) and HCC (31%). Thus, the particular interest was to explore whether those models would present with so called "angiogenetic switch", progressing from FCA into HCC.

Firstly, preforming a detailed background and resources analysis. Later on, identifying lesions according to diagnostic criteria. For the purpose of studying and comparing vasculature structures, we characterized the vessels of pre-neoplastic foci of cellular alteration (FCA) and hepatocellular carcinoma (HCC) by using tissue-based techniques. Immunohistochemistry stainings: CD31, Collagen IV, α-SMA, Desmin. Combined with stainings such as Ki-67 for the nuclear proliferation comparison, LYVE1 for identification of lymphovascular proliferation and at first, we used VEGF164 due to its homogenous cytoplasmic staining we used afterwards VEGF-A mRNA. CD31 and α-SMA are the classic vascular marker that are widely used in the research world, especially on rodents [171, 241, 248-253]. The other vascular markers that we selected were Desmin and Collagen IV, which were described in microvasculature papers also in [241, 249, 254]. Further computer assisted analysis to better understand if and how vascular remodeling appears in rodent models for liver tumorigenesis.

We focused on accessing FCA versus HCC:

- Identifying common vascular markers that could be used on mice
- Comparing the vasculature with subgroups of vessel sizes
- Assessing the vessels by using different vasculature markers
- Assessing if the angiogenesis present in liver rodent models
- Analyzing if there is a correlation between vessel distribution and lesion types.
- Statistically comparing the microvessel analysis data and interpreting the findings.

6 MATERIALS AND METHODS

All of the materials and methods were previously published in my 2022 Cells paper "Vascular Remodeling Is a Crucial Event in the Early Phase of Hepatocarcinogenesis in Rodent Models for Liver Tumorigenesis" Cells 2022, 11(14), 2129 [255]; except Ki-67 and VEGF164 results – they are described in details here.

6.1 TISSUE COLLECTION

A total of 25 formalin fixed paraffin-embedded (FFPE) samples from GEMM for liver tumorigenesis were used. All tissue samples of mice were processed at the Comparative Experimental Pathology (CEP) at the Institute of Pathology, Technical University Munich (TUM). Animals were initially provided to our collaboration partners (J.G.) by the Welcome Trust Sanger Institute, Genome Campus, Hinxton, Cambridge, CB10 1SA, UK. Experiments were approved by the local ethical committees in both the UK and Germany (TV 55.2-2532.Vet_02-16-143, government of Oberbayern; year of approval included in number). Mice were all kept under standard laboratory conditions (12 h day/night cycle, water and standard diet ad libitum, no special diet). Only samples from animals originating from end-point studies were included. Samples from animals with unclear/insufficient extent of genetic knockdown were excluded from this study. Those 25 FFPE blocks were from KRAS, KRAS/adenosine kinase (Adk) and KRAS/ nuclear factor IA (Nfia) GEMMs were included in the study [178]. The genetic background has been already been extensively described in the paper of Steiger et al. [178].

The FFPE blocks were sequentially cut (2-3µm) on tissue slides, and Thermo Scientific HM 340 was used as cutting machine. Later they were stained with hematoxylin and eosin (H&E) according to standard protocols. Slides were then independently evaluated by me and under supervision of experienced liver and comparative pathologist Prof. Dr. med. Carolin Mogler; and diagnosed according to existing guidelines for diagnosis of proliferative liver lesions in rodents mentioned above [217]. Lesions with morphological diagnosis of FCA (clear cell, basophilic and eosinophilic subtype) and HCC were then selected for this study.

6.2 IMMUNOHISTOCHEMISTRY

The vasculature was characterized by immunohistochemistry including stainings for the intralesional vasculature of FCA and HCC including stainings for CD31 (1:100; DIA-310, Dianova, Hamburg, Germany), Collagen IV (1:50; CL50451AP, Cedarlane, Ontario, Canada), α-Smooth muscle actin (α-SMA) (1:500; ab5694, Abcam, Cambridge, UK), LYVE1 (1:7000; ab33682, Abcam, Cambridge, UK), Desmin (1:50; M0760, DAKO, Santa Clara, United States), Ki-67 (1:50, ab16667, Abcam, Cambridge, UK), VEGF164 (1:20; AF-493-NA, Bio-Techne, Minneapolis, United States) and using standard protocols [256, 257]. All the immunohistochemistry stainings were performed by me and with the help and guidance of our lab technicians Maximilian Guenzl and Annett Hering. Stainings were performed on Bond-Max Rxm and Bond-Max Rx from Leica Biosystems, Nussloch, Germany. Further description in detail in the Table 1.

TABLE 1

Immunohistochemistry table

Stainings	Code	Manufacturer	Dilution	Visualization	Antigen retrieval protocol
1. CD31	DIA-310	Dianova, Hamburg, Germany	1:100	3,3'-Diaminobenzidin (DAB)	Epitope-Retrieval 2 (EDTA-Buffer) for 30 min. Order number: AR9640
2. Collagne IV	CL50451AP	Cedarlane, Ontario, Canada	1:50	3,3'-Diaminobenzidin (DAB)	Enzyme 1 (Proteinase K) for 10 min. Order number: AR9551
3. VEGF164	AF-493-NA	Bio-Techne, Minneapolis, United States	1:20	3,3'-Diaminobenzidin (DAB)	Enzyme 1 (Proteinase K) for 15 min. Order number: AR9551
4. α-SMA	ab5694	Abcam, Cambridge, UK	1:500	3,3'-Diaminobenzidin (DAB)	Epitope-Retrieval 1 (Citrat-Buffer) for 20 min. Order number: AR9961
5. Desmin	M0760	DAKO, Santa Clara, United States	1:50	3,3'-Diaminobenzidin (DAB)	Epitope-Retrieval 1 (Citrat-Buffer) for 30 min. Order number: AR9961
6. LYVE1	ab33682	Abcam, Cambridge, UK	1:7000	3,3'-Diaminobenzidin (DAB)	Epitope-Retrieval 2 (EDTA-Buffer) for 30 min. Order number: AR9640
7. Ki-67	ab16667	Abcam, Cambridge, UK	1:50	3,3'-Diaminobenzidin (DAB)	Epitope-Retrieval 1 (Citrat-Buffer) for 20 min. Order number: AR9961

Table 1. Immunohistochemistry table. The detailed information on immunohistochemistry stainings.

6.3 RNASCOPE TECHNOLOGY (*IN-SITU* HYBRIDIZATION (ISH) AND IMMUNOHISTOCHEMISTRY)

RNAscope technology is the combination of the *in-situ* RNA analysis and the immunohistochemistry technique together. Levels of vascular endothelial growth factor A (VEGF-A) mRNA were assessed by RNAscope (RNAscope multiplex fluorescent reagent Kit v2 Assay, 323100-USM, ACD, Newark, United States) according to the manufacturer´s protocol. Analysis was performed by Maximillian Guenzl and our collaboration partner Thomas Leibing, University Hospital Mannheim, Germany. Evaluation and interpretation of the results done by me and help of a postdoc Sabrina Sarkar Rim.

6.4 COMPUTER-ASSISTED IMAGE ANALYSIS

Slides were scanned using a slide scanner, Aperio AT2 (Leica Biosystems, Nussloch, Germany) at the magnification of 40X. With the guidance of my supervisor and expert pathologists Dr. med. Carolin Mogler, I have manually annotated the selected regions of interest (ROIs) on Aperio ImageScope software (Version 12.4.0.7018, Leica Biosystems). Further computational analysis was performed by me and with help of post-doc Sabrina Sarkar Rim in the determination of computer algorithm.

The staining for α-SMA and desmin were analyzed with using the Aperio ImageScope software with an algorithm, 'Positive Pixel Count v9' as previously described [258]. The default set of parameters of the algorithm was modified according to the stain contrast and intensity of the scanned images. The algorithm measured the intensity of the stain (brown signal) for the whole section. The total positive pixel was then normalized to the total area of the tissue section (pixel/mm^2).

For counting Ki67-positive cells, a modified version of the 'Nuclear v9' algorithm on Aperio ImageScope software (Version 12.4.0.7018, Leica Biosystems, Wetzlar, Germany) was used. The percentage of cells with positive immunostaining was defined as the Ki-67 proliferation index.

For quantifying VEGF-A expression, an open-source image analysis software, 'QuPath' (version 0.2.3, Queen's University Belfast, Ireland) was used [259]. The ROIs annotated on ImageScope were transferred as xml files onto QuPath using a software script developed by the QuPath developer. Firstly, cells were segmented using a modified 'Cell detection'

algorithm. For probe VEGF- A detection, the 'Subcellular detection' algorithm was chosen and a detection threshold was adjusted interactively until all the probe dots are detected. The minimum and maximum spot size ranged from 0.5μm^2 to 3μm^2. Larger areas were considered as clusters of spots. Total number of subcellular spots of clusters for each ROI was counted.

Analysis of intra-tumoral vasculature was performed using computational approaches. Microvessel density (MVD) was assessed using Definiens Tissue Studio of CD31 and Collagen IV- stained vessels were analyzed by Definiens Architect (version XD 64 2.7, Definiens AG, Munich, Germany) using the algorithm, 'Marker Area Detection'. ROIs were transferred from ImageScope using a default feature in Definiens. Blood vessel size was defined in accordance and of published literature in rats was Julia C. D'Souza et al., which defined the blood vessels sizes according to their diameter as small vessels (5 to 15um in diameter), medium vessels (16 to 50um), and large vessels (>50um) [260]. In our case, the vessel classification was based on the area. The vessel areas of each subgroup were measured manually by randomly annotating the vessels of the lesions, then taking the average of the vessel area, in order to set the criteria. Then after setting the criteria, the size of the vessels was used to automatically define 3 groups of vessels, defining small (< 150 μm^2), medium (150-500 μm^2), large (> 500 μm^2). Computer analyzed quantitative vessel data was normalized accordingly as a ratio, providing three values for each vessel group: stained vessel area per total lesion area, stained vessel number per total lesion area and average staining intensity of the lesion.

Heatmaps were generated based on the density of the three vessel subgroups mentioned above, using Definiens Architect (version XD 64 2.7, Definiens AG, Munich, Germany). The heatmap evaluation was performed according to published literature [261], including colored-coded evaluation of density of marker expression (green color for the lowest density, yellow color for medium density, red color for the highest density). The analysis was done semi-quantitively, according to the highest hotspot locations (marked in red color) within the lesion (FCA or HCC) based on their computer-defined location (peripheral or central part of the lesion/intralesional). Each slide was evaluated by 2 independent investigators me and postdoc Sabrina Sarkar Rim. The hotspot was referred to the highest density of micro-vessel area (small/medium/large).

LYVE1 expression was evaluated semi-quantitative and given as percentage (%) of vasculature/lesion stained for LYVE1.

6.5 STATISTICAL ANALYSIS

Statistical analyses were performed by me, using GraphPad Prism 9 (GraphPad Software, Inc., San Diego, United States) and IBM SPSS Statistics (version 28, IBM Corporation, Armonk, New York, United States). The cut off for statistical significance was p value ≤ 0.05. The selection of statistical test was done according to the normal distribution tests (Shapiro-Wilk and Kolmogorov-Smirnov test). If groups were not normally distributed then nonparametric test (Mann-Whitney U test) was performed, whereas if groups were normally distributed unpaired T-test was performed. The heatmap analysis was statistically compared with Fisher's Exact test. Statistical supervision and guidance were performed by Dr. Katty Castillo and Birgit Waschulzik, Institute of Medical Informatics, Statistics and Epidemiology, Technical University of Munich (TUM).

7 RESULTS

The main results are published in my 2022 Cells paper "Vascular Remodeling Is a Crucial Event in the Early Phase of Hepatocarcinogenesis in Rodent Models for Liver Tumorigenesis" Cells 2022, 11(14), 2129 [255].

7.1 COHORT

A total of 262 FCAs and 36 HCCs were identified by histological classification Manual annotation for further computational analysis of H&E staining was performed (Figure 6 A–D) and immunohistochemistry staining of CD31 (Figure 6 E-F) and Collagen IV (Figure 6 G-H). Median FCA lesion in the cohort was 4.83 mm (ranging from 0.07–9.603 mm) and distributed multifocally up to 70 lesions per slide. The median HCC lesion size was 9.85 mm (range: 0.523–19.18 mm) and distributed mostly as one lesion per slide. Based on H&E morphology, FCA showed a homogenous vascular pattern with a predominant appearance of narrow vessels. The HCC sample, however, especially larger specimens, presented with a more inhomogeneous pattern including areas of narrow but also dilated and angled vessels surrounding tumor cell clusters. Necrosis was not observable within the smaller tumor nodules (FCA/HCC) but detectable in the larger HCC nodules.

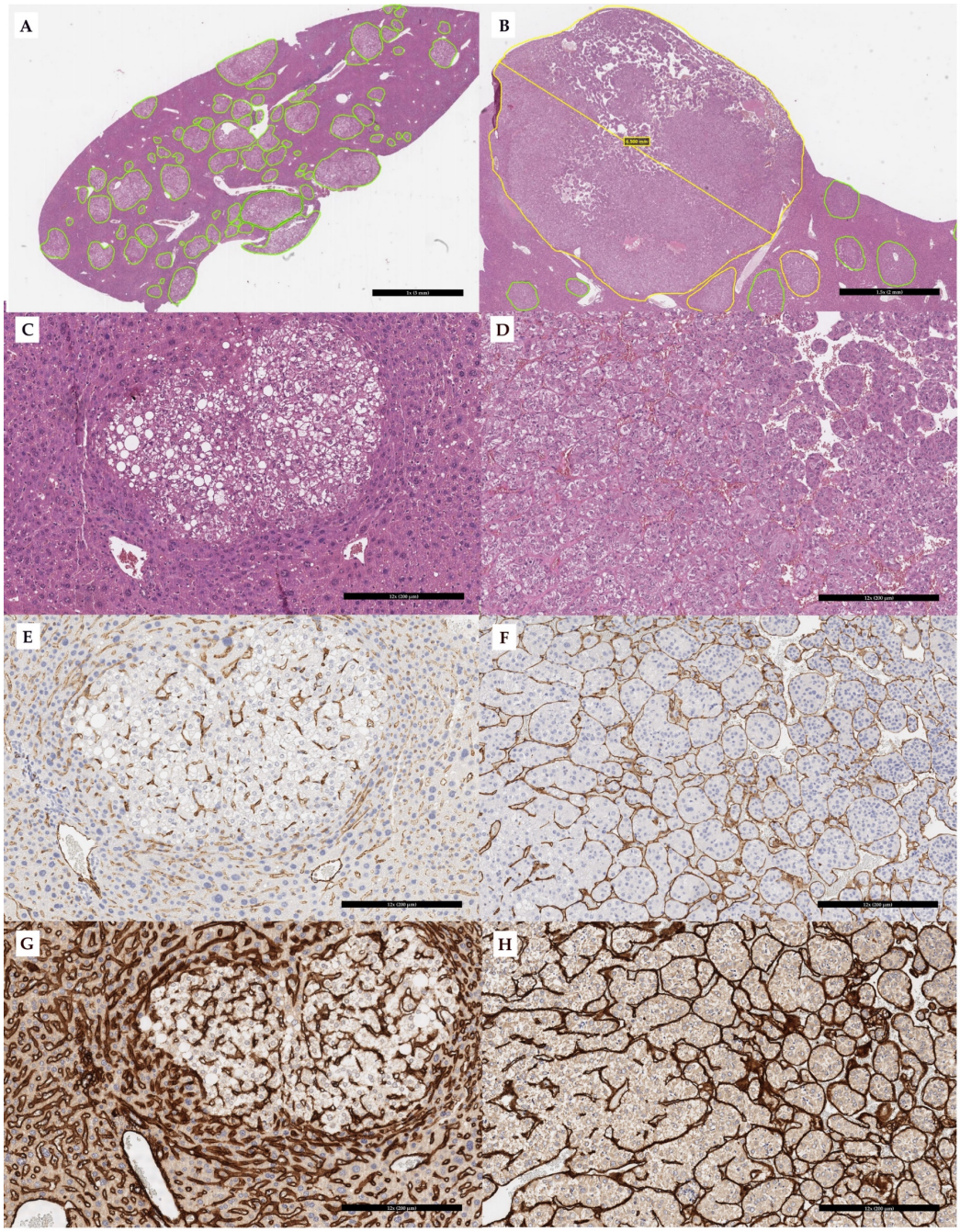

Figure 6. Annotation and immunostaining of foci of cellular alteration (FCA) and hepatocellular carcinoma (HCC).

FCA annotated with green color in H&E (A); HCC annotated with yellow color in H&E (B); representative image of FCA (C) (H&E) and HCC (D) (H&E); CD31 immunostaining in FCA (E) and HCC (F). Collagen IV immunostaining in FCA (G) and HCC (H). Scale bar (A, B): 1mm (magnification 1×), 2 mm (magnification 1.5×). Scale bar (C–F): 200 μm (magnification 12×).

7.2 MICROVESSEL DENSITY ANALYSIS & EXPRESSION OF CD31, COLLAGEN IV

In the subsequent computational analysis, the total number of vessels, assessed by CD31 and Collagen IV, was significantly higher in FCAs than in HCCs (Figure 7 A, B). Analysis of staining intensities showed opposite results, where HCC presented with a stronger CD31 staining intensity but not Collagen IV (Figure 7 C, D). The total area of CD31 stained vessels were observed to be higher in the HCC than in the FCA (Figure 7 E, p value = 0.2344). Nevertheless, no differences were observed in total area covered by intralesional vessels (Figure 7 E, F).

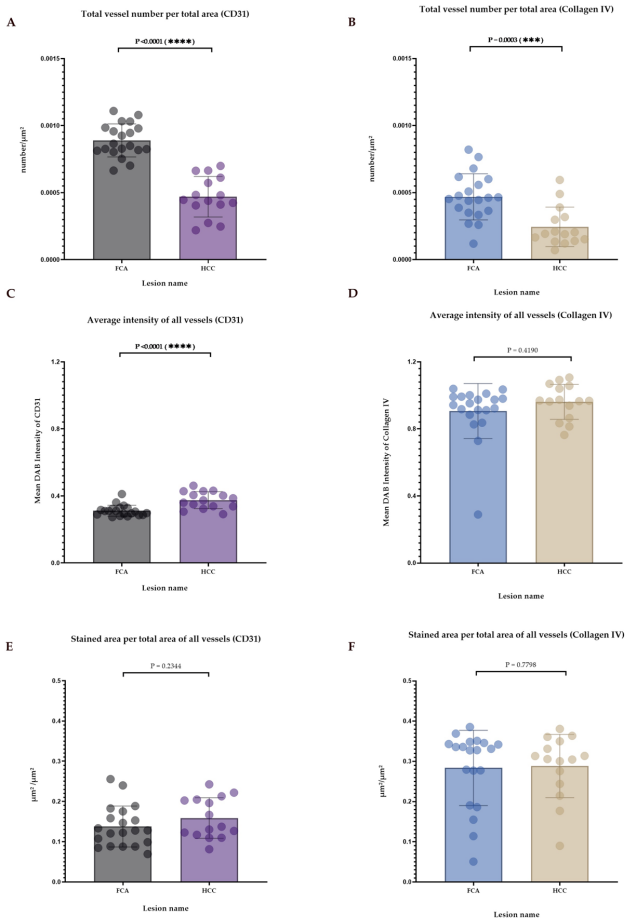

Figure 7. Detailed vessel analysis by CD31 and Collagen IV in FCA and HCC.
Total number of vessels in FCA versus HCC by CD31 (A) and Collagen IV (B); average staining intensity of vessels by CD31 (C) and Collagen IV (D). No differences were observed in total vessel area: CD31 (E) and Collagen IV (F). Error bars show the mean and standard deviation for each lesion. p-values: Not statistically significant p value > 0.05; for statistical significance, accepted *** = p value ≤ 0.001, ≤ and **** = p value ≤ 0.0001.

For a more detailed analysis of the vessels according to their size (small, medium, large), a computer-assisted subgrouping of the vessels was performed on CD31 and Collagen IV stained vessels (Figure 8 A-H).

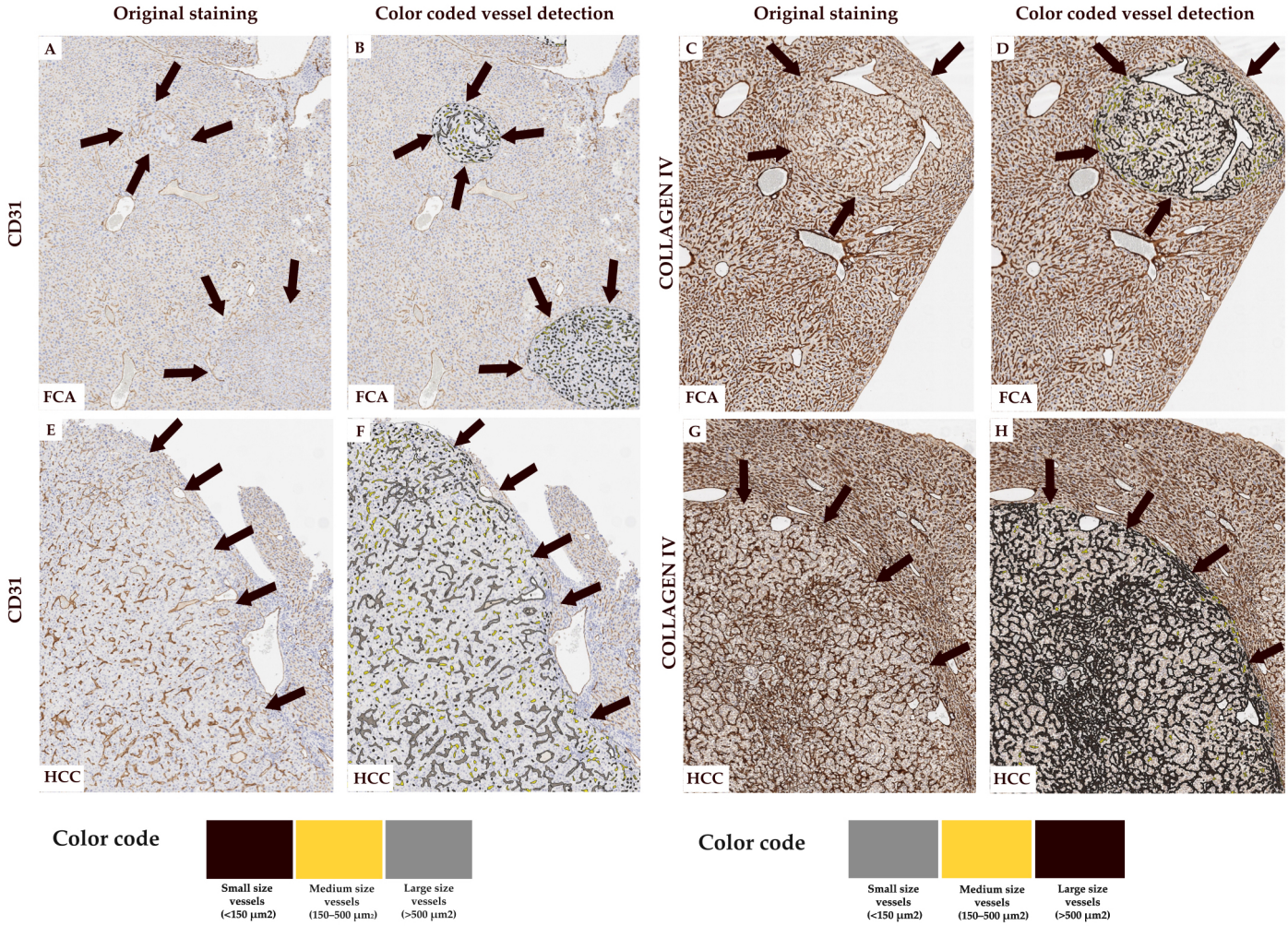

Figure 8. Computer-assisted subgrouping of vessels.
CD31-based vessel subgrouping (A-B, E-F) for FCA (A) and CD31 (B) subgroups and HCC (E) and CD31 (F) subgroups. Collagen IV-based vessel subgrouping (C–D, G-H) for FCA (C) and Collagen IV (D) subgroups and HCC (G) and Collagen IV (H) subgroups. Arrows mark the lesion in (A–H). Magnification 5×. Color coding of subgroups:
(A-B, E-F) Black-colored areas highlight small-sized vessels (<150 µm²), yellow-colored areas highlight medium-sized vessels (150–500 µm²), and grey-colored areas highlight large-sized vessels (>500 µm²).
(C–D, G-H) Grey-colored areas highlight small-sized vessels (<150 µm²), yellow-colored areas highlight medium-sized vessels (150–500 µm²), and black-colored areas highlight large-sized vessels (>500 µm²).

Following the subgrouping, the comparison within subgroups were done on CD31 and Collagen IV: vessel numbers, in all three vessel subgroups FCA lesions have a higher number of vessels both in CD31 and Collagen IV stains (Figure 9 A-B, D-F), except in the number of CD31 stained large vessels showed to be have almost same number in FCA and HCC (Figure 9 C, p value = 0.3997). Regarding the comparison of the vessel area in small and medium size vessels in both CD31 and Collagen IV showed a significant amount of areas covered with FCA (Figure 9 G-H, J-K). On the contrary, the large vessels in CD31 (Figure 9 I) and Collagen IV have bigger areas covered with HCC (Figure 9 L, p value = 0.2877).

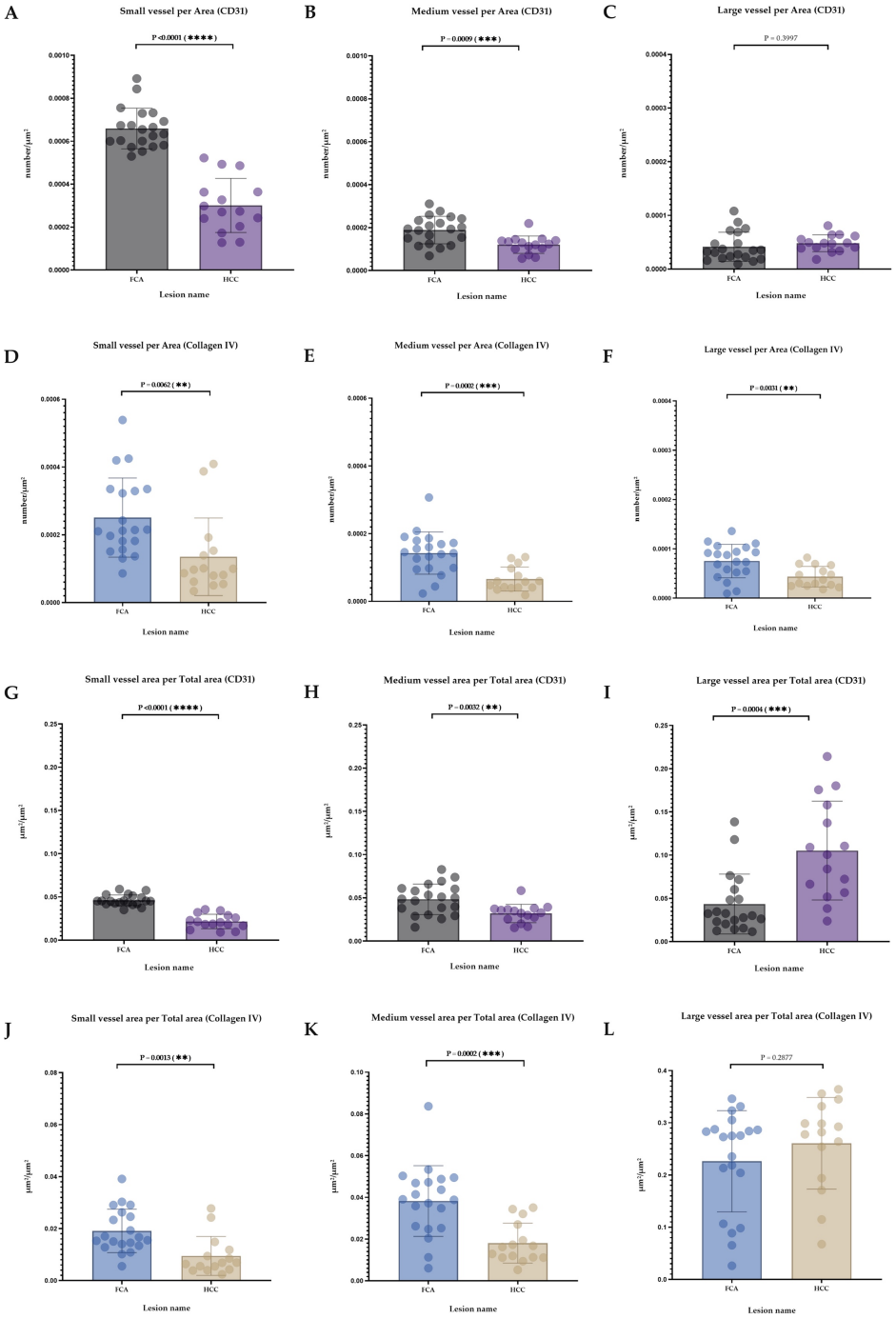

Figure 9. Analysis of vessel area and vessel number per lesion.
Evaluation of subgrouped vessels per area in CD31 (A–C) and Collagen IV staining (D-F). Subgrouped vessels per total area in CD31 (G–I) and Collagen IV staining (J-L). Error bars show the mean and standard deviation for each lesion. *p*-values: not statistically significant p value > 0.05; for statistical significance, accepted p value ≤ 0.05., **=p value ≤ 0.01, *** = p value ≤ 0.001, and **** = p value ≤ 0.0001.

The last part of analysis was the evaluation of average staining intensity, where HCC have a stronger intensity in CD31 small, medium and large vessels (Figure 10 A-C), whereas the intensity of Collagen IV had no significant difference (Figure 10 D-F).

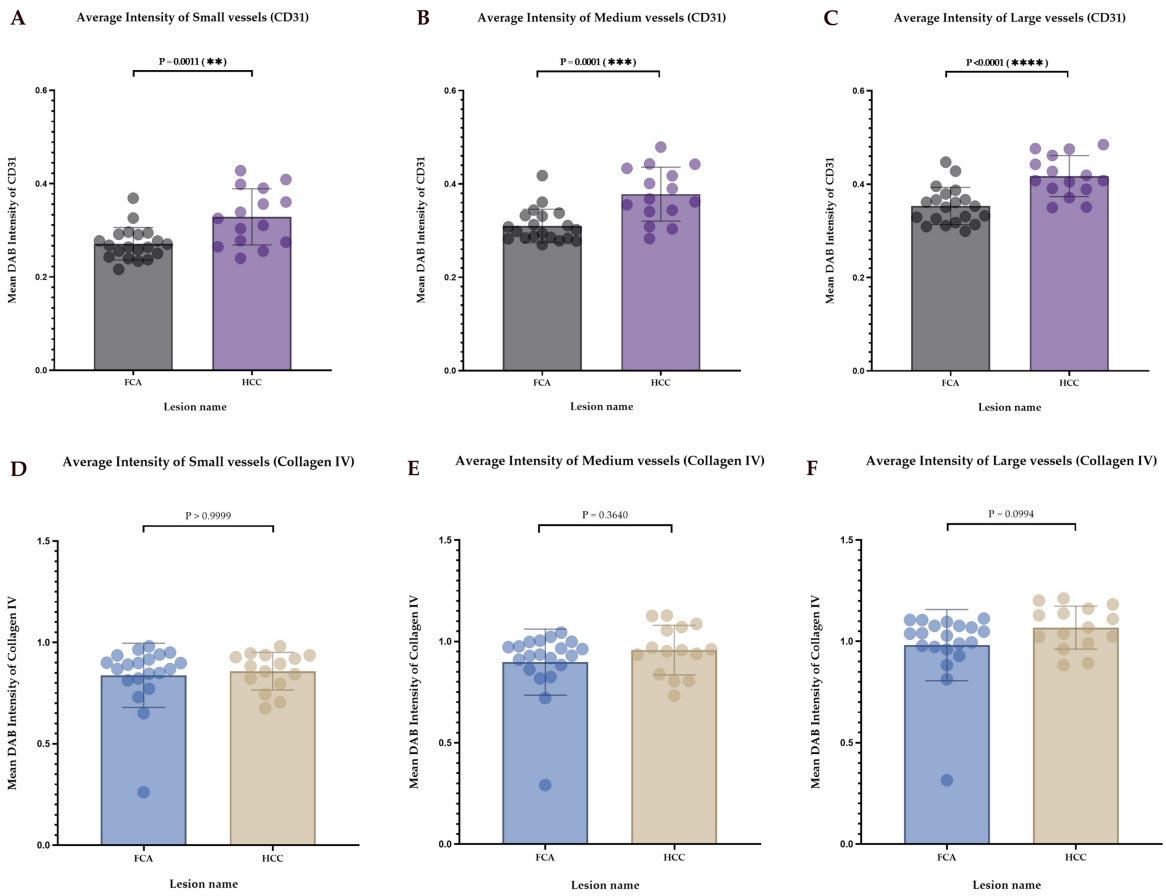

Figure 10. Analysis of staining intensity per lesion of CD31- and Collagen IV-stained vessels (A–F).
Error bars indicate the mean and standard deviation for each lesion. p-values: not statistically significant p value > 0.05; for statistical significance, accepted p value ≤ 0.05. ** = p value ≤ 0.01, *** = p value ≤ 0.001, and ****= p value ≤ 0.0001.

7.3 HEATMAP ANALYSIS OF CD31 AND COLLAGEN IV

The heatmap evaluation was based on the hotspot density of CD31 and Collagen IV stained vessels, showing the distribution as the green areas defined as having the least density, the yellow color show medium density and the red areas show the highest in density.

In the CD31 stained vessels, small and medium- size vessels are predominantly located in the central part of the FCA lesions (Figure 11 B-E). On the contrary, in the HCC lesion these vessels located in the periphery of the lesion (Figure 11 F-G). Heatmap analysis of Collagen IV stained vessels, only small-size vessels tend to be located in the center of the FCA lesion, whereas in the HCC those vessels were mostly located in the periphery of the lesion (Figure 11 I-J). In the correlation test of medium and large- size vessels no correlation of vessels and location in the lesions was observable (Figure 11 K-N, p value > 0.05). The original immunohistochemically stained pictures with the annotations are Figure 11 A, 11 H.

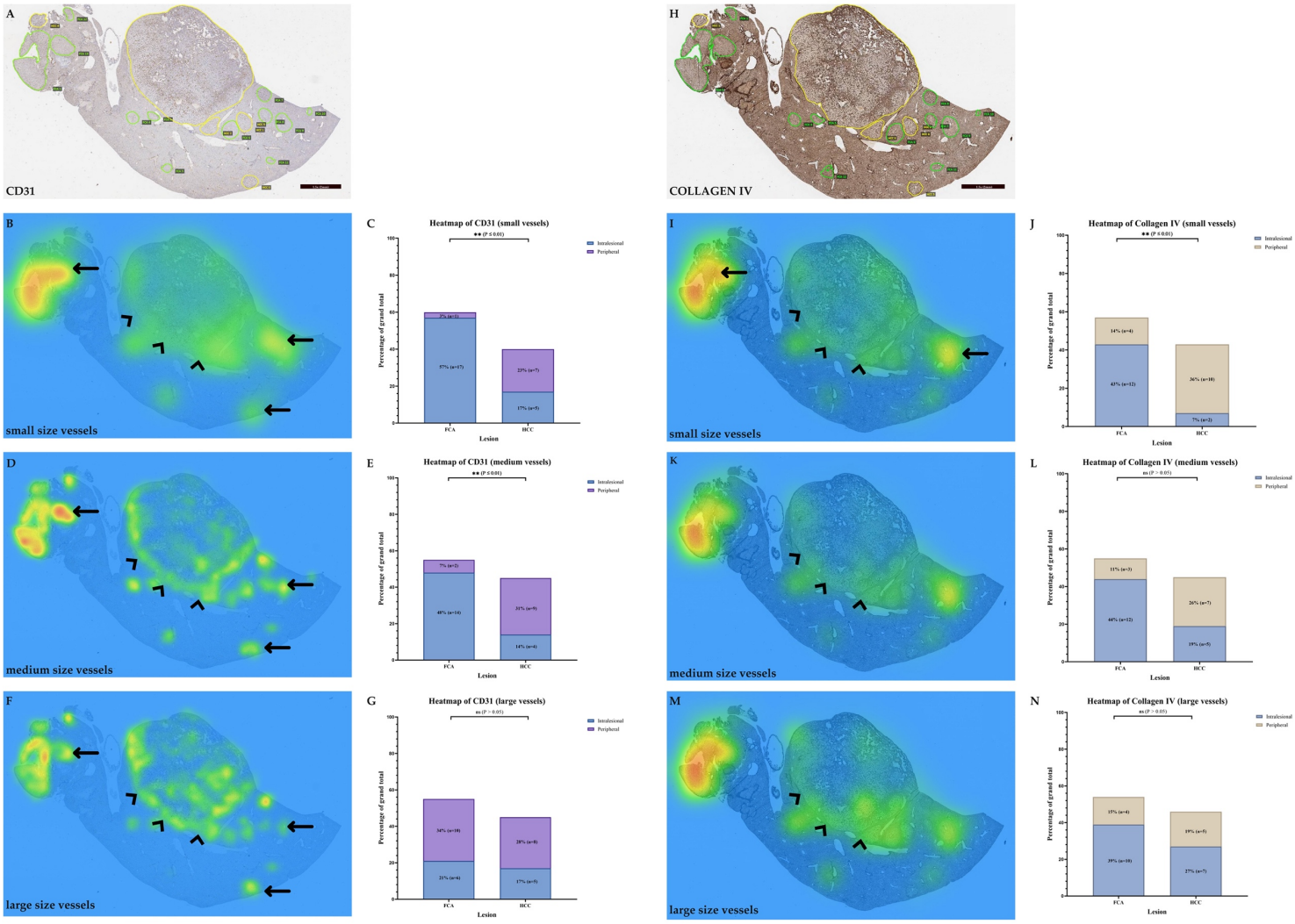

Figure 11. Heatmap of vessel distribution according to size. (Modified from Tulessin et al., Cells 2022, [255]). Annotated FCA (encircled green) and HCC (encircled yellow) in CD31 staining. (A) Distribution of the vessel according to their size in small- sized vessels (B, C), medium-sized vessels (D, E) and large-sized vessels (F, G) show a predominant location of small- and medium-sized vessels in the center (intralesional) of FCA, whereas the small- and medium-sized vessels in HCC mostly located at the periphery of HCC (arrowheads). In Collagen IV (H) small vessels located in the center (intralesional) of FCA but at the periphery of HCC, with shift towards the periphery in medium- and large-sized vessels (I–N). Color coding of heatmap: Green color indicates lowest density; yellow color indicates medium density and red color indicates highest density. Scale bar (A, B): 2 mm (magnification 1.5×). *p*-values: not statistically significant p value > 0.05; for statistical significance, accepted p value ≤ 0.05. **= p value ≤ 0.01, N = number of hotspots identified in each slide and lesion for further in-depth analysis.

7.4 α-SMA AND DESMIN

The general expression of α-SMA (Fig. 12 A-B) and desmin (Figure 12 E-F) was weak in both FCA and HCC lesions, therefore our approach was to count the pixels and evaluate the intensity. In the analysis of α-SMA staining, the number of pixels were prominently higher in HCC as compared to FCA (Figure 12 C, *p* value = 0.0360), but in desmin pixel count we have observed that FCAs have a higher number of pixels, however did not show significant difference between those two lesions (Figure 12 G). The intensity of α-SMA staining both lesions had almost same intensity (Figure 12 D, *p* value = 0.3220) and desmin staining FCA presented with a stronger intensity as compared to HCC (Figure 12 H, *p* value = 0.1326).

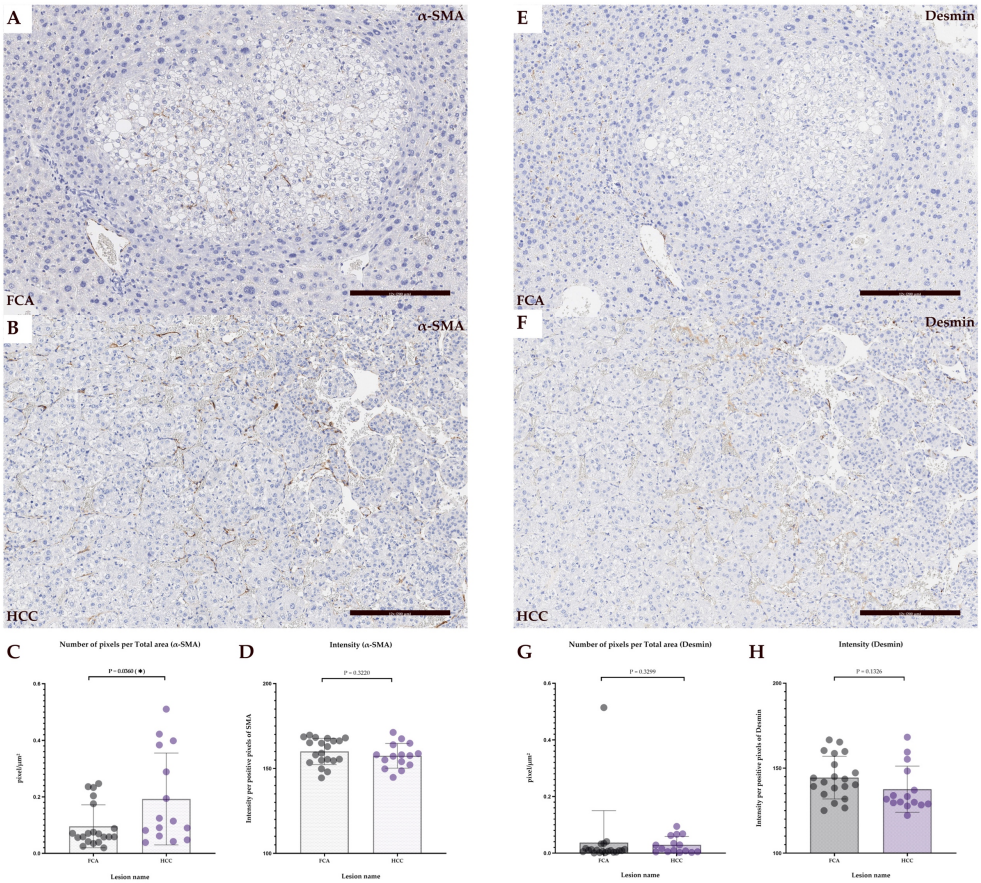

Figure 12. Analysis of vessels per lesion for expression of smooth muscle actin (α-SMA) and desmin.
(A-B) Immunostaining of α-SMA in FCA and HCC, (C) number of α-SMA positive pixel/αtotal area and (D) intensity of α-SMA/positive pixel. (E-F) Immunostaining of desmin in FCA and HCC, (G) number of desmin positive pixel/αtotal area and (H) intensity of desmin/positive pixel. Error bars indicate mean and standard deviation for each lesion. For statistical significance, accepted *p* value: *= *p* value ≤ 0.05. Scale bars: A, B, E, F: 200 μm (12× magnification).

7.5 IMMUNOHISTOCHEMICAL VEGF164 AND VEGF-A mRNA ANALYSIS

The VEGF164 staining was performed before VEGF-A mRNA analysis, it was found to be strongly cytoplasmic-stained in homogenous manner (Figure 13 A-B).

Here in our results, the expression of the VEGF-A mRNA was analyzed with the QuPath program (Figure 13 C, D). Firstly, we detected and counted spots and clusters per cell in FCAs and HCCs separately, clusters were considered as more than 1 spot. In the VEGF-A expression analysis of combined spots and clusters per cell together were observed to be higher in the HCC, than HCC (Figure 13 E, p value = 0.4376). After comparing clusters and spot per cell separately, in both FCA and HCC no statistical significance was found (Figure 13 F-G).

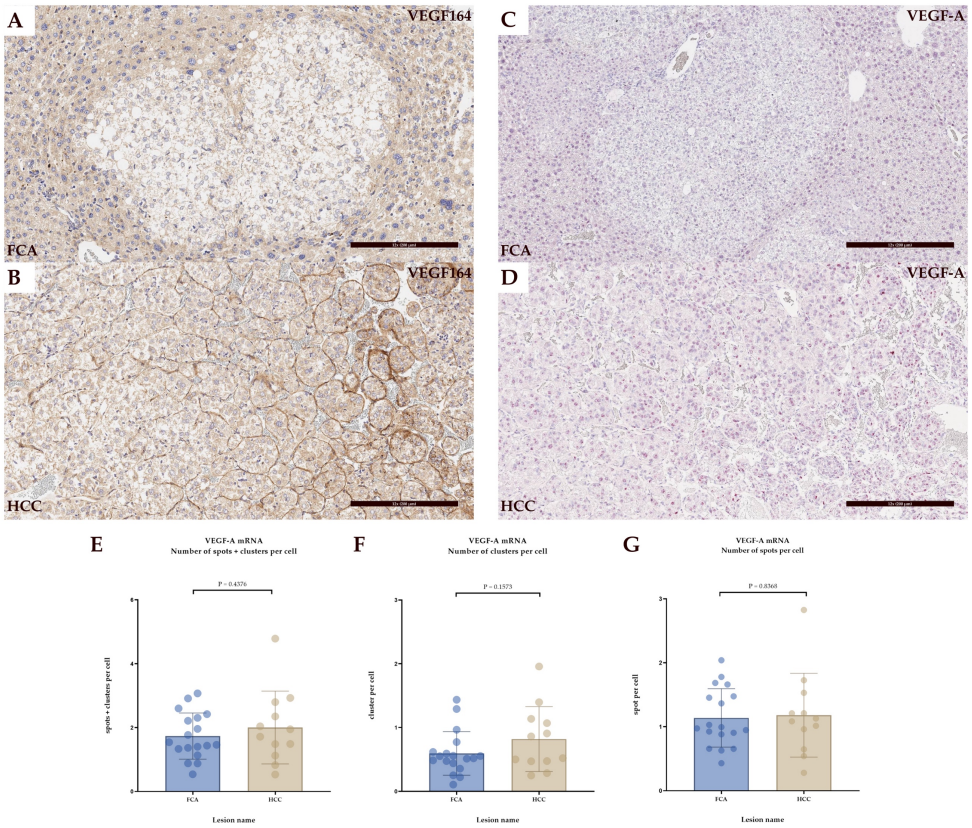

Figure 13. Analysis of vessels per lesion for expression of VEGF164 and VEGF mRNA.
(A-B) Immunostaining of VEGF164 in FCA and HCC, (C-D) mRNA in situ hybridization of VEGF-A in FCA and HCC, (E) Number of VEGF positive spots and clusters per cell, (F) Number of VEGF positive clusters per cell (G) Number of VEGF positive spots per cell. Error bars indicate mean and standard deviation for each lesion. For statistical significance, accepted p value: * = p value ≤ 0.05. Scale bars: A- D: 200µm (12× magnification).

7.6 LYVE1 (LYMPHO-VASCULAR MARKER) & KI-67 (PROLIFERATION MARKER)

In the LYVE1 analysis, the expression of the staining was found to be in diffuse manner, predominantly expressed in the healthy liver tissue as compared to liver lesions. Moreover, the expression was found to be more prominent in the sinusoids and in the periphery of bigger FCAs and HCC, but not in small FCAs. Nevertheless, statistically no differences in the overall expression levels were observed (Figure 14 A, C, E; *p* value = 0.9484).

In the Ki-67 analysis, which is a nuclear proliferation marker (Figure 14 B, D) the average percentage of Ki-67 expression did not show significant differences between FCA and HCC (Figure 14 F, *p* value = 0.0903).

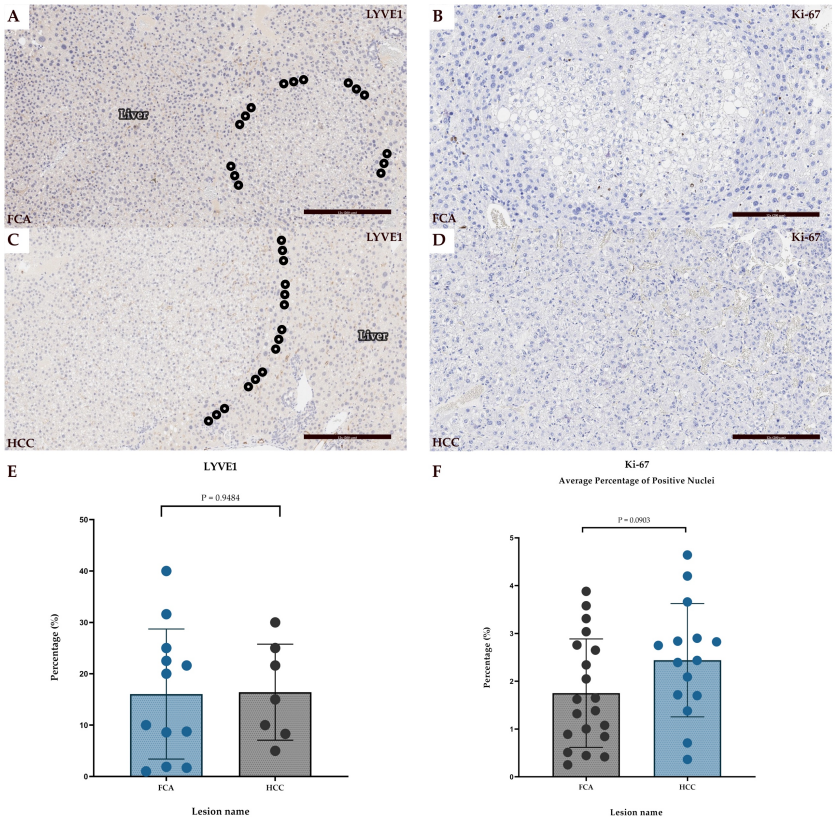

Figure 14. Analysis of vessels per lesion for expression of LYVE1 and Ki-67.
Immunostainings of LYVE1 in FCA and HCC (A, C) showing a weak staining equal or less compared to sinusoidal expression of surrounding liver, dots indicate the lesion area. (E) Semi-quantitative analysis of percentage of LYVE1 positive vessels in FCA and HCC. (B, D) Immunostainings of Ki-67 in FCA and HCC, (F) average percentage of Ki-67 positive nuclei was counted. Error bars indicate mean and standard deviation for each lesion. *p*-values: Statistical significance accepted *p* value ≤ 0.05. *= *p* value ≤ 0.05. Scale bars: A-D: 200µm (12× magnification).

8 DISCUSSION

One of the main aims of this study was to comprehensively investigate vascular changes of pre-malignant and malignant liver lesion in the GEM models for HCC. At the first glance in this study, we have observed a higher amount of FCA lesions were present compared to the HCCs. These observations corroborate the findings of the previous work by Steiger et al, that KRAS models presented with more FCA lesions as compared to the HCC [178]. Currently, there are numerous mouse models that are available for the study of hepatocarcinogenesis [262, 263], which is a favored method for investigating the molecular and histological stages [182, 183]. Particular models of RAS-dependent tumorigenesis have been instrumental in demonstrating the evolution of mouse models of cancer as increasingly accurate representations of human disease [209], which is also considered a relatively frequent mutation found to be involved in the hepatocarcinogenesis [211]. Furthermore, KRAS mutation is found in the vast majority of cancers, and commonly studied in colorectal cancers [264, 265], breast and lung cancers [209]. Although, mouse models dependent on RAS have continued to be at the forefront of mouse modeling, there is still lack of information on KRAS mice models in liver studies, highlighting the need for further investigation in this area [209]. Additionally, the role of the tumor vasculature in either GEMMs or KRAS models is not frequently well addressed by many researchers [241].

One of the other main objectives of this study was to explore the vasculature in detail and assess whether the angiogenetic switch is present in hepatocarcinogenesis of mice, since the current knowledge on vessel sizes and morphological descriptions of vessels in HCC and FCA is limited in mouse models. In this study's vasculature investigation of FCAs, which are premalignant lesions and a counterpart of human dysplastic nodule (DN) [216, 224], FCAs presented with increasing number of vessels, especially small and medium size vessels covered with endothelial and basement membrane cells. In accordance with these results, previous human studies have also demonstrated that new sinusoidal endothelium increases gradually over the stages from LGDN, HGDN to HCC [266], pointing out the presence of sinusoidal capillarization and higher frequency of unpaired arteries [267]. Thus, in correlation with recent studies, my study provides similar and reassuring initial evidence that small and medium size vessels have more of a capillary-like formation in the preneoplastic state, with lesser number of larger vessels.

In the further detailed vessel analysis of the HCC lesions, in comparison to FCA, HCC predominantly presented with large sized vessels, however with lesser distribution of vascular basement membrane and endothelial cells. Hence, one reason for this observation might be that with the progression into HCC, the vessel sprouting begins and forming more of arterial-like vessels, since it is already known that with the tumor progression the requirement for nutrients and oxygen substantially increases [145, 159]. Additionally, vessel leakiness is speculated to contribute to the tumor progression [268], similarly was observed in my study, by the gradual decrease of endothelial and basement membrane cells, which might in result contribute to the onset of vessel leakiness. However, as only tissue sections were investigated in this study, functional analysis to support this hypothesis (such as lectin injection in live mice) was not possible. Interestingly, HCC lesions in our cohort, showed a clear expression of basement membranes in the large vessels representing a more mature phenotype of vasculature. However, in the scientific community, there are some discrepancies regarding the function of vascular basement membrane: some authors postulate that it gets degraded during angiogenesis in the tumor [228, 269, 270]. On the other hand, other authors have stated that it does not get degraded and plays an important role in the endothelial sprouting and neovascularization [271-273]. Findings of this study clearly support the recent ones, through a probable presence of joined work of endothelial cells with the vascular basement membrane on further vessel sprouting and its contribution to the vascular remodeling from FCA to HCC, thus facilitating angiogenesis with upregulating the expression of pro-angiogenic factors, as it was already discussed by other researchers [271, 274].

As the vasculature in tumor lesions differ significantly from normal vessels, tumor blood vessels are characterized by structural and functional abnormalities, which include tortuous and dilated vessels with varying diameters, excessive branching, and shunts [268, 275]. In accordance with these remarks, we have observed not only changes in vessel size and maturity but also in their distribution within the tumor nodules using the heatmap evaluation. The MVD findings were found to be strongly correlated with the vessel analysis, and indicating that small and medium size vessels are highly distributed in the central part of the FCA lesions. Whereas HCC lesions show a shift towards small and medium sized vessels in the outer region, supporting that vascular remodeling in the HCC plays a prominent role in the tumor's infiltrative growth and progression [151-153]. Additionally, my results further support the hypothesis that for further development of the HCC, vascular remodeling with continuous adaptation is required and it is a valuable process for tumor development and differentiation,

as it was previously reported that it is demanded during the transition from developed HCC to more advanced stages [241].

However, one of the challenges in my work was the interpretation of our heatmap analysis and correlation with vessel distribution. Since there is very little information published in the literature on vessel size distribution and appropriate methods for evaluation. One study suggested evaluating the heatmap based on the marker density in the expressed cells [261]. According to the above paper of Böhm et al., we decided for a similar approach and analyzed hotspot areas, with the highest density of expressed vessels. Previous vascular studies have commonly evaluated the hotspot regions manually and calculated the average of positively stained blood vessels in those hotspot areas [266, 276]. However, the detailed MVD analysis of the vasculature in this study has more technological advancement with the usage of computational analysis and software algorithms, providing more accurate and detailed vessel analysis. Moreover, those programs are already widely used in research studies along with routine diagnostics, one of the main advantages of computational analysis is the reduction of the interobserver variance, errors in the diagnosis and classification [277-283]. Nevertheless, it is important to note that the lack of detailed classification of proliferative liver lesions in mice compared to the WHO classification for human liver tumors is a significant limitation [284]. The International Harmonization of Nomenclature and Diagnostic Criteria (INHAND) criteria for murine liver tumors only provides a diagnosis of "HCC" without further sub-classification, as compared to human HCC sub-classifications [216]. Additionally, mouse models used in this study do not develop HCC on a cirrhotic background, which may limit their relevance for studying chronic liver diseases [178].

α-SMA and desmin are common markers that are used to visualize for mural cells, especially pericytes [285-287], which affect the endothelial permeability, proliferation and migration [287]. α-SMA expression in our cohort is in line with previous human studies where the number of pericytes increased with the progression to the HCC [224]. Surprisingly, desmin, another marker for pericytes, was very weakly expressed in both FCA and HCC lesions and did not show any difference. As compared to other studies, where desmin is strongly associated with pericytes recruitment and upregulated in the angiogenesis [241, 287], this was a surprising finding. One possible explanation of the observed low expression of desmin staining in my study could be either due to the difference in type of tumor tissue [287], or due to the antibody used in my study [241].

VEGF is one of the potential predictive biomarkers of the HCC [236, 237], and has a strong association with the advanced disease progression and poor prognosis [13, 152, 153, 159, 166, 240]. There are still some questions, whether the vascular remodeling is driven by hypoxia, activation of oxygen sensors, or an enhancement of VEGF alone [168, 288, 289]. Thus, in this study VEGF164 was first used, however due to its diffuse cytoplasmic staining which was homogeneous in pattern, it was difficult to evaluate by the computer, this finding which was previously seen in the study of Stroescu et al. [290]. Thus, a second technique for a better assessment of VEGF was applied, using RNAscope to detect not the expression on protein level but directly measuring the RNA content of VEGF. VEGF showed to be significantly higher in HCC patients and was proposed to be used as a prognostic marker [291]. In spite of that, in our analysis surprisingly and to some extent contradictory, VEGF-A mRNA did not show any differences between FCA and HCC. However, Hanahan et al. [292] and Lei et al. [163] stated that tumor vasculature is upregulated by VEGF which often in turn has a negative impact on pericytes and basement membrane cells, resulting in the reduction of both of them. As in our study, we observed high pericyte coverage of vessels and basement membrane cells in the HCC, one reason to explain these results in VEGF levels might be that, HCC lesions investigated in our cohort still might be in the early stages of differentiation, where it does not require a high amount of VEGF-A yet. Additionally, in previous human studies, VEGF-A was found to have a negative correlation with the tumor size, meaning that smaller tumors depend on new vessels' formation in order to grow, whereas later in the stage of large tumors it may require other growth factors [293-296]. Thus, published literature provides various insights on VEGF biology; nevertheless, it still remains unclear whether VEGF causes vascular remodeling during early HCC stages. Another explanation could be the absence of fibrosis background of KRAS mice models, since the VEGF expression was found to be higher in liver with fibrotic background which was investigated in human and experimental studies [294, 297, 298].

Regarding the Ki-67 analysis, which is commonly reported in studies as an independent prognostic indicator for patients with HCC [299]. Especially in the human studies Ki-67 was reported to be significant in advanced stages of HCC and associated with poor outcomes [300, 301]. Moreover, higher expression of Ki-67 also correlates with a poor histological differentiation with an increased microvascular invasion [302-304]. Thus, this is another interesting finding that stands out from results reported earlier, that no changes in nuclear proliferation rate of the HCC were observed in this study. One possible explanation here might be that, since we only investigated tissue slides we don´t know when these lesions have developed.

Lastly, LYVE1 is potentially considered to be an independent marker of HCC patient's outcome, since in the detailed Japanese human study [305], it was found to be downregulated with the tumor progression, from well to poorly differentiated HCC. However, LYVE1 analysis in my study didn't present with any differences in expression between FCA or HCC which again might be explainable by the number or degree of development of each lesion. Nonetheless, one finding in our cohort was that LYVE1 positive cells were found to be expressed more in the periphery of the HCC lesion in comparison to FCA. These findings are consistent with previous mice and human studies [306, 307], where they have observed that with tumor growth, LYVE1 expression tends to be located in periphery of the lesion.

This comprehensive computational analysis of FCA and HCC has demonstrated that the mouse models investigated in this study, mimic vascular remodeling in human hepatocarcinogenesis both morphologically and phenotypically. Therefore, these KRAS models can be utilized for investigating vascular therapeutic approaches [308], as well as for basic research questions concerning molecular pathways during the early stages of tumor development [309].

8.1 CONCLUSION AND FUTURE PERSPECTIVES

Hepatocellular carcinoma (HCC) is a leading cause of cancer-related deaths worldwide, due to its highly vascularized properties [1, 3]. Angiogenesis is a pivotal process in the progression of hepatocellular carcinoma (HCC) and its precursor lesions. This study demonstrated that mouse models for hepatocarcinogenesis could serve as proper model to address specific questions on vascular remodeling and the angiogenic switch in HCC.

Furthermore, our computer-assisted assessment of the vasculature could serve as a valuable tool for the accurate diagnosis of proliferative lesions in rodent liver tumor models. This approach may eventually assist in distinguishing between pre-cancerous and cancerous liver lesions and establishing vessel criteria for diagnosis. We hope that this area of research will pique the interest of more scientists to delve into the vascular differentiation of these lesions. However, further exploration of the molecular basis of angiogenesis and the identification of specific vascular genes in the FCA and HCC lesions is necessary to improve our understanding of hepatocarcinogenesis. Genetic alterations play a critical role in the progression of HCC and underline the importance of further investigations in this area [148, 225, 310, 311].

A simplified graphical summary could be found in Figure 15 [255].

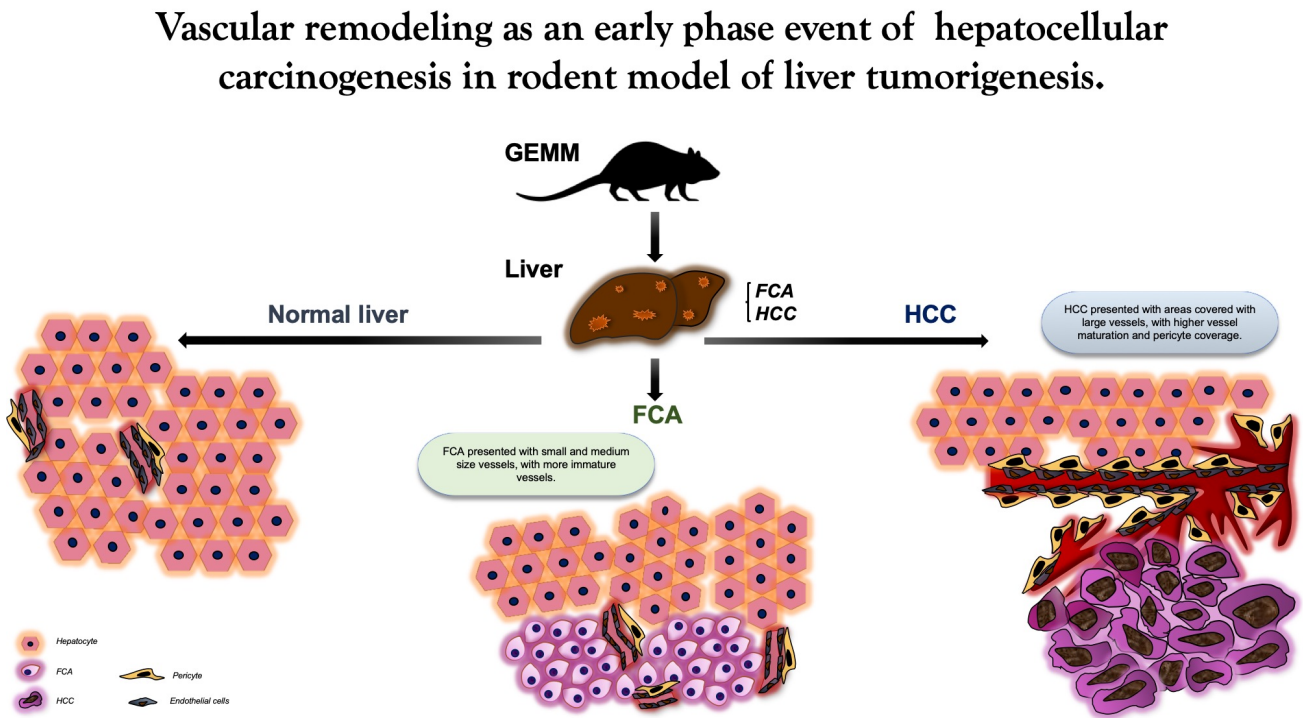

Figure 15. Simplified summary of results. (Unchanged figure taken from Tulessin et al. Vascular Remodeling Is a Crucial Event in the Early Phase of Hepatocarcinogenesis in Rodent Models for Liver Tumorigenesis. Cells, 2022 2022 Jul 6;11(14) [255]).

9 ACKNOWLEDGMENTS

This research project has been a long and challenging journey, spanning several years and multiple institutions. Coming originally from Kazakhstan, later on pursuing medical studies in Turkey, afterwards coming to Germany to gain research experience and medical experience. During this time, I have been fortunate enough to receive a great deal of support, guidance, and encouragement from many individuals and organizations, without which this research would not have been possible.

First and foremost, I would like to express my deepest gratitude to my supervisor, Prof. Dr. med. Carolin Mogler, for her unwavering support, guidance, and belief in me. I consider myself extremely lucky to have had the opportunity to work under her guidance, and I am deeply grateful for the valuable knowledge, experience, and expertise that she shared with me throughout this journey. Her encouragement and motivation were crucial to my success, and I cannot thank her enough.

I would also like to extend my sincere thanks to Dr. med. Ursula Ehmer, PhD; who provided me with excellent support from Internal medicine prospective. Her guidance and encouragement have been invaluable, and I am grateful for her insights and support during my research.

I am grateful to my family, especially my parents, they were supporting and believing in me throughout my medical studies. In addition, I would like to thank my friends, and professors from my medical school, for their unwavering support and encouragement throughout this journey. Their constant encouragement, love, and support have helped me stay focused and motivated even during the most challenging times.

Special thanks go to Dr. Katty Castillo and Birgit Waschulzik from the Institute of Medical Informatics, Statistics, and Epidemiology, Technical University of Munich (TUM), for providing me with invaluable statistical guidance. Their expertise and knowledge have been instrumental in the successful completion of this research. I would also like to express my gratitude to the Department of Pathology, especially Prof. Dr. Weichert for allowing me to do my research and Comparative Experimental Pathology technicians, especially Maximillian Guenzl and Annett Hering, for their technical support and assistance throughout the project. Their help was invaluable in ensuring the success of the research.

Finally, I would like to thank the collaborative research consortium (CRC) 1366 for their financial support (MD stipendiary), which made this research possible.

In conclusion, I am grateful to all the individuals and organizations who have supported me throughout this research journey. Their guidance, encouragement, and support have been invaluable, and I could not have achieved this without them.

10 REFERENCES

1. Sung, H., Ferlay, J., Siegel, R.L., et al. *Global Cancer Statistics 2020: GLOBOCAN Estimates of Incidence and Mortality Worldwide for 36 Cancers in 185 Countries*. CA Cancer J Clin, 2021. **71**(3): p. 209-249 [DOI: 10.3322/caac.21660].
2. Ferlay, J., Colombet, M., Soerjomataram, I., et al., *Cancer statistics for the year 2020: An overview.* Int J Cancer, 2021. **149**(4): p. 778-789 [DOI: 10.1002/ijc.33588].
3. Siegel, R.L., Miller, K.D. and Jemal, A., *Cancer statistics, 2020.* CA Cancer J Clin, 2020. **70**(1): p. 7-30 [DOI: 10.3322/caac.21590].
4. Ferlay, J., Colombet, M., Soerjomataram, I., et al., *Estimating the global cancer incidence and mortality in 2018: GLOBOCAN sources and methods.* Int J Cancer, 2019. **144**(8): p. 1941-1953 [DOI: 10.1002/ijc.31937].
5. Salleng, K.J., Revetta, F.L., Deane, N.G., et al., *The Applicability of a Human Immunohistochemical Panel to Mouse Models of Hepatocellular Neoplasia.* Comp Med, 2015. **65**(5): p. 398-408 [PMCID: PMC4617330].
6. Caldwell, S. and Park, S.H., *The epidemiology of hepatocellular cancer: from the perspectives of public health problem to tumor biology.* J Gastroenterol, 2009. **44** (Suppl 19): p. 96-101 [DOI: 10.1007/s00535-008-2258-6].
7. Llovet, J.M., Kelley, R.K., Villanueva, A., et al., *Hepatocellular carcinoma.* Nat Rev Dis Primers, 2021. **7**(1) [DOI: 10.1038/s41572-020-00240-3].
8. Global Cancer Observatory. *Cancer Tomorrow*. Estimated number of new cases from 2020 to 2040, Both sexes, age [0-85+] 2020; International Agency for Research on Cancer 2023. [Available from: https://gco.iarc.fr/tomorrow/en/dataviz/bars?mode=cancer&group_populations=1&multiple_cancers=1&cancers=11_39].
9. Global Cancer Observatory, *Estimated number of incident cases and deaths liver, both sexes, all ages in (Incidence and Mortality)* 2020. [png]. International Agency for Research on Cancer 2023 (Cancer Today). GLOBOCAN 2020. [Available from: https://gco.iarc.fr/today/online-analysis-multi-bars?v=2020&mode=population&mode_population=countries&population=900&populations=900&key=total&sex=0&cancer=11&type=0&statistic=5&prevalence=0&population_group=5&ages_group%5B%5D=0&ages_group%5B%5D=17&nb_items=10&group_cancer=1&include_nmsc=0&include_nmsc_other=1&type_multiple=%257B%2522inc%2522%253Atrue%252C%2522mort%2522%253Atrue%252C%2522prev%2522%253Afalse%257D&orientation=horizontal&type_sort=0&type_nb_items=%257B%2522top%2522%253Atrue%252C%2522bottom%2522%253Afalse%257D&population_group_list=8,40,112,56,70,100,191,196,203,208,233,246,250,276,300,348,352,372,380,428,440,442,470,499,807,578,616,620,498,642,643,688,703,705,724,752,756,528,804,826&population_group_globocan_id=908].
10. Rahib, L., Smith, B.D., Aizenberg, R., et al., *Projecting cancer incidence and deaths to 2030: the unexpected burden of thyroid, liver, and pancreas cancers in the United States.* Cancer Res, 2014. **74**(11): p. 2913-2921 [DOI: 10.1158/0008-5472.Can-14-0155].

11. Samant, H., Amiri, H.S. and Zibari, G.B., *Addressing the worldwide hepatocellular carcinoma: epidemiology, prevention and management.* J Gastrointest Oncol, 2021. **12**(Suppl 2): p. S361-S373 [DOI: 10.21037/jgo.2020.02.08].
12. Younossi, Z.M. and Henry, L., *Epidemiology of non-alcoholic fatty liver disease and hepatocellular carcinoma.* JHEP Rep, 2021. **3**(4) [DOI: 10.1016/j.jhepr.2021.100305].
13. Furuta, K., Guo, Q., Hirsova, P., et al., *Emerging Roles of Liver Sinusoidal Endothelial Cells in Nonalcoholic Steatohepatitis.* Biology (Basel), 2020. **9**(11) [DOI: 10.3390/biology9110395].
14. American Cancer Society. *Liver Cancer Risk Factors*. 2019, March 21; cancers.org. [Available from: https://www.cancer.org/cancer/liver-cancer/causes-risks-prevention/risk-factors.html].
15. Wong, S.W., Ting, Y.W. and Chan, W.K., *Epidemiology of non-alcoholic fatty liver disease-related hepatocellular carcinoma and its implications.* JGH Open, 2018. **2**(5): p. 235-241 [DOI: 10.1002/jgh3.12070].
16. LaBrecque, D.R., Abbas, Z., Anania, F., et al., *World Gastroenterology Organisation global guidelines: Nonalcoholic fatty liver disease and nonalcoholic steatohepatitis.* J Clin Gastroenterol, 2014. **48**(6): p. 467-473 [DOI: 10.1097/mcg.0000000000000116].
17. Sanyal, A.J., Yoon, S.K. and Lencioni, R., *The etiology of hepatocellular carcinoma and consequences for treatment.* Oncologist, 2010. **15** (Suppl 4): p. 14-22 [DOI: 10.1634/theoncologist.2010-S4-14].
18. Huang, D.Q., Singal, A.G., Kono, Y., et al., *Changing global epidemiology of liver cancer from 2010 to 2019: NASH is the fastest growing cause of liver cancer.* Cell Metab, 2022. **34**(7): p. 969-977.e962 [DOI: 10.1016/j.cmet.2022.05.003].
19. Park, J.W., Chen, M., Colombo, M., et al., *Global patterns of hepatocellular carcinoma management from diagnosis to death: the BRIDGE Study.* Liver Int, 2015. **35**(9): p. 2155-2166 [DOI: 10.1111/liv.12818].
20. Ringelhan, M., McKeating, J.A. and Protzer, U., *Viral hepatitis and liver cancer.* Philos Trans R Soc Lond B Biol Sci, 2017. **372**(1732) [DOI: 10.1098/rstb.2016.0274].
21. The European Union HCV Collaborators, *Hepatitis C virus prevalence and level of intervention required to achieve the WHO targets for elimination in the European Union by 2030: a modelling study.* Lancet Gastroenterol Hepatol, 2017. **2**(5): p. 325-336 [DOI: 10.1016/s2468-1253(17)30045-6].
22. Schweitzer, A., Horn, J., Mikolajczyk, R.T., et al., *Estimations of worldwide prevalence of chronic hepatitis B virus infection: a systematic review of data published between 1965 and 2013.* Lancet, 2015. **386**(10003): p. 1546-1555 [DOI: 10.1016/s0140-6736(15)61412-x].
23. Global Cancer Observatory, *Estimated number of new cases in 2020, World, both sexes, all ages*. 2020. [png]. International Agency for Research on Cancer 2023 (Cancer Today). GLOBOCAN 2020. [Available from: https://gco.iarc.fr/today/online-analysis-pie?v=2020&mode=cancer&mode_population=continents&population=900&populations=900&key=total&sex=0&cancer=39&type=0&statistic=5&prevalence=0&population_group=0&ages_group%5B%5D=0&ages_group%5B%5D=17&nb_items=7&group_cancer=1&include_nmsc=1&include_nmsc_other=1&half_pie=0&donut=0].
24. Global Cancer Observatory, *Estimated number of deaths in 2020, World, both sexes, all ages*. 2020. [png]. International Agency for Research on Cancer 2023 (Cancer Today). GLOBOCAN 2020. [Available from: https://gco.iarc.fr/today/online-analysis-pie?v=2020&mode=cancer&mode_population=continents&population=900&populations=900&key=total&sex=0&cancer=39&type=1&statistic=5&prevalence=0&population_group=0&ages_g

roup%5B%5D=0&ages_group%5B%5D=17&nb_items=7&group_cancer=1&include_nmsc=1&include_nmsc_other=1&half_pie=0&donut=0].
25. World Health Organization. *Global health sector strategy on viral hepatitis 2016-2021. Towards ending viral hepatitis*. 2016; World Health Organization. [Available from: https://apps.who.int/iris/handle/10665/246177].
26. World Health Organization. *Fact sheet (Hepatitis B)*. 2022, June 24; World Health Organization [Available from: https://www.who.int/news-room/fact-sheets/detail/hepatitis-b].
27. World Health Organization. *Fact sheet (Hepatitis C)*. 2022, June 24; World Health Organization [Available from: https://www.who.int/news-room/fact-sheets/detail/hepatitis-c].
28. Echeverría, N., Comas, V., Aldunate, F., et al., *In the era of rapid mRNA-based vaccines: Why is there no effective hepatitis C virus vaccine yet?* World J Hepatol, 2021. **13**(10): p. 1234-1268 [DOI: 10.4254/wjh.v13.i10.1234].
29. Duncan, J.D., Urbanowicz, R.A., Tarr, A.W., et al., *Hepatitis C Virus Vaccine: Challenges and Prospects.* Vaccines (Basel), 2020. **8**(1) [DOI: 10.3390/vaccines8010090].
30. Bailey, J.R., Barnes, E. and Cox, A.L., *Approaches, Progress, and Challenges to Hepatitis C Vaccine Development.* Gastroenterology, 2019. **156**(2): p. 418-430 [DOI: 10.1053/j.gastro.2018.08.060].
31. European Centre for Disease Prevention and Control. *Hepatitis C - Annual Epidemiological Report for 2019*. 2021; ECDC. [Available from: https://www.ecdc.europa.eu/sites/default/files/documents/AER-Hepatitis-C-2019.pdf].
32. Ninio, L., Nissani, A., Meirson, T., et al., *Hepatitis C Virus Enhances the Invasiveness of Hepatocellular Carcinoma via EGFR-Mediated Invadopodia Formation and Activation.* Cells, 2019. **8**(11) [DOI: 10.3390/cells8111395].
33. Khatun, M. and Ray, R.B., *Mechanisms Underlying Hepatitis C Virus-Associated Hepatic Fibrosis.* Cells, 2019. **8**(10): p. 1249 [DOI: 10.3390/cells8101249].
34. Sheena, B.S., Hiebert, L., Han, H., et al., *Global, regional, and national burden of hepatitis B, 1990-2019: a systematic analysis for the Global Burden of Disease Study 2019.* Lancet Gastroenterol Hepatol, 2022. **7**(9): p. 796-829 [DOI: 10.1016/S2468-1253(22)00124-8].
35. European Centre for Disease Prevention and Control. *Hepatitis B - Annual Epidemiological Report for 2019*. 2021; ECDC. [Available from: https://www.ecdc.europa.eu/en/publications-data/hepatitis-b-annual-epidemiological-report-2019].
36. Zamor, P.J., deLemos, A.S. and Russo, M.W., *Viral hepatitis and hepatocellular carcinoma: etiology and management.* J Gastrointest Oncol, 2017. **8**(2): p. 229-242 [DOI: 10.21037/jgo.2017.03.14].
37. Trépo, C., Chan, H.L. and Lok, A., *Hepatitis B virus infection.* Lancet, 2014. **384**(9959): p. 2053-2063 [DOI: 10.1016/s0140-6736(14)60220-8].
38. Iannacone, M. and Guidotti, L.G., *Immunobiology and pathogenesis of hepatitis B virus infection.* Nat Rev Immunol, 2022. **22**(1): p. 19-32 [DOI: 10.1038/s41577-021-00549-4].
39. Salpini, R., D'Anna, S., Benedetti, L., et al., *Hepatitis B virus DNA integration as a novel biomarker of hepatitis B virus-mediated pathogenetic properties and a barrier to the current strategies for hepatitis B virus cure.* Front Microbiol, 2022. **13** [DOI: 10.3389/fmicb.2022.972687].
40. Rizzo, G.E.M., Cabibbo, G. and Craxì, A., *Hepatitis B Virus-Associated Hepatocellular Carcinoma.* Viruses, 2022. **14**(5) [DOI: 10.3390/v14050986].
41. Jiang, Y., Han, Q., Zhao, H., et al., *The Mechanisms of HBV-Induced Hepatocellular Carcinoma.* J Hepatocell Carcinoma, 2021. **8**: p. 435-450 [DOI: 10.2147/jhc.S307962].

42. Levrero, M. and Zucman-Rossi, J., *Mechanisms of HBV-induced hepatocellular carcinoma.* J Hepatol, 2016. **64**(1 Suppl): p. S84-S101 [DOI: 10.1016/j.jhep.2016.02.021].
43. Ringelhan, M., O'Connor, T., Protzer, U., et al., *The direct and indirect roles of HBV in liver cancer: prospective markers for HCC screening and potential therapeutic targets.* J Pathol, 2015. **235**(2): p. 355-367 [DOI: 10.1002/path.4434].
44. Jiang, Z., Jhunjhunwala, S., Liu, J., et al., *The effects of hepatitis B virus integration into the genomes of hepatocellular carcinoma patients.* Genome Res, 2012. **22**(4): p. 593-601 [DOI: 10.1101/gr.133926.111].
45. Kawai-Kitahata, F., Asahina, Y., Tanaka, S., et al., *Comprehensive analyses of mutations and hepatitis B virus integration in hepatocellular carcinoma with clinicopathological features.* J Gastroenterol, 2016. **51**(5): p. 473-486 [DOI: 10.1007/s00535-015-1126-4].
46. Sung, W.K., Zheng, H., Li, S., et al. *Genome-wide survey of recurrent HBV integration in hepatocellular carcinoma.* Nat Genet, 2012. **44**(7): p. 765-769 [DOI: 10.1038/ng.2295].
47. Jiang, S., Yang, Z., Li, W., et al., *Re-evaluation of the carcinogenic significance of hepatitis B virus integration in hepatocarcinogenesis.* PLoS One, 2012. **7**(9) [DOI: 10.1371/journal.pone.0040363].
48. Murakami, Y., Saigo, K., Takashima, H., et al., *Large scaled analysis of hepatitis B virus (HBV) DNA integration in HBV related hepatocellular carcinomas.* Gut, 2005. **54**(8): p. 1162-1168 [DOI: 10.1136/gut.2004.054452].
49. Shi, Y., Wu, Y.H., Wu, W., et al., *Association between occult hepatitis B infection and the risk of hepatocellular carcinoma: a meta-analysis.* Liver Int, 2012. **32**(2): p. 231-240 [DOI: 10.1111/j.1478-3231.2011.02481.x].
50. Ohkubo, K., Kato, Y., Ichikawa, T., et al., *Viral load is a significant prognostic factor for hepatitis B virus-associated hepatocellular carcinoma.* Cancer, 2002. **94**(10): p. 2663-2668 [DOI: 10.1002/cncr.10557].
51. Chan, H.L., Hui, A.Y., Wong, M.L., et al., *Genotype C hepatitis B virus infection is associated with an increased risk of hepatocellular carcinoma.* Gut, 2004. **53**(10): p. 1494-1498 [DOI: 10.1136/gut.2003.033324].
52. Orito, E., Ichida, T., Sakugawa, H., et al., *Geographic distribution of hepatitis B virus (HBV) genotype in patients with chronic HBV infection in Japan.* Hepatology, 2001. **34**(3): p. 590-594 [DOI: 10.1053/jhep.2001.27221].
53. Elizalde, M.M., Mojsiejczuk, L., Speroni, M., et al., *Molecular and biological characterization of hepatitis B virus subgenotype F1b clusters: Unraveling its role in hepatocarcinogenesis.* Front Microbiol, 2022. **13** [DOI: 10.3389/fmicb.2022.946703].
54. Liu, Z., Zhang, Y., Xu, M., et al., *Distribution of hepatitis B virus genotypes and subgenotypes: A meta-analysis.* Medicine (Baltimore), 2021. **100**(50) [DOI: 10.1097/md.0000000000027941].
55. McMahon, B.J., *The influence of hepatitis B virus genotype and subgenotype on the natural history of chronic hepatitis B.* Hepatol Int, 2009. **3**(2): p. 334-342 [DOI: 10.1007/s12072-008-9112-z].
56. Shen, C., Jiang, X., Li, M., et al., *Hepatitis Virus and Hepatocellular Carcinoma: Recent Advances.* Cancers (Basel), 2023. **15**(2) [DOI: 10.3390/cancers15020533].
57. Stella, L., Santopaolo, F., Gasbarrini, A., et al., *Viral hepatitis and hepatocellular carcinoma: From molecular pathways to the role of clinical surveillance and antiviral treatment.* World J Gastroenterol, 2022. **28**(21): p. 2251-2281 [DOI: 10.3748/wjg.v28.i21.2251].

58. Sausen, D.G., Shechter, O., Bietsch, W., et al., *Hepatitis B and Hepatitis D Viruses: A Comprehensive Update with an Immunological Focus.* Int J Mol Sci, 2022. **23**(24) [DOI: 10.3390/ijms232415973].
59. Ferrante, N.D. and Lo Re, V., 3rd, *Epidemiology, Natural History, and Treatment of Hepatitis Delta Virus Infection in HIV/Hepatitis B Virus Coinfection.* Curr HIV/AIDS Rep, 2020. **17**(4): p. 405-414 [DOI: 10.1007/s11904-020-00508-z].
60. Puigvehí, M., Moctezuma-Velázquez, C., Villanueva, A., et al., *The oncogenic role of hepatitis delta virus in hepatocellular carcinoma.* JHEP Rep, 2019. **1**(2): p. 120-130 [DOI: 10.1016/j.jhepr.2019.05.001].
61. Miao, Z., Zhang, S., Ou, X., et al., *Estimating the Global Prevalence, Disease Progression, and Clinical Outcome of Hepatitis Delta Virus Infection.* J Infect Dis, 2020. **221**(10): p. 1677-1687 [DOI: 10.1093/infdis/jiz633].
62. Zhang, Z. and Urban, S., *Interplay between Hepatitis D Virus and the Interferon Response.* Viruses, 2020. **12**(11) [DOI: 10.3390/v12111334].
63. Roulot, D., Brichler, S., Layese, R., et al., *Origin, HDV genotype and persistent viremia determine outcome and treatment response in patients with chronic hepatitis delta.* J Hepatol, 2020. **73**(5): p. 1046-1062 [DOI: 10.1016/j.jhep.2020.06.038].
64. Axley, P., Ahmed, Z., Ravi, S., et al., *Hepatitis C Virus and Hepatocellular Carcinoma: A Narrative Review.* J Clin Transl Hepatol, 2018. **6**(1): p. 79-84 [DOI: 10.14218/jcth.2017.00067].
65. Lin, M.V., King, L.Y. and Chung, R.T., *Hepatitis C virus-associated cancer.* Annu Rev Pathol, 2015. **10**: p. 345-370 [DOI: 10.1146/annurev-pathol-012414-040323].
66. Mahmoudvand, S., Shokri, S., Taherkhani, R., et al., *Hepatitis C virus core protein modulates several signaling pathways involved in hepatocellular carcinoma.* World J Gastroenterol, 2019. **25**(1): p. 42-58 [DOI: 10.3748/wjg.v25.i1.42].
67. Vescovo, T., Refolo, G., Vitagliano, G., et al., *Molecular mechanisms of hepatitis C virus–induced hepatocellular carcinoma.* Clinical Microbiology and Infection, 2016. **22**(10): p. 853-861 [DOI: https://doi.org/10.1016/j.cmi.2016.07.019].
68. Lemon, S.M. and McGivern, D.R., *Is hepatitis C virus carcinogenic?* Gastroenterology, 2012. **142**(6): p. 1274-1278 [DOI: 10.1053/j.gastro.2012.01.045].
69. Zhu, Z., Wilson, A.T., Gopalakrishna, K., et al. *Hepatitis C virus core protein enhances Telomerase activity in Huh7 cells.* J Med Virol, 2010. **82**(2): p. 239-248 [DOI: 10.1002/jmv.21644].
70. Alisi, A., Giambartolomei, S., Cupelli, F., et al., *Physical and functional interaction between HCV core protein and the different p73 isoforms.* Oncogene, 2003. **22**(17): p. 2573-2580 [DOI: 10.1038/sj.onc.1206333].
71. Schulze-Krebs, A., Preimel, D., Popov, Y., et al., *Hepatitis C virus-replicating hepatocytes induce fibrogenic activation of hepatic stellate cells.* Gastroenterology, 2005. **129**(1): p. 246-258 [DOI: 10.1053/j.gastro.2005.03.089].
72. Mavilia, M.G. and Wu, G.Y., *HBV-HCV Coinfection: Viral Interactions, Management, and Viral Reactivation.* J Clin Transl Hepatol, 2018. **6**(3): p. 296-305 [DOI: 10.14218/jcth.2018.00016].
73. Chu, C.J. and Lee, S.D., *Hepatitis B virus/hepatitis C virus coinfection: epidemiology, clinical features, viral interactions and treatment.* J Gastroenterol Hepatol, 2008. **23**(4): p. 512-520 [DOI: 10.1111/j.1440-1746.2008.05384.x].

74. Sagnelli, E., Coppola, N., Marrocco, C., et al., *Hepatitis C virus superinfection in hepatitis B virus chronic carriers: a reciprocal viral interaction and a variable clinical course.* J Clin Virol, 2006. **35**(3): p. 317-320 [DOI: 10.1016/j.jcv.2005.10.006].
75. Liu, C.J., Sheen, I.S., Chen, C.Y., et al., *Ledipasvir/Sofosbuvir for Patients Coinfected With Chronic Hepatitis C and Hepatitis B in Taiwan: Follow-up at 108 Weeks Posttreatment.* Clin Infect Dis, 2022. **75**(3): p. 453-459 [DOI: 10.1093/cid/ciab971].
76. Pol, S., Haour, G., Fontaine, H., et al., *The negative impact of HBV/HCV coinfection on cirrhosis and its consequences.* Aliment Pharmacol Ther, 2017. **46**(11-12): p. 1054-1060 [DOI: 10.1111/apt.14352].
77. Jamma, S., Hussain, G. and Lau, D.T.Y., *Current Concepts of HBV/HCV Coinfection: Coexistence, but Not Necessarily in Harmony.* Current Hepatitis Reports, 2010. **9**(4): p. 260-269 [DOI: 10.1007/s11901-010-0060-4].
78. Huang, D.Q., Mathurin, P., Cortez-Pinto, H., et al., *Global epidemiology of alcohol-associated cirrhosis and HCC: trends, projections and risk factors.* Nat Rev Gastroenterol Hepatol, 2023. **20**(1): p. 37-49 [DOI: 10.1038/s41575-022-00688-6].
79. Matsushita, H. and Takaki, A., *Alcohol and hepatocellular carcinoma.* BMJ Open Gastroenterol, 2019. **6**(1) [DOI: 10.1136/bmjgast-2018-000260].
80. Crabb, D.W., Im, G.Y., Szabo, G., et al., *Diagnosis and Treatment of Alcohol-Associated Liver Diseases: 2019 Practice Guidance From the American Association for the Study of Liver Diseases.* Hepatology, 2020. **71**(1): p. 306-333 [DOI: 10.1002/hep.30866].
81. Scoccianti, C., Cecchini, M., Anderson, A.S., et al., *European Code against Cancer 4th Edition: Alcohol drinking and cancer.* Cancer Epidemiol, 2016. **45**: p. 181-188 [DOI: 10.1016/j.canep.2016.09.011].
82. Welzel, T.M., Graubard, B.I., Quraishi, S., et al., *Population-attributable fractions of risk factors for hepatocellular carcinoma in the United States.* Am J Gastroenterol, 2013. **108**(8): p. 1314-1321 [DOI: 10.1038/ajg.2013.160].
83. World Health Organization. *Global health risks : mortality and burden of disease attributable to selected major risks*. 2009; World Health Organization. [Available from: https://apps.who.int/iris/handle/10665/44203].
84. Ganne-Carrié, N., Chaffaut, C., Bourcier, V., et al., *Estimate of hepatocellular carcinoma incidence in patients with alcoholic cirrhosis.* J Hepatol, 2018. **69**(6): p. 1274-1283 [DOI: 10.1016/j.jhep.2018.07.022].
85. Tsai, M.C., Yang, S.S., Lin, C.C., et al., *Association of Heavy Alcohol Intake and ALDH2 rs671 Polymorphism With Hepatocellular Carcinoma and Mortality in Patients With Hepatitis B Virus-Related Cirrhosis.* JAMA Netw Open, 2022. **5**(7) [DOI: 10.1001/jamanetworkopen.2022.23511].
86. Lin, C.W., Lin, C.C., Mo, L.R., et al., *Heavy alcohol consumption increases the incidence of hepatocellular carcinoma in hepatitis B virus-related cirrhosis.* J Hepatol, 2013. **58**(4): p. 730-735 [DOI: 10.1016/j.jhep.2012.11.045].
87. Osna, N.A., Donohue, T.M., Jr. and Kharbanda, K.K., *Alcoholic Liver Disease: Pathogenesis and Current Management.* Alcohol Res, 2017. **38**(2): p. 147-161 [PMCID: PMC5513682].
88. Seitz, H.K. and Stickel, F., *Molecular mechanisms of alcohol-mediated carcinogenesis.* Nature Reviews Cancer, 2007. **7**(8): p. 599-612 [DOI: 10.1038/nrc2191].

89. Seitz, H.K. and Stickel, F., *Acetaldehyde as an underestimated risk factor for cancer development: role of genetics in ethanol metabolism.* Genes Nutr, 2010. **5**(2): p. 121-128 [DOI: 10.1007/s12263-009-0154-1].
90. Beland, F.A., Benson, R.W., Mellick, P.W., et al., *Effect of ethanol on the tumorigenicity of urethane (ethyl carbamate) in B6C3F1 mice.* Food Chem Toxicol, 2005. **43**(1): p. 1-19 [DOI: 10.1016/j.fct.2004.07.018].
91. Soffritti, M., Belpoggi, F., Cevolani, D., et al., *Results of long-term experimental studies on the carcinogenicity of methyl alcohol and ethyl alcohol in rats.* Ann N Y Acad Sci, 2002. **982**(1): p. 46-69 [DOI: 10.1111/j.1749-6632.2002.tb04924.x].
92. Watabiki, T., Okii, Y., Tokiyasu, T., et al., *Long-term ethanol consumption in ICR mice causes mammary tumor in females and liver fibrosis in males.* Alcohol Clin Exp Res, 2000. **24**(4): p. 117s-122s [DOI: 10.1111/j.1530-0277.2000.tb00025.x].
93. Paradis, V., Scoazec, J.Y., Köllinger, M., et al., *Cellular and subcellular localization of acetaldehyde-protein adducts in liver biopsies from alcoholic patients.* J Histochem Cytochem, 1996. **44**(9): p. 1051-1057 [DOI: 10.1177/44.9.8773571].
94. Siegmund, S.V., Dooley, S. and Brenner, D.A., *Molecular mechanisms of alcohol-induced hepatic fibrosis.* Dig Dis, 2005. **23**(3-4): p. 264-274 [DOI: 10.1159/000090174].
95. Collier, J.D., Bassendine, M.F., Burt, A.D., et al., *Characterisation of the DNA repair enzyme for O(6)-methylguanine in cirrhosis.* J Hepatol, 1996. **25**(2): p. 158-165 [DOI: 10.1016/s0168-8278(96)80068-7].
96. Lieber, C.S., *Alcoholic fatty liver: its pathogenesis and mechanism of progression to inflammation and fibrosis.* Alcohol, 2004. **34**(1): p. 9-19 [DOI: 10.1016/j.alcohol.2004.07.008].
97. Linhart, K., Bartsch, H. and Seitz, H.K., *The role of reactive oxygen species (ROS) and cytochrome P-450 2E1 in the generation of carcinogenic etheno-DNA adducts.* Redox Biol, 2014. **3**: p. 56-62 [DOI: 10.1016/j.redox.2014.08.009].
98. Sharma, P. and Arora, A., *Clinical presentation of alcoholic liver disease and non-alcoholic fatty liver disease: spectrum and diagnosis.* Transl Gastroenterol Hepatol, 2020. **5** [DOI: 10.21037/tgh.2019.10.02].
99. Åberg, F., Helenius-Hietala, J., Puukka, P., et al. *Interaction between alcohol consumption and metabolic syndrome in predicting severe liver disease in the general population*. Hepatology, 2018. **67**(6): p. 2141-2149 [DOI: 10.1002/hep.29631].
100. Schwarzinger, M., Baillot, S., Yazdanpanah, Y., et al., *Contribution of alcohol use disorders on the burden of chronic hepatitis C in France, 2008–2013: A nationwide retrospective cohort study.* Journal of Hepatology, 2017. **67**(3): p. 454-461 [DOI: https://doi.org/10.1016/j.jhep.2017.03.031].
101. Singal, A.K., Kuo, Y.F. and Anand, B.S., *Hepatitis C virus infection in alcoholic hepatitis: prevalence patterns and impact on in-hospital mortality.* Eur J Gastroenterol Hepatol, 2012. **24**(10): p. 1178-1184 [DOI: 10.1097/MEG.0b013e328355cce0].
102. Hart, C.L., Morrison, D.S., Batty, G.D., et al., *Effect of body mass index and alcohol consumption on liver disease: analysis of data from two prospective cohort studies.* Bmj, 2010. **340** [DOI: 10.1136/bmj.c1240].
103. Fletcher, L.M., Dixon, J.L., Purdie, D.M., et al., *Excess alcohol greatly increases the prevalence of cirrhosis in hereditary hemochromatosis.* Gastroenterology, 2002. **122**(2): p. 281-289 [DOI: https://doi.org/10.1053/gast.2002.30992].

104. Vancells Lujan, P., Viñas Esmel, E. and Sacanella Meseguer, E., *Overview of Non-Alcoholic Fatty Liver Disease (NAFLD) and the Role of Sugary Food Consumption and Other Dietary Components in Its Development.* Nutrients, 2021. **13**(5) [DOI: 10.3390/nu13051442].
105. Cotter, T.G. and Rinella, M., *Nonalcoholic Fatty Liver Disease 2020: The State of the Disease.* Gastroenterology, 2020. **158**(7): p. 1851-1864 [DOI: 10.1053/j.gastro.2020.01.052].
106. Younossi, Z.M., *Non-alcoholic fatty liver disease - A global public health perspective.* J Hepatol, 2019. **70**(3): p. 531-544 [DOI: 10.1016/j.jhep.2018.10.033].
107. Estes, C., Razavi, H., Loomba, R., et al., *Modeling the epidemic of nonalcoholic fatty liver disease demonstrates an exponential increase in burden of disease.* Hepatology, 2018. **67**(1): p. 123-133 [DOI: 10.1002/hep.29466].
108. McGlynn, K.A., Petrick, J.L. and El-Serag, H.B., *Epidemiology of Hepatocellular Carcinoma.* Hepatology, 2021. **73** (Suppl 1): p. 4-13 [DOI: 10.1002/hep.31288].
109. Lazarus, J.V., Colombo, M., Cortez-Pinto, H., et al., *NAFLD — sounding the alarm on a silent epidemic.* Nature Reviews Gastroenterology & Hepatology, 2020. **17**(7): p. 377-379 [DOI: 10.1038/s41575-020-0315-7].
110. Kim, D., Li, A.A., Gadiparthi, C., et al., *Changing Trends in Etiology-Based Annual Mortality From Chronic Liver Disease, From 2007 Through 2016.* Gastroenterology, 2018. **155**(4): p. 1154-1163.e1153 [DOI: 10.1053/j.gastro.2018.07.008].
111. Estes, C., Anstee, Q.M., Arias-Loste, M.T., et al., *Modeling NAFLD disease burden in China, France, Germany, Italy, Japan, Spain, United Kingdom, and United States for the period 2016–2030.* Journal of Hepatology, 2018. **69**(4): p. 896-904 [DOI: https://doi.org/10.1016/j.jhep.2018.05.036].
112. Younossi, Z., Anstee, Q.M., Marietti, M., et al., *Global burden of NAFLD and NASH: trends, predictions, risk factors and prevention.* Nat Rev Gastroenterol Hepatol, 2018. **15**(1): p. 11-20 [DOI: 10.1038/nrgastro.2017.109].
113. Calle, E.E., Rodriguez, C., Walker-Thurmond, K., et al., *Overweight, obesity, and mortality from cancer in a prospectively studied cohort of U.S. adults.* N Engl J Med, 2003. **348**(17): p. 1625-1638 [DOI: 10.1056/NEJMoa021423].
114. Powell, E.E., Wong, V.W. and Rinella, M., *Non-alcoholic fatty liver disease.* Lancet, 2021. **397**(10290): p. 2212-2224 [DOI: 10.1016/s0140-6736(20)32511-3].
115. Zhang, C. and Yang, M., *Current Options and Future Directions for NAFLD and NASH Treatment.* Int J Mol Sci, 2021. **22**(14): p. 7571 [DOI: 10.3390/ijms22147571].
116. Campbell, P.T., Newton, C.C., Freedman, N.D., et al., *Body Mass Index, Waist Circumference, Diabetes, and Risk of Liver Cancer for U.S. Adults.* Cancer Res, 2016. **76**(20): p. 6076-6083 [DOI: 10.1158/0008-5472.Can-16-0787].
117. Marchesini, G., Brizi, M., Bianchi, G., et al., *Nonalcoholic fatty liver disease: a feature of the metabolic syndrome.* Diabetes, 2001. **50**(8): p. 1844-1850 [DOI: 10.2337/diabetes.50.8.1844].
118. Mittal, S., El-Serag, H.B., Sada, Y.H., et al., *Hepatocellular Carcinoma in the Absence of Cirrhosis in United States Veterans is Associated With Nonalcoholic Fatty Liver Disease.* Clin Gastroenterol Hepatol, 2016. **14**(1): p. 124-131.e121 [DOI: 10.1016/j.cgh.2015.07.019].
119. Huang, T.S., Lin, C.L., Lu, M.J., et al., *Diabetes, hepatocellular carcinoma, and mortality in hepatitis C-infected patients: A population-based cohort study.* J Gastroenterol Hepatol, 2017. **32**(7): p. 1355-1362 [DOI: 10.1111/jgh.13670].

120. Li, X., Xu, H., Gao, Y., et al., *Diabetes mellitus increases the risk of hepatocellular carcinoma in treatment-naïve chronic hepatitis C patients in China.* Medicine (Baltimore), 2017. **96**(13): p. e6508 [DOI: 10.1097/md.0000000000006508].
121. Parthasarathy, G., Revelo, X. and Malhi, H., *Pathogenesis of Nonalcoholic Steatohepatitis: An Overview.* Hepatol Commun, 2020. **4**(4): p. 478-492 [DOI: 10.1002/hep4.1479].
122. Schuster, S., Cabrera, D., Arrese, M., et al., *Triggering and resolution of inflammation in NASH.* Nat Rev Gastroenterol Hepatol, 2018. **15**(6): p. 349-364 [DOI: 10.1038/s41575-018-0009-6].
123. Vescovo, T., Refolo, G., Vitagliano, G., et al., *Molecular mechanisms of hepatitis C virus-induced hepatocellular carcinoma.* Clin Microbiol Infect, 2016. **22**(10): p. 853-861 [DOI: 10.1016/j.cmi.2016.07.019].
124. Ganz, M. and Szabo, G., *Immune and inflammatory pathways in NASH.* Hepatol Int, 2013. **7**(Suppl 2): p. 771-781 [DOI: 10.1007/s12072-013-9468-6].
125. Petrick, J.L., Campbell, P.T., Koshiol, J., et al., *Tobacco, alcohol use and risk of hepatocellular carcinoma and intrahepatic cholangiocarcinoma: The Liver Cancer Pooling Project.* Br J Cancer, 2018. **118**(7): p. 1005-1012 [DOI: 10.1038/s41416-018-0007-z].
126. Jacob, L., Freyn, M., Kalder, M., et al., *Impact of tobacco smoking on the risk of developing 25 different cancers in the UK: a retrospective study of 422,010 patients followed for up to 30 years.* Oncotarget, 2018. **9**(25): p. 17420-17429 [DOI: 10.18632/oncotarget.24724].
127. Warren, G.W. and Cummings, K.M., *Tobacco and lung cancer: risks, trends, and outcomes in patients with cancer.* Am Soc Clin Oncol Educ Book, 2013. **33**: p. 359-364 [DOI: 10.14694/EdBook_AM.2013.33.359].
128. Saha, S.P., Bhalla, D.K., Whayne, T.F., Jr., et al., *Cigarette smoke and adverse health effects: An overview of research trends and future needs.* Int J Angiol, 2007. **16**(3): p. 77-83 [DOI: 10.1055/s-0031-1278254].
129. Sasco, A.J., Secretan, M.B. and Straif, K., *Tobacco smoking and cancer: a brief review of recent epidemiological evidence.* Lung Cancer, 2004. **45** (Suppl 2): p. S3-9 [DOI: 10.1016/j.lungcan.2004.07.998].
130. National Toxicology Program. *Report on Carcinogens, Fifteenth Edition*. 2021, December 21; NTP. [Available from: https://ntp.niehs.nih.gov/go/roc15].
131. Premkumar, M. and Anand, A.C., *Tobacco, Cigarettes, and the Liver: The Smoking Gun.* J Clin Exp Hepatol, 2021. **11**(6): p. 700-712 [DOI: 10.1016/j.jceh.2021.07.016].
132. Wang, S., Sugamori, K.S., Tung, A., et al., *N-hydroxylation of 4-aminobiphenyl by CYP2E1 produces oxidative stress in a mouse model of chemically induced liver cancer.* Toxicol Sci, 2015. **144**(2): p. 393-405 [DOI: 10.1093/toxsci/kfv006].
133. Poirier, M.C. and Beland, F.A., *DNA adduct measurements and tumor incidence during chronic carcinogen exposure in rodents.* Environ Health Perspect, 1994. **102**(Suppl 6): p. 161-165 [DOI: 10.1289/ehp.94102s6161].
134. Yang, D., Kim, J.W., Jeong, H., et al., *Effects of maternal cigarette smoke exposure on the progression of nonalcoholic steatohepatitis in offspring mice.* Toxicol Res, 2023. **39**(1): p. 91-103 [DOI: 10.1007/s43188-022-00153-1].
135. Barsouk, A., Thandra, K.C., Saginala, K., et al., *Chemical Risk Factors of Primary Liver Cancer: An Update.* Hepat Med, 2020. **12**: p. 179-188 [DOI: 10.2147/hmer.S278070].
136. Liu, Y. and Wu, F., *Global burden of aflatoxin-induced hepatocellular carcinoma: a risk assessment.* Environ Health Perspect, 2010. **118**(6): p. 818-824 [DOI: 10.1289/ehp.0901388].

137. Magnussen, A. and Parsi, M.A., *Aflatoxins, hepatocellular carcinoma and public health.* World J Gastroenterol, 2013. **19**(10): p. 1508-1512 [DOI: 10.3748/wjg.v19.i10.1508].
138. Long, X.D., Ma, Y., Zhou, Y.F., et al., *XPD codon 312 and 751 polymorphisms, and AFB1 exposure, and hepatocellular carcinoma risk.* BMC Cancer, 2009. **9** [DOI: 10.1186/1471-2407-9-400].
139. Wang, J.S. and Groopman, J.D., *DNA damage by mycotoxins.* Mutat Res, 1999. **424**(1-2): p. 167-181 [DOI: 10.1016/s0027-5107(99)00017-2].
140. Farazi, P.A. and DePinho, R.A., *Hepatocellular carcinoma pathogenesis: from genes to environment.* Nature Reviews Cancer, 2006. **6**(9): p. 674-687 [DOI: 10.1038/nrc1934].
141. Galle, P.R., Forner, A., Llovet, J.M., et al., *EASL Clinical Practice Guidelines: Management of hepatocellular carcinoma.* Journal of Hepatology, 2018. **69**(1): p. 182-236 [DOI: https://doi.org/10.1016/j.jhep.2018.03.019].
142. Forner, A., Reig, M. and Bruix, J., *Hepatocellular carcinoma.* Lancet, 2018. **391**(10127): p. 1301-1314 [DOI: 10.1016/s0140-6736(18)30010-2].
143. Kim, Y., Sills, R.C. and Houle, C.D., *Overview of the molecular biology of hepatocellular neoplasms and hepatoblastomas of the mouse liver.* Toxicol Pathol, 2005. **33**(1): p. 175-180 [DOI: 10.1080/01926230590522130].
144. Tahmasebi Birgani, M. and Carloni, V., *Tumor Microenvironment, a Paradigm in Hepatocellular Carcinoma Progression and Therapy.* Int J Mol Sci, 2017. **18**(2) [DOI: 10.3390/ijms18020405].
145. Hernandez-Gea, V., Toffanin, S., Friedman, S.L., et al., *Role of the microenvironment in the pathogenesis and treatment of hepatocellular carcinoma.* Gastroenterology, 2013. **144**(3): p. 512-527 [DOI: 10.1053/j.gastro.2013.01.002].
146. Wu, S.D., Ma, Y.S., Fang, Y., et al., *Role of the microenvironment in hepatocellular carcinoma development and progression.* Cancer Treat Rev, 2012. **38**(3): p. 218-225 [DOI: 10.1016/j.ctrv.2011.06.010].
147. Johnston, M.P. and Khakoo, S.I., *Immunotherapy for hepatocellular carcinoma: Current and future.* World J Gastroenterol, 2019. **25**(24): p. 2977-2989 [DOI: 10.3748/wjg.v25.i24.2977].
148. Zucman-Rossi, J., Villanueva, A., Nault, J.C., et al. *Genetic Landscape and Biomarkers of Hepatocellular Carcinoma.* Gastroenterology, 2015. **149**(5): p. 1226-1239.e1224 [DOI: 10.1053/j.gastro.2015.05.061].
149. Laurent-Puig, P. and Zucman-Rossi, J., *Genetics of hepatocellular tumors.* Oncogene, 2006. **25**(27): p. 3778-3786 [DOI: 10.1038/sj.onc.1209547].
150. Vanderborght, B., Lefere, S., Vlierberghe, H.V., et al., *The Angiopoietin/Tie2 Pathway in Hepatocellular Carcinoma.* Cells, 2020. **9**(11) [DOI: 10.3390/cells9112382].
151. Lugano, R., Ramachandran, M. and Dimberg, A., *Tumor angiogenesis: causes, consequences, challenges and opportunities.* Cell Mol Life Sci, 2020. **77**(9): p. 1745-1770 [DOI: 10.1007/s00018-019-03351-7].
152. Moawad, A.W., Szklaruk, J., Lall, C., et al., *Angiogenesis in Hepatocellular Carcinoma; Pathophysiology, Targeted Therapy, and Role of Imaging.* J Hepatocell Carcinoma, 2020. **7**: p. 77-89 [DOI: 10.2147/jhc.S224471].
153. Morse, M.A., Sun, W., Kim, R., et al., *The Role of Angiogenesis in Hepatocellular Carcinoma.* Clin Cancer Res, 2019. **25**(3): p. 912-920 [DOI: 10.1158/1078-0432.Ccr-18-1254].
154. Atanasov, G., Dino, K., Schierle, K., et al., *Angiogenic inflammation and formation of necrosis in the tumor microenvironment influence patient survival after radical surgery for de novo hepatocellular carcinoma in non-cirrhosis.* World J Surg Oncol, 2019. **17**(1) [DOI: 10.1186/s12957-019-1756-8].

155. Quaglia, A., *Hepatocellular carcinoma: a review of diagnostic challenges for the pathologist.* J Hepatocell Carcinoma, 2018. **5**: p. 99-108 [DOI: 10.2147/jhc.S159808].
156. Ghouri, Y., Mian, I. and Rowe, J., *Review of hepatocellular carcinoma: Epidemiology, etiology, and carcinogenesis.* Journal of Carcinogenesis, 2017. **16**(1) [DOI: 10.4103/jcar.JCar_9_16].
157. Yang, Z.F. and Poon, R.T., *Vascular changes in hepatocellular carcinoma.* Anat Rec (Hoboken), 2008. **291**(6): p. 721-734 [DOI: 10.1002/ar.20668].
158. Yao, C., Wu, S., Kong, J., et al., *Angiogenesis in hepatocellular carcinoma: mechanisms and anti-angiogenic therapies.* Cancer Biol Med, 2023. **20**(1): p. 25-43 [DOI: 10.20892/j.issn.2095-3941.2022.0449].
159. Zhu, A.X., Duda, D.G., Sahani, D.V., et al., *HCC and angiogenesis: possible targets and future directions.* Nat Rev Clin Oncol, 2011. **8**(5): p. 292-301 [DOI: 10.1038/nrclinonc.2011.30].
160. Fleischer, J.R., Jodszuweit, C.A., Ghadimi, M., et al., *Vascular Heterogeneity With a Special Focus on the Hepatic Microenvironment.* Front Physiol, 2020. **11** [DOI: 10.3389/fphys.2020.591901].
161. Natarajan, V., Harris, E.N. and Kidambi, S., *SECs (Sinusoidal Endothelial Cells), Liver Microenvironment, and Fibrosis.* Biomed Res Int, 2017. **2017** [DOI: 10.1155/2017/4097205].
162. Augustin, H.G. and Koh, G.Y., *Organotypic vasculature: From descriptive heterogeneity to functional pathophysiology.* Science, 2017. **357**(6353): p. eaal2379 [DOI: 10.1126/science.aal2379].
163. Lei, L., Ei Mourabit, H., Housset, C., et al., *Role of Angiogenesis in the Pathogenesis of NAFLD.* J Clin Med, 2021. **10**(7) [DOI: 10.3390/jcm10071338].
164. Coulon, S., Heindryckx, F., Geerts, A., et al., *Angiogenesis in chronic liver disease and its complications.* Liver Int, 2011. **31**(2): p. 146-162 [DOI: 10.1111/j.1478-3231.2010.02369.x].
165. Motz, G.T. and Coukos, G., *The parallel lives of angiogenesis and immunosuppression: cancer and other tales.* Nat Rev Immunol, 2011. **11**(10): p. 702-711 [DOI: 10.1038/nri3064].
166. Horwitz, E., Stein, I., Andreozzi, M., et al., *Human and mouse VEGFA-amplified hepatocellular carcinomas are highly sensitive to sorafenib treatment.* Cancer Discov, 2014. **4**(6): p. 730-743 [DOI: 10.1158/2159-8290.Cd-13-0782].
167. Turlin, B., Le Quilleuc, D., Leroyer, P., et al., *High vascular endothelial growth factor (VEGF) expression in chemically-induced hepatic microcancers in mice.* J Hepatol, 2002. **37**(5): p. 620-624 [DOI: 10.1016/s0168-8278(02)00249-0].
168. Poon, R.T., Fan, S.T. and Wong, J., *Clinical implications of circulating angiogenic factors in cancer patients.* J Clin Oncol, 2001. **19**(4): p. 1207-1225 [DOI: 10.1200/jco.2001.19.4.1207].
169. Holmes, D.I. and Zachary, I., *The vascular endothelial growth factor (VEGF) family: angiogenic factors in health and disease.* Genome Biol, 2005. **6**(2): p. 209 [DOI: 10.1186/gb-2005-6-2-209].
170. Finn, R.S., Qin, S., Ikeda, M., et al., *Atezolizumab plus Bevacizumab in Unresectable Hepatocellular Carcinoma.* N Engl J Med, 2020. **382**(20): p. 1894-1905 [DOI: 10.1056/NEJMoa1915745].
171. Finn, R.S., Bentley, G., Britten, C.D., et al., *Targeting vascular endothelial growth factor with the monoclonal antibody bevacizumab inhibits human hepatocellular carcinoma cells growing in an orthotopic mouse model.* Liver Int, 2009. **29**(2): p. 284-290 [DOI: 10.1111/j.1478-3231.2008.01762.x].
172. Ferrara, N., Hillan, K.J. and Novotny, W., *Bevacizumab (Avastin), a humanized anti-VEGF monoclonal antibody for cancer therapy.* Biochem Biophys Res Commun, 2005. **333**(2): p. 328-335 [DOI: 10.1016/j.bbrc.2005.05.132].
173. Saviano, A., Roehlen, N., Virzì, A., et al., *Stromal and Immune Drivers of Hepatocarcinogenesis*, in *Hepatocellular Carcinoma: Translational Precision Medicine Approaches*, Y. Hoshida, Editor. 2019: Cham (CH).Chapter 15. p. 317-331].

174. Affo, S., Yu, L.X. and Schwabe, R.F., *The Role of Cancer-Associated Fibroblasts and Fibrosis in Liver Cancer.* Annu Rev Pathol, 2017. **12**: p. 153-186 [DOI: 10.1146/annurev-pathol-052016-100322].
175. Lin, N., Chen, Z., Lu, Y., et al., *Role of activated hepatic stellate cells in proliferation and metastasis of hepatocellular carcinoma.* Hepatol Res, 2015. **45**(3): p. 326-336 [DOI: 10.1111/hepr.12356].
176. Taura, K., De Minicis, S., Seki, E., et al., *Hepatic stellate cells secrete angiopoietin 1 that induces angiogenesis in liver fibrosis.* Gastroenterology, 2008. **135**(5): p. 1729-1738 [DOI: 10.1053/j.gastro.2008.07.065].
177. De Minicis, S., Kisseleva, T., Francis, H., et al., *Liver carcinogenesis: rodent models of hepatocarcinoma and cholangiocarcinoma.* Dig Liver Dis, 2013. **45**(6): p. 450-459 [DOI: 10.1016/j.dld.2012.10.008].
178. Steiger, K., Gross, N., Widholz, S.A., et al., *Genetically Engineered Mouse Models of Liver Tumorigenesis Reveal a Wide Histological Spectrum of Neoplastic and Non-Neoplastic Liver Lesions.* Cancers (Basel), 2020. **12**(8) [DOI: 10.3390/cancers12082265].
179. Blidisel, A., Marcovici, I., Coricovac, D., et al., *Experimental Models of Hepatocellular Carcinoma—A Preclinical Perspective.* Cancers, 2021. **13**(15) [DOI: 10.3390/cancers13153651].
180. Lee, J.S., Grisham, J.W. and Thorgeirsson, S.S., *Comparative functional genomics for identifying models of human cancer.* Carcinogenesis, 2005. **26**(6): p. 1013-1020 [DOI: 10.1093/carcin/bgi030].
181. Vandamme, T.F., *Use of rodents as models of human diseases.* J Pharm Bioallied Sci, 2014. **6**(1): p. 2-9 [DOI: 10.4103/0975-7406.124301].
182. Cho, K., Ro, S.W., Seo, S.H., et al., *Genetically Engineered Mouse Models for Liver Cancer.* Cancers (Basel), 2019. **12**(1) [DOI: 10.3390/cancers12010014].
183. Heindryckx, F., Colle, I. and Van Vlierberghe, H., *Experimental mouse models for hepatocellular carcinoma research.* International Journal of Experimental Pathology, 2009. **90**(4): p. 367-386 [DOI: https://doi.org/10.1111/j.1365-2613.2009.00656.x].
184. Klaunig, J.E., Pereira, M.A., Ruch, R.J., et al., *Dose-response relationship of diethylnitrosamine-initiated tumors in neonatal balb/c mice: effect of phenobarbital promotion.* Toxicol Pathol, 1988. **16**(3): p. 381-385 [DOI: 10.1177/019262338801600310].
185. de Lima, V.M., Oliveira, C.P., Alves, V.A., et al., *A rodent model of NASH with cirrhosis, oval cell proliferation and hepatocellular carcinoma.* J Hepatol, 2008. **49**(6): p. 1055-1061 [DOI: 10.1016/j.jhep.2008.07.024].
186. Knight, B., Yeoh, G.C., Husk, K.L., et al., *Impaired preneoplastic changes and liver tumor formation in tumor necrosis factor receptor type 1 knockout mice.* J Exp Med, 2000. **192**(12): p. 1809-1818 [DOI: 10.1084/jem.192.12.1809].
187. McGlynn, K.A., Hunter, K., LeVoyer, T., et al., *Susceptibility to aflatoxin B1-related primary hepatocellular carcinoma in mice and humans.* Cancer Res, 2003. **63**(15): p. 4594-4601 [PMID: 12907637].
188. Kelland, L.R., *Of mice and men: values and liabilities of the athymic nude mouse model in anticancer drug development.* Eur J Cancer, 2004. **40**(6): p. 827-836 [DOI: 10.1016/j.ejca.2003.11.028].
189. Frese, K.K. and Tuveson, D.A., *Maximizing mouse cancer models.* Nat Rev Cancer, 2007. **7**(9): p. 645-658 [DOI: 10.1038/nrc2192].
190. McGivern, D.R. and Lemon, S.M., *Virus-specific mechanisms of carcinogenesis in hepatitis C virus associated liver cancer.* Oncogene, 2011. **30**(17): p. 1969-1983 [DOI: 10.1038/onc.2010.594].

191. Kamegaya, Y., Hiasa, Y., Zukerberg, L., et al., *Hepatitis C virus acts as a tumor accelerator by blocking apoptosis in a mouse model of hepatocarcinogenesis.* Hepatology, 2005. **41**(3): p. 660-667 [DOI: 10.1002/hep.20621].
192. Tsuge, M., *Are Humanized Mouse Models Useful for Basic Research of Hepatocarcinogenesis through Chronic Hepatitis B Virus Infection?* Viruses, 2021. **13**(10) [DOI: 10.3390/v13101920].
193. Schieck, A., Schulze, A., Gähler, C., et al., *Hepatitis B virus hepatotropism is mediated by specific receptor recognition in the liver and not restricted to susceptible hosts.* Hepatology, 2013. **58**(1): p. 43-53 [DOI: 10.1002/hep.26211].
194. Lee, J.-S., Chu, I.-S., Mikaelyan, A., et al., *Application of comparative functional genomics to identify best-fit mouse models to study human cancer.* Nature Genetics, 2004. **36**(12): p. 1306-1311 [DOI: 10.1038/ng1481].
195. de La Coste, A., Romagnolo, B., Billuart, P., et al., *Somatic mutations of the beta-catenin gene are frequent in mouse and human hepatocellular carcinomas.* Proc Natl Acad Sci U S A, 1998. **95**(15): p. 8847-8851 [DOI: 10.1073/pnas.95.15.8847].
196. Colnot, S., Decaens, T., Niwa-Kawakita, M., et al., *Liver-targeted disruption of Apc in mice activates beta-catenin signaling and leads to hepatocellular carcinomas.* Proc Natl Acad Sci U S A, 2004. **101**(49): p. 17216-17221 [DOI: 10.1073/pnas.0404761101].
197. Borlak, J., Meier, T., Halter, R., et al., *Epidermal growth factor-induced hepatocellular carcinoma: gene expression profiles in precursor lesions, early stage and solitary tumours.* Oncogene, 2005. **24**(11): p. 1809-1819 [DOI: 10.1038/sj.onc.1208196].
198. Tönjes, R.R., Löhler, J., O'Sullivan, J.F., et al., *Autocrine mitogen IgEGF cooperates with c-myc or with the Hcs locus during hepatocarcinogenesis in transgenic mice.* Oncogene, 1995. **10**(4): p. 765-768 [PMID: 7862454].
199. Baek, H.J., Lim, S.C., Kitisin, K., et al., *Hepatocellular cancer arises from loss of transforming growth factor beta signaling adaptor protein embryonic liver fodrin through abnormal angiogenesis.* Hepatology, 2008. **48**(4): p. 1128-1137 [DOI: 10.1002/hep.22460].
200. Nicholes, K., Guillet, S., Tomlinson, E., et al., *A mouse model of hepatocellular carcinoma: ectopic expression of fibroblast growth factor 19 in skeletal muscle of transgenic mice.* Am J Pathol, 2002. **160**(6): p. 2295-2307 [DOI: 10.1016/s0002-9440(10)61177-7].
201. Khodayari, N., Wang, R.L., Oshins, R., et al., *The Mechanism of Mitochondrial Injury in Alpha-1 Antitrypsin Deficiency Mediated Liver Disease.* International Journal of Molecular Sciences, 2021. **22**(24) [DOI: 10.3390/ijms222413255].
202. Geller, S.A., Nichols, W.S., Kim, S., et al., *Hepatocarcinogenesis is the sequel to hepatitis in Z#2 alpha 1-antitrypsin transgenic mice: histopathological and DNA ploidy studies.* Hepatology, 1994. **19**(2): p. 389-397 [DOI: 10.1002/hep.1840190218].
203. Campbell, J.S., Hughes, S.D., Gilbertson, D.G., et al., *Platelet-derived growth factor C induces liver fibrosis, steatosis, and hepatocellular carcinoma.* Proc Natl Acad Sci U S A, 2005. **102**(9): p. 3389-3394 [DOI: 10.1073/pnas.0409722102].
204. Schnur, J., Oláh, J., Szepesi, A., et al., *Thioacetamide-induced hepatic fibrosis in transforming growth factor beta-1 transgenic mice.* Eur J Gastroenterol Hepatol, 2004. **16**(2): p. 127-133 [DOI: 10.1097/00042737-200402000-00002].
205. Sanderson, N., Factor, V., Nagy, P., et al., *Hepatic expression of mature transforming growth factor beta 1 in transgenic mice results in multiple tissue lesions.* Proc Natl Acad Sci U S A, 1995. **92**(7): p. 2572-2576 [DOI: 10.1073/pnas.92.7.2572].

206. Martínez-Chantar, M.L., Vázquez-Chantada, M., Ariz, U., et al., *Loss of the glycine N-methyltransferase gene leads to steatosis and hepatocellular carcinoma in mice.* Hepatology, 2008. **47**(4): p. 1191-1199 [DOI: 10.1002/hep.22159].
207. Liu, S.P., Li, Y.S., Chen, Y.J., et al., *Glycine N-methyltransferase-/- mice develop chronic hepatitis and glycogen storage disease in the liver.* Hepatology, 2007. **46**(5): p. 1413-1425 [DOI: 10.1002/hep.21863].
208. Watanabe, S., Horie, Y., Kataoka, E., et al., *Non-alcoholic steatohepatitis and hepatocellular carcinoma: lessons from hepatocyte-specific phosphatase and tensin homolog (PTEN)-deficient mice.* J Gastroenterol Hepatol, 2007. **22** (Suppl 1): p. S96-S100 [DOI: 10.1111/j.1440-1746.2006.04665.x].
209. O'Hagan, R.C. and Heyer, J., *KRAS Mouse Models: Modeling Cancer Harboring KRAS Mutations.* Genes Cancer, 2011. **2**(3): p. 335-343 [DOI: 10.1177/1947601911408080].
210. Downward, J., *Targeting RAS signalling pathways in cancer therapy.* Nat Rev Cancer, 2003. **3**(1): p. 11-22 [DOI: 10.1038/nrc969].
211. Calvisi, D.F., Ladu, S., Gorden, A., et al., *Ubiquitous activation of Ras and Jak/Stat pathways in human HCC.* Gastroenterology, 2006. **130**(4): p. 1117-1128 [DOI: 10.1053/j.gastro.2006.01.006].
212. Chung, S.I., Moon, H., Kim, D.Y., et al., *Development of a transgenic mouse model of hepatocellular carcinoma with a liver fibrosis background.* BMC Gastroenterol, 2016. **16** [DOI: 10.1186/s12876-016-0423-6].
213. Chow, E.K., Fan, L.L., Chen, X., et al., *Oncogene-specific formation of chemoresistant murine hepatic cancer stem cells.* Hepatology, 2012. **56**(4): p. 1331-1341 [DOI: 10.1002/hep.25776].
214. Zhang, G., Budker, V. and Wolff, J.A., *High levels of foreign gene expression in hepatocytes after tail vein injections of naked plasmid DNA.* Hum Gene Ther, 1999. **10**(10): p. 1735-1737 [DOI: 10.1089/10430349950017734].
215. Liu, S., Huang, F., Ru, G., et al., *Mouse Models of Hepatocellular Carcinoma: Classification, Advancement, and Application.* Front Oncol, 2022. **12** [DOI: 10.3389/fonc.2022.902820].
216. Thoolen, B., Ten Kate, F.J., van Diest, P.J., et al., *Comparative histomorphological review of rat and human hepatocellular proliferative lesions.* J Toxicol Pathol, 2012. **25**(3): p. 189-199 [DOI: 10.1293/tox.25.189].
217. Thoolen, B., Maronpot, R.R., Harada, T., et al., *Proliferative and nonproliferative lesions of the rat and mouse hepatobiliary system.* Toxicol Pathol, 2010. **38**(7 Suppl): p. 5s-81s [DOI: 10.1177/0192623310386499].
218. Kolaja, K.L. and Klaunig, J.E., *Vitamin E modulation of hepatic focal lesion growth in mice.* Toxicol Appl Pharmacol, 1997. **143**(2): p. 380-387 [DOI: 10.1006/taap.1996.8089].
219. International Consensus Group for Hepatocellular Neoplasia, *Pathologic diagnosis of early hepatocellular carcinoma: a report of the international consensus group for hepatocellular neoplasia.* Hepatology, 2009. **49**(2): p. 658-664 [DOI: 10.1002/hep.22709].
220. Kojiro, M. and Roskams, T., *Early hepatocellular carcinoma and dysplastic nodules.* Semin Liver Dis, 2005. **25**(2): p. 133-142 [DOI: 10.1055/s-2005-871193].
221. International Working Party, *Terminology of nodular hepatocellular lesions.* Hepatology, 1995. **22**(3): p. 983-993 [DOI: 10.1016/0270-9139(95)90324-0].
222. Marquardt, J.U., Andersen, J.B. and Thorgeirsson, S.S., *Functional and genetic deconstruction of the cellular origin in liver cancer.* Nat Rev Cancer, 2015. **15**(11): p. 653-667 [DOI: 10.1038/nrc4017].

223. Bannasch, P., Haertel, T. and Su, Q., *Significance of Hepatic Preneoplasia in Risk Identification and Early Detection of Neoplasia *.* Toxicologic Pathology, 2003. **31**(1): p. 134-139 [DOI: 10.1080/01926230390173923].
224. Roncalli, M., Roz, E., Coggi, G., et al., *The vascular profile of regenerative and dysplastic nodules of the cirrhotic liver: implications for diagnosis and classification.* Hepatology, 1999. **30**(5): p. 1174-1178 [DOI: 10.1002/hep.510300507].
225. Dhanasekaran, R., Bandoh, S. and Roberts, L.R., *Molecular pathogenesis of hepatocellular carcinoma and impact of therapeutic advances.* F1000Res, 2016. **5**(879) [DOI: 10.12688/f1000research.6946.1].
226. Katayama, Y., Uchino, J., Chihara, Y., et al., *Tumor Neovascularization and Developments in Therapeutics.* Cancers (Basel), 2019. **11**(3) [DOI: 10.3390/cancers11030316].
227. Naumov, G.N., Akslen, L.A. and Folkman, J., *Role of angiogenesis in human tumor dormancy: animal models of the angiogenic switch.* Cell Cycle, 2006. **5**(16): p. 1779-1787 [DOI: 10.4161/cc.5.16.3018].
228. Gupta, M.K. and Qin, R.Y., *Mechanism and its regulation of tumor-induced angiogenesis.* World J Gastroenterol, 2003. **9**(6): p. 1144-1155 [DOI: 10.3748/wjg.v9.i6.1144].
229. Bergers, G. and Benjamin, L.E., *Tumorigenesis and the angiogenic switch.* Nature Reviews Cancer, 2003. **3**(6): p. 401-410 [DOI: 10.1038/nrc1093].
230. Sugimachi, K., Tanaka, S., Terashi, T., et al., *The mechanisms of angiogenesis in hepatocellular carcinoma: angiogenic switch during tumor progression.* Surgery, 2002. **131**(1 Suppl): p. S135-S141 [DOI: 10.1067/msy.2002.119365].
231. Papetti, M. and Herman, I.M., *Mechanisms of normal and tumor-derived angiogenesis.* Am J Physiol Cell Physiol, 2002. **282**(5): p. C947-C970 [DOI: 10.1152/ajpcell.00389.2001].
232. Yancopoulos, G.D., Davis, S., Gale, N.W., et al., *Vascular-specific growth factors and blood vessel formation.* Nature, 2000. **407**(6801): p. 242-248 [DOI: 10.1038/35025215].
233. Compagni, A., Wilgenbus, P., Impagnatiello, M.A., et al., *Fibroblast growth factors are required for efficient tumor angiogenesis.* Cancer Res, 2000. **60**(24): p. 7163-7169 [PMID: 11156426].
234. Heindryckx, F., Mertens, K., Charette, N., et al., *Kinetics of angiogenic changes in a new mouse model for hepatocellular carcinoma.* Mol Cancer, 2010. **9** [DOI: 10.1186/1476-4598-9-219].
235. Geerts, A.M., De Vriese, A.S., Vanheule, E., et al., *Increased angiogenesis and permeability in the mesenteric microvasculature of rats with cirrhosis and portal hypertension: an in vivo study.* Liver Int, 2006. **26**(7): p. 889-898 [DOI: 10.1111/j.1478-3231.2006.01308.x].
236. Qi, Y., Song, Y., Cai, M., et al., *Vascular endothelial growth factor A is a potential prognostic biomarker and correlates with immune cell infiltration in hepatocellular carcinoma.* Journal of Cellular and Molecular Medicine, 2023. **27**(4): p. 538-552 [DOI: https://doi.org/10.1111/jcmm.17678].
237. Lacin, S. and Yalcin, S., *The Prognostic Value of Circulating VEGF-A Level in Patients With Hepatocellular Cancer.* Technol Cancer Res Treat, 2020. **19**: p. 1-8 [DOI: 10.1177/1533033820971677].
238. Ho, M.C., Chen, C.N., Lee, H., et al., *Placenta growth factor not vascular endothelial growth factor A or C can predict the early recurrence after radical resection of hepatocellular carcinoma.* Cancer Lett, 2007. **250**(2): p. 237-249 [DOI: 10.1016/j.canlet.2006.10.005].

239. Amini, A., Masoumi Moghaddam, S., Morris, D.L., et al., *The critical role of vascular endothelial growth factor in tumor angiogenesis.* Curr Cancer Drug Targets, 2012. **12**(1): p. 23-43 [DOI: 10.2174/156800912798888956].
240. Chiang, D.Y., Villanueva, A., Hoshida, Y., et al., *Focal gains of VEGFA and molecular classification of hepatocellular carcinoma.* Cancer Res, 2008. **68**(16): p. 6779-6788 [DOI: 10.1158/0008-5472.Can-08-0742].
241. Runge, A., Hu, J., Wieland, M., et al., *An inducible hepatocellular carcinoma model for preclinical evaluation of antiangiogenic therapy in adult mice.* Cancer Res, 2014. **74**(15): p. 4157-4169 [DOI: 10.1158/0008-5472.Can-13-2311].
242. Medina, J., Arroyo, A.G., Sánchez-Madrid, F., et al., *Angiogenesis in chronic inflammatory liver disease.* Hepatology, 2004. **39**(5): p. 1185-1195 [DOI: 10.1002/hep.20193].
243. Semela, D. and Dufour, J.F., *Angiogenesis and hepatocellular carcinoma.* J Hepatol, 2004. **41**(5): p. 864-880 [DOI: 10.1016/j.jhep.2004.09.006].
244. Kornek, M., Raskopf, E., Tolba, R., et al., *Accelerated orthotopic hepatocellular carcinomas growth is linked to increased expression of pro-angiogenic and prometastatic factors in murine liver fibrosis.* Liver Int, 2008. **28**(4): p. 509-518 [DOI: 10.1111/j.1478-3231.2008.01670.x].
245. Liu, K., Zhang, X., Xu, W., et al., *Targeting the vasculature in hepatocellular carcinoma treatment: Starving versus normalizing blood supply.* Clin Transl Gastroenterol, 2017. **8**(6): p. e98 [DOI: 10.1038/ctg.2017.28].
246. Haratake, J. and Scheuer, P.J., *An immunohistochemical and ultrastructural study of the sinusoids of hepatocellular carcinoma.* Cancer, 1990. **65**(9): p. 1985-1993 [DOI: 10.1002/1097-0142(19900501)65:9<1985::aid-cncr2820650918>3.0.co;2-c].
247. Isomura, T. and Nakashima, T., *Ultrastructure of human hepatocellular carcinoma.* Acta Pathol Jpn, 1980. **30**(5): p. 713-726 [DOI: 10.1111/j.1440-1827.1980.tb00969.x].
248. Edrei, Y., Gross, E., Corchia, N., et al., *Vascular profile characterization of liver tumors by magnetic resonance imaging using hemodynamic response imaging in mice.* Neoplasia, 2011. **13**(3): p. 244-253 [DOI: 10.1593/neo.101354].
249. Yasui, Y., Toyoda, K. and Imai, K., *A primary hepatic malignant mesenchymal tumor with myofibrogenic differentiation in a B6C3F1 mouse.* Toxicol Pathol, 2009. **37**(2): p. 244-248 [DOI: 10.1177/0192623308329341].
250. Man, K., Ng, K.T., Lo, C.M., et al., *Ischemia-reperfusion of small liver remnant promotes liver tumor growth and metastases--activation of cell invasion and migration pathways.* Liver Transpl, 2007. **13**(12): p. 1669-1677 [DOI: 10.1002/lt.21193].
251. Wang, D., Stockard, C.R., Harkins, L., et al., *Immunohistochemistry in the evaluation of neovascularization in tumor xenografts.* Biotech Histochem, 2008. **83**(3-4): p. 179-189 [DOI: 10.1080/10520290802451085].
252. Frachon, S., Gouysse, G., Dumortier, J., et al., *Endothelial cell marker expression in dysplastic lesions of the liver: an immunohistochemical study.* J Hepatol, 2001. **34**(6): p. 850-857 [DOI: 10.1016/s0168-8278(01)00049-6].
253. Morinaga, S., Imada, T., Shimizu, A., et al., *Angiogenesis in hepatocellular carcinoma as evaluated by alpha smooth muscle actin immunohistochemistry.* Hepatogastroenterology, 2001. **48**(37): p. 224-228 [PMID: 11268971].

254. Corliss, B.A., Mathews, C., Doty, R., et al., *Methods to label, image, and analyze the complex structural architectures of microvascular networks.* Microcirculation, 2019. **26**(5): p. e12520 [DOI: 10.1111/micc.12520].
255. Tulessin, M., Sarker, R.S.J., Griger, J., et al., *Vascular Remodeling Is a Crucial Event in the Early Phase of Hepatocarcinogenesis in Rodent Models for Liver Tumorigenesis.* Cells, 2022. **11**(14) [DOI: 10.3390/cells11142129].
256. Ballke, S., Heid, I., Mogler, C., et al., *Correlation of in vivo imaging to morphomolecular pathology in translational research: challenge accepted.* EJNMMI Res, 2021. **11**(1) [DOI: 10.1186/s13550-021-00826-2].
257. Steiger, K., Ballke, S., Yen, H.Y., et al., *[Histopathological research laboratories in translational research : Conception and integration into the infrastructure of pathological institutes]. German.* Pathologe, 2019. **40**(2): p. 172-178 [DOI: 10.1007/s00292-018-0458-2].
258. Brazdziute, E. and Laurinavicius, A., *Digital pathology evaluation of complement C4d component deposition in the kidney allograft biopsies is a useful tool to improve reproducibility of the scoring.* Diagn Pathol, 2011. **6**(Suppl 1) [DOI: 10.1186/1746-1596-6-s1-s5].
259. Bankhead, P., Loughrey, M.B., Fernández, J.A., et al., *QuPath: Open source software for digital pathology image analysis.* Sci Rep, 2017. **7**(1) [DOI: 10.1038/s41598-017-17204-5].
260. D'Souza, J.C., Sultan, L.R., Hunt, S.J., et al., *Microbubble-enhanced ultrasound for the antivascular treatment and monitoring of hepatocellular carcinoma.* Nanotheranostics, 2019. **3**(4): p. 331-341 [DOI: 10.7150/ntno.39514].
261. Böhm, J., Muenzner, J.K., Caliskan, A., et al., *Loss of enhancer of zeste homologue 2 (EZH2) at tumor invasion front is correlated with higher aggressiveness in colorectal cancer cells.* J Cancer Res Clin Oncol, 2019. **145**(9): p. 2227-2240 [DOI: 10.1007/s00432-019-02977-1].
262. Du, Y., Zhang, W., Qiu, H., et al., *Mouse Models of Liver Parenchyma Injuries and Regeneration.* Front Cell Dev Biol, 2022. **10** [DOI: 10.3389/fcell.2022.903740].
263. Brown, Z.J., Heinrich, B. and Greten, T.F., *Mouse models of hepatocellular carcinoma: an overview and highlights for immunotherapy research.* Nature Reviews Gastroenterology & Hepatology, 2018. **15**(9): p. 536-554 [DOI: 10.1038/s41575-018-0033-6].
264. Maitra, R., Thavornwatanayong, T., Venkatesh, M.K., et al., *Development and Characterization of a Genetic Mouse Model of KRAS Mutated Colorectal Cancer.* Int J Mol Sci, 2019. **20**(22) [DOI: 10.3390/ijms20225677].
265. Di Nicolantonio, F. and Bardelli, A., *Mouse models of Kras-mutant colorectal cancer: valuable GEMMs for drug testing?* Clin Cancer Res, 2013. **19**(11): p. 2794-2796 [DOI: 10.1158/1078-0432.Ccr-13-0339].
266. Paschoal, J.P., Bernardo, V., Canedo, N.H., et al., *Microvascular density of regenerative nodule to small hepatocellular carcinoma by automated analysis using CD105 and CD34 immunoexpression.* BMC Cancer, 2014. **14** [DOI: 10.1186/1471-2407-14-72].
267. Nascimento, C., Caroli-Bottino, A., Paschoal, J., et al., *Vascular Immunohistochemical Markers: Contributions to Hepatocellular Nodule Diagnosis in Explanted Livers.* Transplantation Proceedings, 2009. **41**(10): p. 4211-4213 [DOI: https://doi.org/10.1016/j.transproceed.2009.09.068].
268. Hashizume, H., Baluk, P., Morikawa, S., et al., *Openings between defective endothelial cells explain tumor vessel leakiness.* Am J Pathol, 2000. **156**(4): p. 1363-1380 [DOI: 10.1016/s0002-9440(10)65006-7].

269. Denekamp, J., *Review article: angiogenesis, neovascular proliferation and vascular pathophysiology as targets for cancer therapy.* Br J Radiol, 1993. **66**(783): p. 181-196 [DOI: 10.1259/0007-1285-66-783-181].
270. Kalebic, T., Garbisa, S., Glaser, B., et al., *Basement membrane collagen: degradation by migrating endothelial cells.* Science, 1983. **221**(4607): p. 281-283 [DOI: 10.1126/science.6190230].
271. Baluk, P., Morikawa, S., Haskell, A., et al., *Abnormalities of basement membrane on blood vessels and endothelial sprouts in tumors.* Am J Pathol, 2003. **163**(5): p. 1801-1815 [DOI: 10.1016/s0002-9440(10)63540-7].
272. Egginton, S., Zhou, A.L., Brown, M.D., et al., *Unorthodox angiogenesis in skeletal muscle.* Cardiovasc Res, 2001. **49**(3): p. 634-646 [DOI: 10.1016/s0008-6363(00)00282-0].
273. Jerdan, J.A., Michels, R.G. and Glaser, B.M., *Extracellular matrix of newly forming vessels--an immunohistochemical study.* Microvasc Res, 1991. **42**(3): p. 255-265 [DOI: 10.1016/0026-2862(91)90060-o].
274. Yang, W., Li, Z., Qin, R., et al., *YY1 Promotes Endothelial Cell-Dependent Tumor Angiogenesis in Hepatocellular Carcinoma by Transcriptionally Activating VEGFA.* Front Oncol, 2019. **9** [DOI: 10.3389/fonc.2019.01187].
275. Carmeliet, P. and Jain, R.K., *Angiogenesis in cancer and other diseases.* Nature, 2000. **407**(6801): p. 249-257 [DOI: 10.1038/35025220].
276. Chen, Y.W., Pan, H.B., Tseng, H.H., et al., *Assessment of blood flow in hepatocellular carcinoma: correlations of computed tomography perfusion imaging and circulating angiogenic factors.* Int J Mol Sci, 2013. **14**(9): p. 17536-17552 [DOI: 10.3390/ijms140917536].
277. Yaghjyan, L., Heng, Y.J., Baker, G.M., et al., *Reliability of CD44, CD24, and ALDH1A1 immunohistochemical staining: Pathologist assessment compared to quantitative image analysis.* Front Med (Lausanne), 2022. **9** [DOI: 10.3389/fmed.2022.1040061].
278. Baker, G.M., Bret-Mounet, V.C., Wang, T., et al., *Immunohistochemistry scoring of breast tumor tissue microarrays: A comparison study across three software applications.* J Pathol Inform, 2022. **13** [DOI: 10.1016/j.jpi.2022.100118].
279. Siddiqui, I., Bilkey, J., McKee, T.D., et al., *Digital quantitative tissue image analysis of hypoxia in resected pancreatic ductal adenocarcinomas.* Front Oncol, 2022. **12** [DOI: 10.3389/fonc.2022.926497].
280. Cui, M. and Zhang, D.Y., *Artificial intelligence and computational pathology.* Laboratory Investigation, 2021. **101**(4): p. 412-422 [DOI: 10.1038/s41374-020-00514-0].
281. Cizkova, K., Foltynkova, T., Gachechiladze, M., et al., *Comparative Analysis of Immunohistochemical Staining Intensity Determined by Light Microscopy, ImageJ and QuPath in Placental Hofbauer Cells.* Acta Histochem Cytochem, 2021. **54**(1): p. 21-29 [DOI: 10.1267/ahc.20-00032].
282. Aeffner, F., Zarella, M.D., Buchbinder, N., et al. *Introduction to Digital Image Analysis in Whole-slide Imaging: A White Paper from the Digital Pathology Association.* Journal of Pathology Informatics, 2019. **10**(1): [DOI: 10.4103/jpi.jpi_82_18].
283. Korbar, B., Olofson, A.M., Miraflor, A.P., et al., *Deep Learning for Classification of Colorectal Polyps on Whole-slide Images.* J Pathol Inform, 2017. **8**(1) [DOI: 10.4103/jpi.jpi_34_17].
284. Nagtegaal, I.D., Odze, R.D., Klimstra, D., et al., *The 2019 WHO classification of tumours of the digestive system.* Histopathology, 2020. **76**(2): p. 182-188 [DOI: 10.1111/his.13975].
285. Zhang, Z.S., Zhou, H.N., He, S.S., et al., *Research advances in pericyte function and their roles in diseases.* Chin J Traumatol, 2020. **23**(2): p. 89-95 [DOI: 10.1016/j.cjtee.2020.02.006].

286. Nasarre, P., Thomas, M., Kruse, K., et al., *Host-derived angiopoietin-2 affects early stages of tumor development and vessel maturation but is dispensable for later stages of tumor growth.* Cancer Res, 2009. **69**(4): p. 1324-1333 [DOI: 10.1158/0008-5472.Can-08-3030].
287. Morikawa, S., Baluk, P., Kaidoh, T., et al., *Abnormalities in pericytes on blood vessels and endothelial sprouts in tumors.* Am J Pathol, 2002. **160**(3): p. 985-1000 [DOI: 10.1016/s0002-9440(10)64920-6].
288. Vizio, B., Bosco, O., David, E., et al., *Cooperative Role of Thrombopoietin and Vascular Endothelial Growth Factor-A in the Progression of Liver Cirrhosis to Hepatocellular Carcinoma.* Int J Mol Sci, 2021. **22**(4) [DOI: 10.3390/ijms22041818].
289. Ma, M., Hua, S., Li, G., et al., *Prolyl hydroxylase domain protein 3 and asparaginyl hydroxylase factor inhibiting HIF-1 levels are predictive of tumoral behavior and prognosis in hepatocellular carcinoma.* Oncotarget, 2017. **8**(8): p. 12983-13002 [DOI: 10.18632/oncotarget.14677].
290. Stroescu, C., Dragnea, A., Ivanov, B., et al., *Expression of p53, Bcl-2, VEGF, Ki67 and PCNA and prognostic significance in hepatocellular carcinoma.* J Gastrointestin Liver Dis, 2008. **17**(4): p. 411-417 [PMID: 19104702].
291. Poon, R.T., Lau, C.P., Cheung, S.T., et al., *Quantitative correlation of serum levels and tumor expression of vascular endothelial growth factor in patients with hepatocellular carcinoma.* Cancer Res, 2003. **63**(12): p. 3121-3126 [PMID: 12810638].
292. Hanahan, D. and Coussens, L.M., *Accessories to the crime: functions of cells recruited to the tumor microenvironment.* Cancer Cell, 2012. **21**(3): p. 309-322 [DOI: 10.1016/j.ccr.2012.02.022].
293. de Oliveira, A., Castanhole-Nunes, M.M.U., Biselli-Chicote, P.M., et al., *Differential expression of angiogenesis-related miRNAs and VEGFA in cirrhosis and hepatocellular carcinoma.* Arch Med Sci, 2020. **16**(5): p. 1150-1157 [DOI: 10.5114/aoms.2020.97967].
294. Giatromanolaki, A., Kotsiou, S., Koukourakis, M.I., et al., *Angiogenic factor expression in hepatic cirrhosis.* Mediators Inflamm, 2007. **2007** [DOI: 10.1155/2007/67187].
295. El-Assal, O.N., Yamanoi, A., Soda, Y., et al., *Clinical significance of microvessel density and vascular endothelial growth factor expression in hepatocellular carcinoma and surrounding liver: possible involvement of vascular endothelial growth factor in the angiogenesis of cirrhotic liver.* Hepatology, 1998. **27**(6): p. 1554-1562 [DOI: 10.1002/hep.510270613].
296. Yamaguchi, R., Yano, H., Iemura, A., et al., *Expression of vascular endothelial growth factor in human hepatocellular carcinoma.* Hepatology, 1998. **28**(1): p. 68-77 [DOI: 10.1002/hep.510280111].
297. Yoshiji, H., Kuriyama, S., Yoshii, J., et al., *Vascular endothelial growth factor and receptor interaction is a prerequisite for murine hepatic fibrogenesis.* Gut, 2003. **52**(9): p. 1347-1354 [DOI: 10.1136/gut.52.9.1347].
298. Corpechot, C., Barbu, V., Wendum, D., et al., *Hypoxia-induced VEGF and collagen I expressions are associated with angiogenesis and fibrogenesis in experimental cirrhosis.* Hepatology, 2002. **35**(5): p. 1010-1021 [DOI: 10.1053/jhep.2002.32524].
299. King, K.L., Hwang, J.J., Chau, G.Y., et al., *Ki-67 expression as a prognostic marker in patients with hepatocellular carcinoma.* J Gastroenterol Hepatol, 1998. **13**(3): p. 273-279 [DOI: 10.1111/j.1440-1746.1998.01555.x].
300. Mohamed, W.S., Omar, M.M., Khayri, T.M., et al., *Assessment of the Proliferative Marker Ki-67 and p53 Protein Expression in HBV- and HCV-related Hepatocellular Carcinoma Cases in Egypt.* Int J Health Sci (Qassim), 2008. **2**(1): p. 27-34 [PMCID: PMC3068722].

301. Nakanishi, K., Sakamoto, M., Yamasaki, S., et al., *Akt phosphorylation is a risk factor for early disease recurrence and poor prognosis in hepatocellular carcinoma.* Cancer, 2005. **103**(2): p. 307-312 [DOI: 10.1002/cncr.20774].
302. Huang, Z., Zhou, P., Li, S., et al., *Prediction of the Ki-67 marker index in hepatocellular carcinoma based on Dynamic Contrast-Enhanced Ultrasonography with Sonazoid.* Insights into Imaging, 2022. **13**(1) [DOI: 10.1186/s13244-022-01320-6].
303. Koskinas, J., Petraki, K., Kavantzas, N., et al., *Hepatic expression of the proliferative marker Ki-67 and p53 protein in HBV or HCV cirrhosis in relation to dysplastic liver cell changes and hepatocellular carcinoma.* Journal of Viral Hepatitis, 2005. **12**(6): p. 635-641 [DOI: https://doi.org/10.1111/j.1365-2893.2005.00635.x].
304. D'Errico, A., Grigioni, W.F., Fiorentino, M., et al., *Overexpression of p53 protein and Ki67 proliferative index in hepatocellular carcinoma: an immunohistochemical study on 109 Italian patients.* Pathol Int, 1994. **44**(9): p. 682-687 [DOI: 10.1111/j.1440-1827.1994.tb02947.x].
305. Kitagawa, K., Nakajima, G., Kuramochi, H., et al., *Lymphatic vessel endothelial hyaluronan receptor-1 is a novel prognostic indicator for human hepatocellular carcinoma.* Mol Clin Oncol, 2013. **1**(6): p. 1039-1048 [DOI: 10.3892/mco.2013.167].
306. Carreira, C.M., Nasser, S.M., di Tomaso, E., et al., *LYVE-1 Is Not Restricted to the Lymph Vessels: Expression in Normal Liver Blood Sinusoids and Down-Regulation in Human Liver Cancer and Cirrhosis.* Cancer Research, 2001. **61**(22): p. 8079-8084 [PMID: 11719431].
307. Leu, A.J., Berk, D.A., Lymboussaki, A., et al., *Absence of Functional Lymphatics within a Murine Sarcoma: A Molecular and Functional Evaluation.* Cancer Research, 2000. **60**(16): p. 4324-4327 [PMID: 10969769].
308. Tanaka, S., Sugimachi, K., Yamashita, Y., et al., *Angiogenic switch as a molecular target of malignant tumors.* J Gastroenterol, 2003. **38** (Suppl 15): p. 93-97 [PMID: 12698880].
309. He, L., Tian, D.A., Li, P.Y., et al., *Mouse models of liver cancer: Progress and recommendations.* Oncotarget, 2015. **6**(27): p. 23306-23322 [DOI: 10.18632/oncotarget.4202].
310. Cancer Genome Atlas Research Network, *Comprehensive and Integrative Genomic Characterization of Hepatocellular Carcinoma.* Cell, 2017. **169**(7): p. 1327-1341.e1323 [DOI: 10.1016/j.cell.2017.05.046].
311. Hussain, S.P., Schwank, J., Staib, F., et al., *TP53 mutations and hepatocellular carcinoma: insights into the etiology and pathogenesis of liver cancer.* Oncogene, 2007. **26**(15): p. 2166-2176 [DOI: 10.1038/sj.onc.1210279].

11 LIST OF FIGURES

12 LIST OF TABLES

13 ANNEX

13.1.1 POSTER PRESENTATION AT THE ANNUAL MEETING OF THE GERMAN SOCIETY FOR PATHOLOGY (DGP) IN MÜNSTER, JUNE 2022

CRC1366 Vascular Control of Organ Function

POSTER-CODE: P14.05

Institut für allgemeine Pathologie und pathologische Anatomie
Technische Universität München

Vascular remodeling is a crucial event in the early phase of hepatocarcinogenesis in rodent models for liver tumorigenesis.

Margaret Tulessin [1], Rim Sabrina Jahan Sarker [1], Joscha Griger [2], Wilko Weichert [1], Katja Steiger [1], Carolin Mogler [1]
1. Institute of Pathology, School of Medicine, TU Munich, Munich, Germany
2. Institute of Molecular Oncology and Functional Genomics, TU Munich, Munich, Germany

Introduction

The investigation of hepatocarcinogenesis is one of the major fields of interest in the oncology research and rodent models are commonly used to unravel the pathophysiology of onset and progression of hepatocellular carcinoma (HCC). HCC is a highly vascularized tumor and vascular remodeling is one of the hallmarks in tumor progression. To date, only few detailed data exist about the vasculature and vascular remodeling in rodent models used for hepatocarcinogenesis [1,2]. The aim of this study was, therefore, to perform a comprehensive characterization and comparison of the vasculature in mouse models used for hepatocarcinogenesis studies.

Results

262 FCA lesions and 36 HCC lesions were investigated so far. Analysis included microvessel density (MVD) using CD31 and Collagen IV stainings and pixel analysis of αSMA and Desmin as well as an analysis of LYVE1 staining (Figure 1, 2).

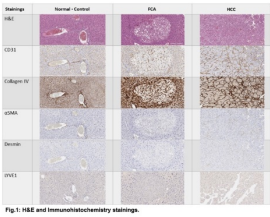

Fig.1: H&E and immunohistochemistry stainings.

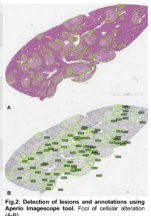

Fig.2: Detection of lesions and annotations using Aperio ImageScope tool. Foci of cellular alteration (A-B).

Furthermore, the size of the vessels were used to automatically define into 3 groups of vessels (small, medium and large) (Figure 3, 4) .

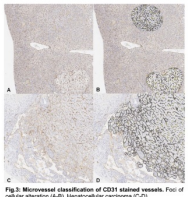

Fig.3: Microvessel classification of CD31 stained vessels. Foci of cellular alteration (A-B). Hepatocellular carcinoma (C-D). Black coloured are small-size (< 150 μm^2), yellow coloured are medium-size (150-500 μm^2), grey coloured are large-size (>500 μm^2).

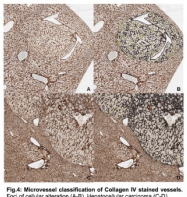

Fig.4: Microvessel classification of Collagen IV stained vessels. Foci of cellular alteration (A-B). Hepatocellular carcinoma (C-D). Grey coloured are small-size (< 150 μm^2), yellow coloured are medium-size (150-500 μm^2), black coloured are large-size (>500 μm^2).

Methods

In this study, formalin fixed paraffin-embedded samples of 25 genetically engineered mice (GEMM) for liver tumorigenesis were used. The liver lesions detected in these slides were analyzed by two experienced liver and comparative pathologists and diagnosed according to the existing guidelines [1]. The vasculature of hepatocellular carcinoma (HCC) and preneoplastic foci of cellular alteration (FCA) were comprehensively characterized by using immunohistochemistry techniques (CD31, Collagen IV, αSMA, Desmin and LYVE1). Computational image analysis was performed to evaluate selected parameters including microvessel density, pericyte coverage, vessel size, intratumoral vessel distribution and architecture using Aperio ImageScope software (Version 12.4.0.7018, Leica Biosystems) and Definiens software programs (Version XD 64 2.7, Definiens AG, Munich, Germany). Statistical analyses were performed with GraphPad Prism 9 (GraphPad Software, Inc., San Diego, United States).

Results

HCC presented with a significant lower number of vessels, but larger vessel size and increased coverage leading to a higher degree of maturation, whereas FCA lesions were presented with a higher microvessel density and a higher amount of smaller but more immature vessels (Figure 5, 6).

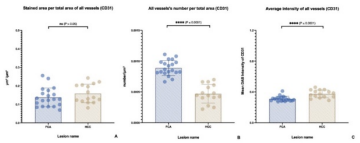

Fig.5: Microvessel analysis of CD31 stained vessels. Error bars indicate mean and standard deviation for each lesion.

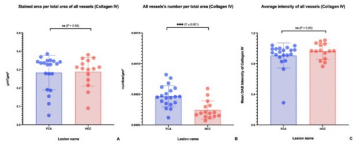

Fig.6: Microvessel analysis of Collagen IV stained vessels. Error bars indicate mean and standard deviation for each lesion.

Conclusion

Our results clearly demonstrate, that vascular remodeling is present in early stages of liver tumorigenesis making mouse models with a histological spectrum of FCA and HCC as an attractive tool for angiogenesis research.

References

[1] Bob Thoolen et al. Proliferative and nonproliferative lesions of the rat and mouse hepatobiliary system. Toxicol Pathol 2010 Dec;38(7 Suppl):5S-81S.doi: 10.1177/0192623310386499.

[2] Bob Thoolen et al. Comparative histomorphological review of rat and human hepatocellular proliferative lesions. J Toxicol Pathol 2012 Sep;25(3):189-99.doi: 10.1293/tox.25.189. Epub 2012 Oct 1.

13.1.2 PUBLICATION IN CELLS (BASEL), JULY 2022

cells

IMPACT FACTOR 7.666

Indexed in: PubMed

Article

Vascular Remodeling Is a Crucial Event in the Early Phase of Hepatocarcinogenesis in Rodent Models for Liver Tumorigenesis

Margaret Tulessin, Rim Sabrina Jahan Sarker, Joscha Griger, Thomas Leibing, Cyrill Geraud, Wilko Weichert, Katja Steiger and Carolin Mogler

MDPI

https://doi.org/10.3390/cells11142129

cells

MDPI

Article

Vascular Remodeling Is a Crucial Event in the Early Phase of Hepatocarcinogenesis in Rodent Models for Liver Tumorigenesis

Margaret Tulessin [1,†], Rim Sabrina Jahan Sarker [1,2,†], Joscha Griger [3], Thomas Leibing [4], Cyrill Geraud [4,5,6], Wilko Weichert [1,2], Katja Steiger [1,2] and Carolin Mogler [1,2,*]

1 Institute of Pathology, School of Medicine, Technical University of Munich (TUM), 81675 Munich, Germany; margaret.tulessin@tum.de (M.T.); sabrina.sarker@tum.de (R.S.J.S.); wilko.weichert@tum.de (W.W.); katja.steiger@tum.de (K.S.)
2 Comparative Experimental Pathology, School of Medicine, Technical University of Munich (TUM), 81675 Munich, Germany
3 Institute of Molecular Oncology and Functional Genomics, School of Medicine, Technical University of Munich (TUM), 81675 Munich, Germany; joscha.griger@tum.de
4 Department of Dermatology, Venereology, and Allergology, University Medical Center and Medical Faculty Mannheim, Heidelberg University, 68167 Mannheim, Germany; thomas.leibing@medma.uni-heidelberg.de (T.L.); cyrill.geraud@umm.de (C.G.)
5 Section of Clinical and Molecular Dermatology, University Medical Center and Medical Faculty Mannheim, Heidelberg University, 68167 Mannheim, Germany
6 European Center for Angioscience (ECAS), Medical Faculty Mannheim, Heidelberg University, 68167 Mannheim, Germany
* Correspondence: carolin.mogler@tum.de; Tel.: +49-894-4140-4166
† These authors contributed equally to this work.

check for updates

Citation: Tulessin, M.; Sarker, R.S.J.; Griger, J.; Leibing, T.; Geraud, C.; Weichert, W.; Steiger, K.; Mogler, C. Vascular Remodeling Is a Crucial Event in the Early Phase of Hepatocarcinogenesis in Rodent Models for Liver Tumorigenesis. *Cells* **2022**, *11*, 2129. https://doi.org/10.3390/cells11142129

Academic Editor: Ezequiel Álvarez

Received: 27 May 2022
Accepted: 1 July 2022
Published: 6 July 2022

Publisher's Note: MDPI stays neutral with regard to jurisdictional claims in published maps and institutional affiliations.

Simple Summary: Hepatocellular carcinoma (HCC) is a highly vascularized tumor and remodeling of the tumor vasculature is one of the hallmarks of tumor progression. Mouse models are elegant tools to study the onset and progression of liver tumors. However, only few data exist on the vasculature and vascular remodeling processes especially in the early phase of hepatocarcinogenesis. The aim of this study was therefore to perform a comprehensive characterization and comparison of the vasculature in mouse models used for hepatocarcinogenesis studies. For this purpose, we characterized the preneoplastic foci of cellular alteration (FCA) and hepatocellular carcinoma (HCC) by using tissue-based techniques and computer-assisted analysis to better understand if and how vascular remodeling appears in rodent models for liver tumorigenesis. Our findings demonstrated crucial differences in the number and size of the vessels, degree of maturation and intratumoral localization of the vasculature in FCA and HCC, clearly indicating that vascular remodeling is an important step in the early phase of liver tumorigenesis of rodent models.

Abstract: The investigation of hepatocarcinogenesis is a major field of interest in oncology research and rodent models are commonly used to unravel the pathophysiology of onset and progression of hepatocellular carcinoma. HCC is a highly vascularized tumor and vascular remodeling is one of the hallmarks of tumor progression. To date, only a few detailed data exist about the vasculature and vascular remodeling in rodent models used for hepatocarcinogenesis. In this study, the vasculature of HCC and the preneoplastic foci of alteration (FCA) of different mouse models with varying genetic backgrounds were comprehensively characterized by using immunohistochemistry (CD31, Collagen IV, αSMA, Desmin and LYVE1) and RNA in situ hybridization (VEGF-A). Computational image analysis was performed to evaluate selected parameters including microvessel density, pericyte coverage, vessel size, intratumoral vessel distribution and architecture using the Aperio ImageScope and Definiens software programs. HCC presented with a significantly lower number of vessels, but larger vessel size and increased coverage, leading to a higher degree of maturation, whereas FCA lesions presented with a higher microvessel density and a higher amount of smaller but more immature vessels. Our results clearly demonstrate that vascular remodeling is present and crucial in

early stages of experimental hepatocarcinogenesis. In addition, our detailed characterization provides a strong basis for further angiogenesis studies in these experimental models.

Keywords: hepatocellular carcinoma; foci of cellular alteration; vessel analysis; vascular remodeling; image analysis; animal model

1. Introduction

Primary liver tumors are the sixth-most commonly diagnosed cancer and third-leading cause of cancer death worldwide [1]. A total of 75–85% of those tumors are hepatocellular carcinoma (HCC) [2–4]. There are several predisposing factors for HCC, including chronic viral hepatitis, cirrhosis, alcohol abuse and non-alcoholic fatty liver disease (NAFLD) [5–13]. Independent of their etiology, HCC are highly vascularized neoplasms in which angiogenesis and vascular remodeling play an important role in tumor onset and progression [14–16]. This so called angiogenic switch is a hallmark in the development of liver cancer including the transformation into a fully arterialized vascular supply, which in turn further promotes tumor growth and disease progression [17]. This process is mainly driven by an imbalance of pro- and antiangiogenic factors caused by continuous tumor cell growth and subsequent development of hypoxia [18]. Regulated by prolyl hydroxylases (PHDs), oxygen sensors (including the family of hypoxia inducible factors such as HIF1alpha) enhance the production of the vascular endothelial growth factor (VEGF), which in turn leads to the formation of new blood vessels [19,20]. Not only VEGF but several other angiogenic molecules have been identified to promote this remodeling including insulin growth factor-2 (IGF-2), platelet-derived growth factor (PDGF) fibroblast growth factor (FGF), thrombospondin (TS) and the angiopoietin family (ANG) [14,17,21,22]. The development of tumor vessels is characterized by the formation of typically irregular-sized and -shaped vessels, with abnormal vascular branching pattern, tortuous properties, a high level of leakiness and partial coverage by pericytes with incomplete basal membrane [16,23]. Ultrastructural findings from electron microscopy studies further identified endothelial cell thickening, reduction or lack of fenestrations, formation of basement membranes, paucity of sinusoidal macrophages and a higher rate of small arterioles with smooth muscle in their walls [23]. In more recent comparative studies, both murine and human HCC presented with a robust loss of differentiation markers in liver sinusoidal endothelial markers (LSEC) [14] and the potency of endothelial cells to lose their polarity, resulting in stratification and protrusion into the vessel lumen [24]. Fully developed HCC tumor nodules in a Cre-inducible mouse model using the SV40 large T antigen were proven to establish a functional vasculature by cooption, remodeling, and angiogenic expansion of the preexisting sinusoidal liver vasculature with increasing signs of vascular immaturity during tumor progression [15]. The vasculature thus undergoes a subsequent transformation and remodeling with loss of the specifically differentiated morphology of healthy liver sinusoids and displaying characteristics of capillary and precapillary blood vessels [23]. Recent studies further discuss the involvement of (secreted) factors such as suppressors of cytokine signaling 2 (SOCS 2) and ATAD2 as a member of the ATP family in HCC progression, molecules well known from physiological liver regeneration [25,26].

Chemically induced or genetically engineered rodent models are widely used to investigate and modulate the process of hepatocarcinogenesis [27]. Both model types typically present with a wide range of histopathological diagnosis [28]. Among these, proliferative preneoplastic lesions such as foci of cellular alteration (FCA) and early (small) hepatocellular carcinoma (HCC) are common findings [29]. In particular, the former are rarely taken into account when performing studies on the development and progression of HCC [27] unless given evidence that FCA (especially clear cell, basophilic and eosinophilic FCA) are very likely to resemble dysplastic nodules (DN) in humans and progression to HCC has been demonstrated [30]. In particular in newly designed genetic mouse models,

little is known on the vasculature in early stages of liver tumorigenesis; and to date, it is not yet fully clarified if the development and progression from FCA to HCC also include mechanisms of vascular remodeling, likewise observed in human hepatocarcinogenesis and some chemically induced models [31]. Our study tries to address these open questions performing a computer-assisted in-depth characterization of the vasculature with focus on proliferative lesions in early stages of tumorigenesis in GEMM.

2. Materials and Methods

Tissue collection: All tissue samples of mice were processed at the Comparative Experimental Pathology (CEP) at the Institute of Pathology, Technical University Munich (TUM). Animals were initially provided to our collaboration partners (J.G.) by the Welcome Trust Sanger Institute, Genome Campus, Hinxton, Cambridge, CB10 1SA, UK. Experiments were approved by the local ethical committees in both the UK and Germany (TV 55.2-2532.Vet_02-16-143, government of Oberbayern; year of approval included in number). Mice were all kept under standard laboratory conditions (12 h day/night cycle, water and standard diet ad libitum, no special diet). Only samples from animals originating from endpoint studies were included. Samples from animals with unclear/insufficient extent of genetic knockdown were excluded from this study. A total of 25 formalin-fixed paraffin-embedded (FFPE) blocks from KRAS [28], KRAS/adenosine kinase (Adk) [32] and KRAS/ nuclear factor IA (Nfia) [33] genetically engineered mice (GEMM) were included in this study. These mice have previously been extensively characterized and chosen for this study due to a high tumor burden including a high percentage of FCA and HCC tumor nodules [28]. No differences in terms of number or distribution of histological diagnosis were observed upon further genetic modification (ADk/Nfia) and all mice were used equally for this study.

The FFPE blocks were cut and tissue slides (2–3 µm) were stained with hematoxylin and eosin (H&E) according to standard protocols. Slides were then independently evaluated by two experienced liver and comparative pathologists (K.S. and C.M.) and diagnosed according to existing guidelines for diagnosis of proliferative liver lesions in rodents [29]. Lesions with definite morphological diagnosis of FCA (clear cell, basophilic and eosinophilic subtype) and HCC were then selected for this study.

Immunohistochemistry: The intralesional vasculature of FCA and HCC was characterized by immunohistochemistry including staining for vascular adhesion molecule CD31 [34] (1:100; DIA-310, Dianova, Hamburg, Germany), Collagen IV [35] (1:50; CL50451AP, Cedarlane, ON, Canada), smooth muscle actin (α-SMA) [24] (1:500; ab5694, Abcam, Cambridge, UK), LYVE1 [36] (1:7000; ab33682, Abcam, Cambridge, UK), and Desmin [15] (1:50; M0760, DAKO, Santa Clara, CA, USA) using standard protocols [37,38].

RNAscope (in situ hybridization (ISH) and immunohistochemistry): Levels of vascular endothelial growth factor A (VEGF-A) were assessed by RNAscope (RNAscope multiplex fluorescent reagent Kit v2 Assay, 323100-USM, ACD, Newark, NJ, USA) according to the manufacturer's protocol.

Computer-assisted image analysis: Slides were scanned using the slide scanner Aperio AT2 (Leica Biosystems, Nussloch, Germany) at a magnification of 40×. Selected regions of interest (ROIs) were then manually annotated the on Aperio ImageScope software (Version 12.4.0.7018, Leica Biosystems). Analysis of intralesional vasculature was performed using computational approaches. Microvessel density (MVD) was assessed using Definiens Tissue Studio of CD31- and Collagen IV-stained vessels were analyzed by Definiens Architect (version XD 64 2.7, Definiens AG, Munich, Germany) using the algorithm 'Marker Area Detection'. ROIs were transferred from ImageScope using a default feature in Definiens. Subgroups of blood vessel size were defined in accordance with published literature of vessel size definitions in rats [39] and adopted for computer-assisted evaluation referring to area (but not diameter). The vessel areas for subgroup analysis were measured by annotating the vessels and calculating the average of vessel area, in order to set the criteria. Size of the vessels was then used to automatically define 3 groups of vessels—small (<150 μm^2),

medium (150–500 μm^2), large (>500 μm^2) vessels. Computer-analyzed quantitative vessel data were normalized accordingly as a ratio, providing three values for each vessel group: stained vessel area per total lesion area, stained vessel number per total lesion area and average staining intensity of the lesion. Heatmaps were generated based on the density of the three vessel subgroups mentioned above, using Definiens Architect (version XD 64 2.7, Definiens AG, Munich, Germany). The heatmap evaluation was performed according to published literature [40], including colored-coded evaluation of density of marker expression (green color for the lowest density, yellow color for medium density, and red color for the highest density). The analysis was performed semi-quantitively, according to the highest hotspot locations (marked in red color) within the lesion (FCA or HCC) based on their computer-defined location (peripheral or central part of the lesion/intralesional). Each slide was evaluated by 2 independent investigators (R.S.J.S. and M.T.). The hotspot was referred to as the highest density of micro-vessel area (small/medium/large).

The staining for αSMA and Desmin were analyzed using the Aperio ImageScope software with the algorithm 'Positive Pixel Count v9' as previously described [12]. The default set of parameters of the algorithm was modified according to the stain contrast and intensity of the scanned images. The algorithm measured the intensity of the stain (brown signal) for the whole section. The total positive pixel was then normalized to the total area of the tissue section (pixel/mm^2). The general expression of αSMA and Desmin was weak in both FCA and HCC lesions; therefore, pixels were counted automatically and intensity evaluated. LYVE1 expression was evaluated semi-quantitative and given as percentage (%) of vasculature/lesion stained for LYVE1.

For quantifying VEGF-A mRNA expression, an open-source image analysis software, 'QuPath' (version 0.2.3, Queen's University Belfast, Ireland) was used [41]. The ROIs annotated on ImageScope were transferred as xml files onto QuPath using a software script developed by the QuPath developer. Firstly, cells were segmented using a modified 'Cell detection' algorithm. For probe (VEGF-A) detection, the 'Subcellular detection' algorithm was chosen and a detection threshold was adjusted interactively until all the probe dots are detected. The minimum and maximum spot size ranged from 0.5 to 3 μm^2. Larger areas were considered as clusters of spots. The total number of subcellular spots of clusters for each ROI was counted.

Statistical analysis: Statistical analyses were performed with GraphPad Prism (GraphPad Software 9.1.1. (223), Inc., San Diego, CA, United States). The cut off for statistical significance was p value ≤ 0.05. The selection of statistical test was performed according to the normal distribution tests (Shapiro–Wilk and Kolmogorov–Smirnov test). If groups were not normally distributed then a non-parametric test (Mann–Whitney U test) was performed, whereas an unpaired T-test was performed if groups were normally distributed. The heatmap analysis was statistically compared with Fisher's eact test. Statistical supervision and guidance were performed by Dr. Katty Castillo and Birgit Waschulzik, Institute of Medical Informatics, Statistics and Epidemiology, Technical University of Munich (TUM), Munich, Germany.

3. Results

A total of 262 FCAs and 36 HCCs were identified by histological classification. Manual annotation for further computational analysis of H&E staining was performed (Figure 1A–D and Supplementary Figure S1). Median FCA lesion in the cohort was 4.83 mm (ranging from 0.07–9.603 mm) and distributed multifocally up to 70 lesions per slide. The median HCC lesion size was 9.85 mm (range: 0.523–19.18 mm) and distributed mostly as one lesion per slide. Based on H&E morphology, FCA showed a homogenous vascular pattern with a predominant appearance of narrow vessels. The HCC sample, however, especially larger specimens, presented with a more inhomogeneous pattern including areas of narrow but also dilated and angled vessels surrounding tumor cell clusters. Necrosis was not observable within the smaller tumor nodules (FCA/HCC) but detectable in the larger HCC nodules. An overview of the various vascular patterns observed in H&E is shown in

Supplementary Figure S1. Immunohistochemical staining was performed against adhesion molecule CD31 to highlight endothelial cells (FCA in Figure 1E, HCC in Figure 1F, additional pictures of different patterns are in Supplementary Figure S1) and Collagen IV to highlight vascular basal membrane components (FCA in Figure 1G, HCC in Figure 1H). In the subsequent computational analysis, the total number of vessels, assessed by CD31 and Collagen IV, was significantly higher in FCAs than in HCCs (Figure 2A,B). Analysis of staining intensities showed opposite results, where HCC presented with a stronger CD31 staining intensity but not Collagen IV (Figure 2C,D). No differences were observed in total area covered by intralesional vessels (Figure 2E,F).

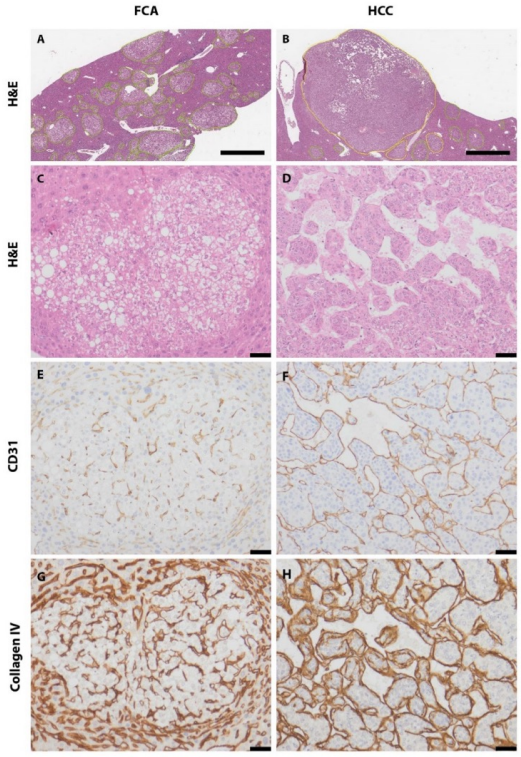

Figure 1. Annotation and immunostaining of foci of cellular alteration (FCA) and hepatocellular carcinoma (HCC). FCA annotated with green color in H&E (**A**); HCC annotated with yellow color in H&E (**B**); representative image of FCA (**C**) (H&E) and HCC (**D**) (H&E); CD31 immunostaining in FCA I and HCC (**E**,**F**). Collagen IV immunostaining in FCA (**G**) and HCC (**H**). Scale bar (**A**,**B**): 2 mm (magnification 1.5×). Scale bar (**C**–**F**): 50 µm (magnification 20×).

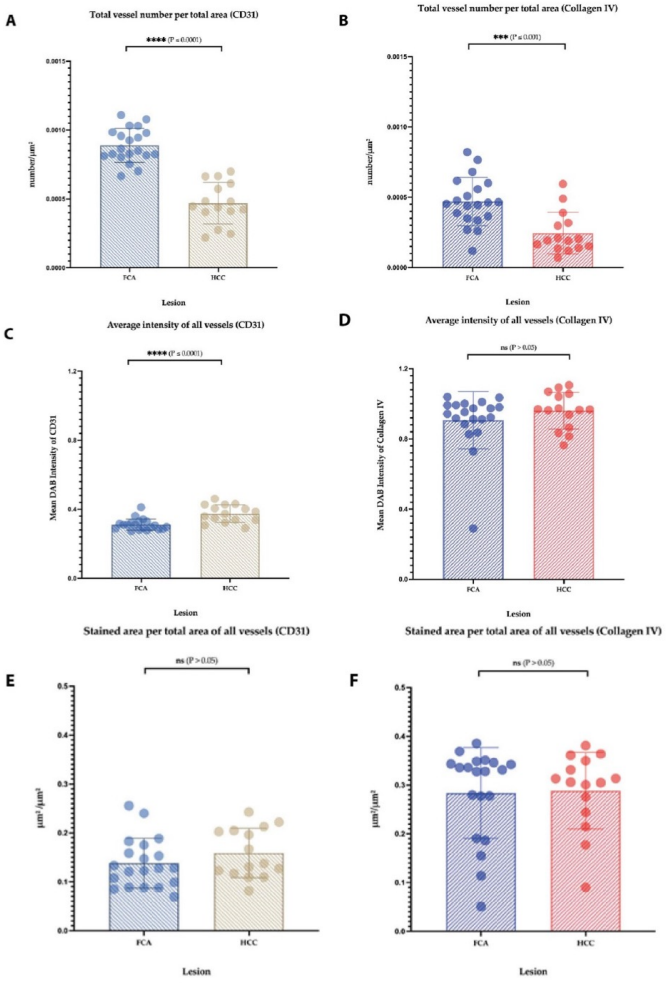

Figure 2. Detailed vessel analysis by CD31 and Collagen IV in FCA and HCC. Total number of vessels in FCA versus HCC by CD31 (**A**) and Collagen IV (**B**); average staining intensity of vessels by CD31 (**C**) and Collagen IV (**D**). No differences were observed in total vessel area: CD31 (**E**) and Collagen IV (**F**). Error bars show the mean and standard deviation for each lesion. *p*-values: Not statistically significant (ns) p value > 0.05; for statistical significance, accepted *** = p value $\leq$ 0.001, and **** = p value $\leq$ 0.0001.

For a detailed vessel analysis according to their size, a subgrouping of vessels was performed on CD31 (Figure 3A–D) and Collagen IV immunostaining (Figure 3E–H) dividing the vessels into small, medium and large (as described earlier in the Material and Methods section). Regarding the vessel area in CD31 staining, a significantly larger area in FCA was

covered by small- and medium-sized vessels (Figure 4A,B), on the contrary HCC presented with a significant amount of large vessel areas (Figure 4C). In Collagen IV-stained vessel areas, and in CD31-stained vessels, FCA presented with a significantly larger area covered by small- and medium-sized vessels (Figure 4D,E), whereas no differences were observed in large vessel areas between FCA and HCC (Figure 4F). Consistent with the finding that a larger area was covered by small- and medium-sized vessels, the total number of small and medium vessels was similarly, significantly higher in FCA as compared to HCC, both in CD31- (Figure 4G–I) and Collagen IV- (Figure 4J,K) stained vessels. In addition, the number of large vessels was significantly higher in FCAs compared to that observed in HCCs, which was demonstrated by Collagen IV positive vessels (Figure 4L). On average staining intensity, HCC again showed a higher CD31 staining intensity in small, medium and large vessels (Figure 5A–C). In contrast, the intensity of Collagen IV staining (Figure 5D–F) did not show significant differences among vessel subgroups (a summary of the distribution of each vessel per subgroup per lesion is provided in Supplementary Figure S2).

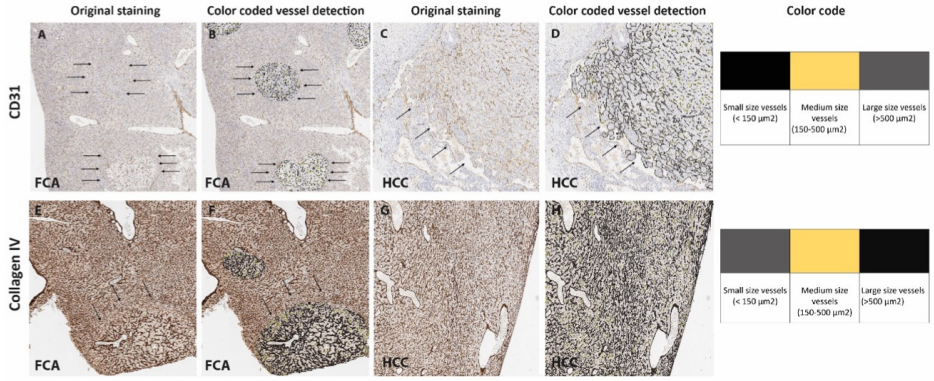

Figure 3. Computer-assisted subgrouping of vessels. CD31-based vessel subgrouping (**A**–**D**) for FCA (**A**) and CD31 (**B**) subgroups and HCC (**C**) and CD31 (**D**) subgroups. Collagen IV-based vessel subgrouping (**E**–**H**) for FI (**E**) and Collagen IV (**F**) subgroups and HCC (**G**) and Collagen IV (**H**) subgroups. Arrows mark the lesion in (**A**–**F**). Magnification 5×. Color coding of subgroups: (**A**,**D**) black-colored areas highlight small-sized vessels (<150 μm^2), yellow-colored areas highlight medium-sized vessels (150–500 μm^2), and grey-colored areas highlight large-sized vessels (>500 μm^2). (**F**,**H**) Grey-colored areas highlight small-sized vessels (<150 μm^2), yellow-colored areas highlight medium-sized vessels (150–500 μm^2), and black-colored areas highlight large-sized vessels (>500 μm^2).

To obtain more detailed information about the intralesional distribution of vessels according to their size, a heatmap evaluation was additionally performed, based on CD31 and Collagen IV-stained and annotated slides (Figure 6A,B). The heatmap analysis of hotspots of CD31-stained vessels showed a strong correlation between vessel distribution and lesion in small- and medium-sized vessels (Figure 6), but not in large-sized vessels. Small- and medium-sized vessels were located more in the central part of the FCAs, compared to HCCs where these sizes of vessels located more in peripherally in the lesion. Regarding the heatmap analysis of Collagen IV-stained vessels, small vessels were predominantly located in the center (intralesional) of FCA, whereas Collagen IV-stained small vessels in the HCC lesions are mostly located peripherally in the lesion.

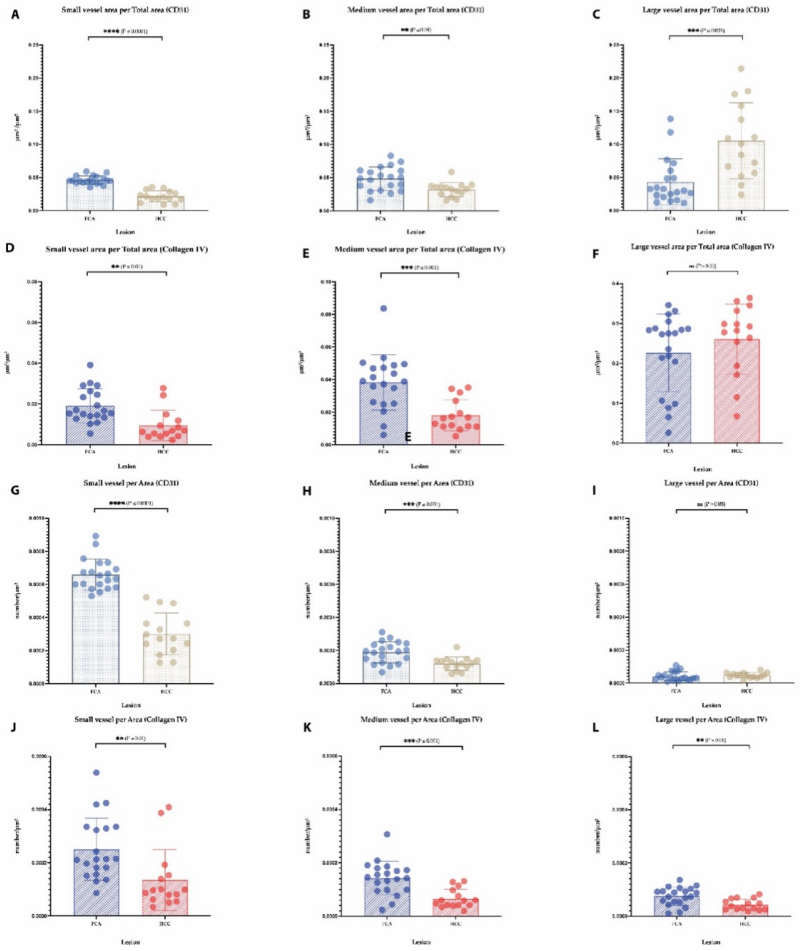

Figure 4. Analysis of vessel area and vessel number per lesion. Evaluation of subgrouped vessels per total area in CD31 (**A–C**) and Collagen IV staining (**D**,**E**,**F**). Subgrouped vessels per area in CD31 (**G–I**) and Collagen IV staining (**J**,**K**,**L**). Error bars show the mean and standard deviation for each lesion. *p*-values: not statistically significant (ns) *p* value > 0.05; for statistical significance, accepted *p* value ≤ 0.05., ** *p* value ≤ 0.01, *** *p* value ≤ 0.001, and **** *p* value ≤ 0.0001.

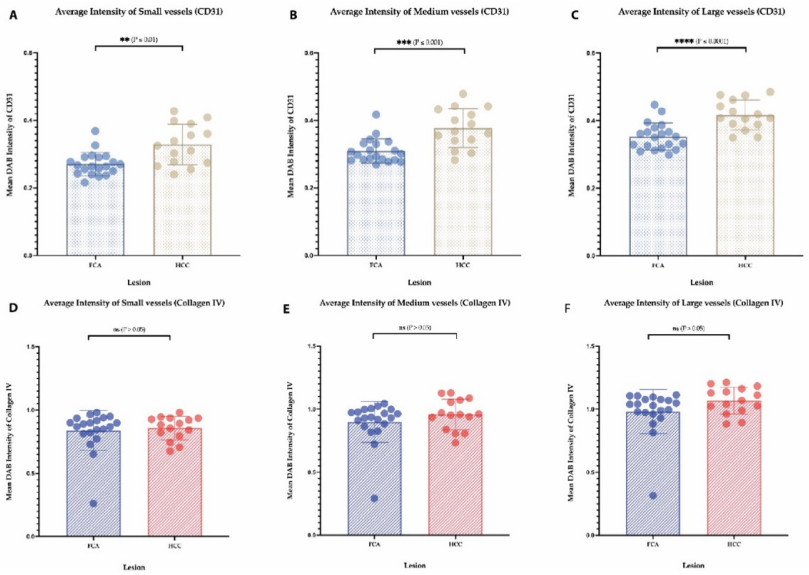

Figure 5. Analysis of staining intensity per lesion of CD31- and Collagen IV-stained vessels (A–F). Error bars indicate the mean and standard deviation for each lesion. *p*-values: Not statistically significant (ns) p value > 0.05; for statistical significance, accepted p value $\leq$ 0.05. ** p value $\leq$ 0.01, *** p value $\leq$ 0.001, and **** p value $\leq$ 0.0001.

In the analysis of αSMA immunostaining, the number of pixels were significantly higher in HCC compared to FCA (Figure 7A,B), reflecting a higher coverage by pericytes. However, staining intensity did not differ between the two groups (Figure 7C). In LYVE1 staining, FCA and HCC vasculature expressed LYVE1 in a diffuse manner (Supplementary Figure S3). In both types of lesions, only weak staining was expressed, predominantly less than in the sinusoids of surrounding healthy liver tissue was found (Supplementary Figure S3A,B). Interestingly, mostly larger FCAs and HCC, but not smaller FCAs, tended to have more LYVE1 expression, pronounced peripherally in the lesions; however, no significant differences were observed (Supplementary Figure S3A,B).

In Desmin staining analysis, neither pixel count nor intensity showed significant differences between FCA and HCC (Supplementary Figure S3C,D). To assess the amount of VEGF-A as a secreted protein, RNAscope was performed. Neither the number of positive spots and/or clusters (either counted separately or commonly) showed significant differences (Supplementary Figure S3E,F). A tabular summary of the main findings including differences in vessel number, vascular size, staining intensity as well as a simplified graphical presentation can be found in Supplementary Figure S4A,B.

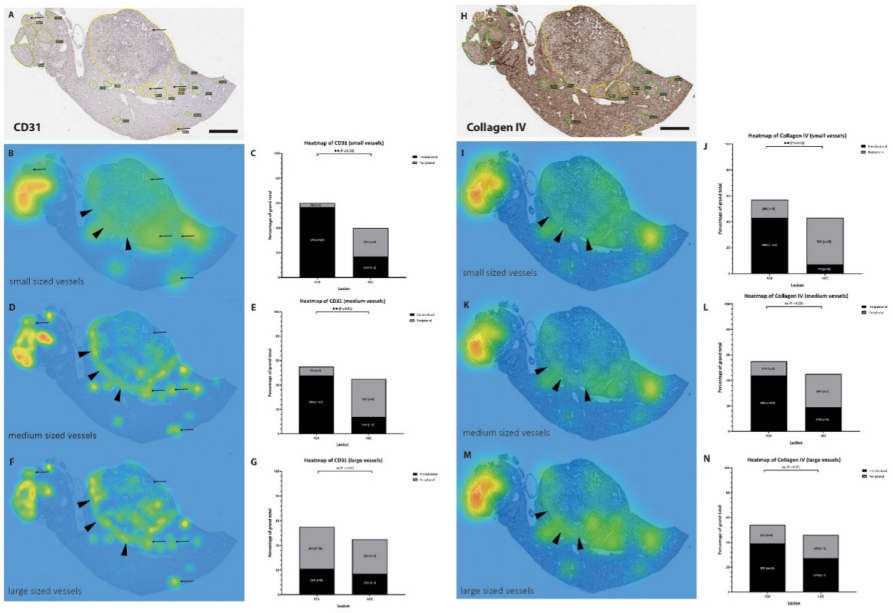

Figure 6. Heatmap of vessel distribution according to size. Annotated FCA (encircled green) and HCC (encircled yellow) in CD31 staining. (**A**) Distribution of the vessel according to their size in small-sized vessels (**B**,**C**), medium-sized vessels (**D**,**E**) and large-sized vessels (**F**,**G**) show a predominant location of small- and medium-sized vessels in the center (intralesional) of FCA, whereas the small- and medium-sized vessels in HCC mostly located at the periphery of HCC (arrowheads). In Collagen IV (**H**) small vessels located in the center (intralesional) of FCA but at the periphery of HCC, with shift towards the periphery in medium- and large-sized vessels (**I**–**N**). Color coding of heatmap: Green color indicates lowest density, yellow color indicates medium density and red color indicates highest density. Scale bar (**A**,**B**): 2 mm (magnification 1×). *p*-values: Not statistically significant (ns) p value > 0.05; for statistical significance, accepted p value $\leq$ 0.05. ** p value $\leq$ 0.01, N = number of hotspots identified in each slide and lesion for further in-depth analysis.

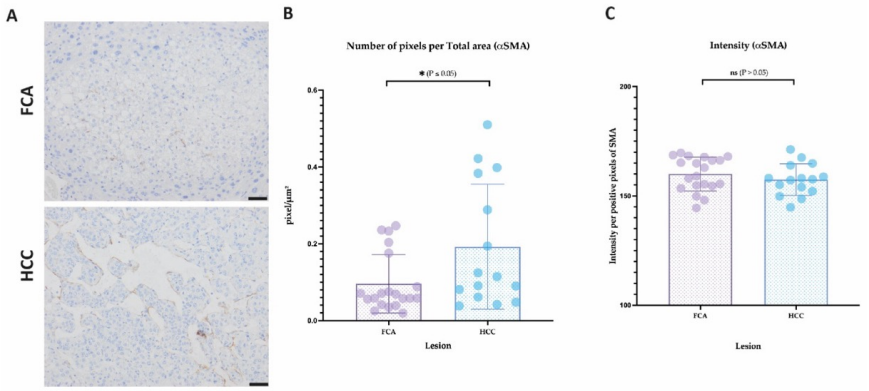

Figure 7. Analysis of vessels per lesion for expression of smooth muscle actin (α-SMA). (**A**) Immunostaining of α-SMA in FCA and HCC, (**B**) number of α-SMA positive pixel/total area and (**C**) intensity of α-SMA/positive pixel. for statistical significance, accepted p value: * p value ≤ 0.05. Scale bar: 50 µm (magnification 20×).

4. Discussion

Hepatocellular carcinoma is among the leading cancer-related causes of death in the world [3]. To date, several mouse models for the study of hepatocarcinogenesis exist; however, available rodent models can be very diverse in terms of tumor development and histological subtypes heavily depending on their strain and biological background [28,42]. Often genetically engineered mice develop cancer without premalignant lesions or early tumors are not detected in the endpoint studies [28,43]. GEMM or chemically induced mouse models are widely used to study specific genes of interest or drug interactions but only few authors specifically address the role of the tumor vasculature [15].

Addressing one of the hallmarks of HCC development and progression, our study was designed to investigate the vasculature in genetic mouse models developing malignant and premalignant lesions to intensively study early vascular events. Our results comprehensively demonstrate very diverse vascular phenotypes in FCA and HCC. FCA presented with a higher number of small- and medium-sized vessels, higher levels of basal membrane components but a lower pericyte coverage. These findings reflect a vascular phenotype of immature small (capillary-like) vessels. Similar to the histological appearance, the vascular profile of FCA therefore closely resembles morphology and immunophenotype of human dysplastic nodules (DN) [34], further supporting the role of FCA as the direct murine counterpart to human DN [30]. In contrast, HCCs were characterized by a lower number of vessels, larger vessel size and a higher degree of pericyte coverage. These substantial changes in vascular architecture and composition define a complex maturation process towards a robust (arterial-like) vasculature capable of supporting proliferating tumor cells with oxygen and nutrients [18]. Similar observations of such an increased arterialized vasculature have been described in rat models of chemically induced hepatocarcinogenesis [31] and some extent also in mouse models for liver cancer [15]. The observed remodeling process from FCA to HCC did not include only vessel formation but also (spontaneous) vessel regression reflected by the decreasing numbers of endothelial cells and simultaneously stable or increasing levels of Collagen IV. The newly developed vessels are presumably functional in early HCC nodules as no tumor cell necrosis or hemorrhage could be detected in the smaller HCC nodules but only in larger [18]. The architectural changes in our mouse HCC mimic in part the "vessels encapsulating tumor clusters (VETC)" pattern commonly described in human HCC of predominantly macrotrabecular subtypes [44]. Furthermore,

not only the size and degree of maturation but also the intralesional distribution of the vessels evolves in the development from FCA to HCC. FCA presented with small- and medium-sized vessels predominantly located in the central areas of the tumor nodules. However, in HCC, a clearly observable shift of small- and medium-sized vessels towards the outer region (periphery) could be observed supporting that vascular remodeling in HCC subsequently progresses to the periphery supporting infiltrative growth and progression of HCC. Similar vascular remodeling has been described in the progression of fully developed HCC to more advanced tumor stages, indicating a continuous vasculature adaption throughout the different stages of tumor development and differentiation [15]. As no significant differences were observed in the cellular levels of VEGF-A between our FCA and HCC, it remains to be speculated whether the involvement of VEGF-A might not yet play a leading role at this early time point or the observed remodeling might not be primarily driven by hypoxia, activation of oxygen sensors and subsequent enhancement of VEGF alone [19].

Our detailed analysis in summary provides clear evidence that the investigated mouse models reflect both morphologically and phenotypically the angiogenic switch in human hepatocarcinogenesis and can be therefore used as a suitable model to study vascular therapeutic approaches [45] or basic research questions in the early phase of tumor development to further unravel molecular pathways [27]. One limitation of this mouse model (precisely any mouse model) includes the general lack of availability of a more detailed classification of proliferative liver lesions compared to the actual WHO classification of human liver tumors [46]. The diagnosis of "HCC" in humans is subdivided in small, early and progressed HCC with precise diagnostic criteria for each category. In murine liver tumors, the INHAND criteria to date only provides the diagnosis of "HCC" without further subclassification [29]. This difference needs to be addressed when discussing different stages of HCC development in terms of sage of mouse models. The mouse models used in our study furthermore do not develop FCA or HCC on a cirrhotic background [28], a condition which should be carefully considered when choosing this model for specific questions on chronic liver diseases [47]. Vascular remodeling is broadly observed in physiological and pathological non-neoplastic liver conditions such as chronic inflammation, regeneration and liver fibrosis [21,23,34,36,48–51]. An emerging role of sinusoidal endothelial cells has recently also been described in the development and progression of non-alcoholic steatohepatitis by altered endocytosis of lipids by the endothelial cells and activation of Kupffer Cells [10,52]. Therefore, it should be taken into account that mouse models developing HCC on a cirrhotic background (such as the MDR2 mouse model [53,54]) should be investigated independently with regard to vascular remodeling and angiogenic switch.

5. Conclusions

Angiogenesis is a vital step in tumor onset and progression in HCC and its precursor lesions. In our research study, we contribute to closure in the gap of knowledge on tumor vasculature in the development of FCA to HCC in rodent hepatocarcinogenesis, by using an in-depth computational analysis of the tumor vasculature. Our results clearly demonstrate that vascular remodeling is present in early stages of liver tumorigenesis making these mouse models with a histological spectrum of FCA and HCC an attractive tool for angiogenesis research purposes.

Supplementary Materials: The following supporting information can be downloaded at: https://www.mdpi.com/article/10.3390/cells11142129/s1, Figure S1: Representative images of the H&E based vascular morphology in small and large Foci of cel-lular alteration (FCA); Figure S2: The distribution of vessels according to size subgroups and investigated parameter; Figure S3: Analysis of vessels per lesion for expression of LYVE, Desmin and VEGF mRNA; Figure S4: Simplified summary of results.

Author Contributions: Conceptual design of this study: M.T., R.S.J.S., K.S., W.W. and C.M. Performance of experiments: M.T., R.S.J.S., K.S., T.L. and C.G. Critical discussion: M.T., R.S.J.S., K.S., J.G., T.L., C.G., W.W. and C.M. All authors have read and agreed to the published version of the manuscript.

Funding: This work was supported by grants from the Deutsche Forschungsgemeinschaft (DFG): C.M project Z02 within CRC1366 "Vascular Control of Organ Function" [project number 39404578], C.G project B03 within CRC1366 [project number 394046768], R.S.J.S. and K.S. project Z02 within CRC1371 [project number 395357507], K.S. and W.W. project Z01 within CRC1335 [project number 360372040].

Acknowledgments: Special thanks for providing statistical guidance go to Katty Castillo and Birgit Waschulzik, Institute of Medical Informatics, Statistics and Epidemiology, Technical University of Munich (TUM). We thank the Comparative Experimental Pathology (School of Medicine, TUM, Munich, Germany) for excellent technical support.

Conflicts of Interest: The authors declare no conflict of interest.

References

1. Ferlay, J.; Colombet, M.; Soerjomataram, I.; Parkin, D.M.; Pineros, M.; Znaor, A.; Bray, F. Cancer statistics for the year 2020: An overview. *Int. J. Cancer* **2021**, *149*, 778–789. [CrossRef] [PubMed]
2. Ferlay, J.; Colombet, M.; Soerjomataram, I.; Mathers, C.; Parkin, D.M.; Pineros, M.; Znaor, A.; Bray, F. Estimating the global cancer incidence and mortality in 2018: GLOBOCAN sources and methods. *Int. J. Cancer* **2019**, *144*, 1941–1953. [CrossRef] [PubMed]
3. Siegel, R.L.; Miller, K.D.; Jemal, A. Cancer statistics, 2020. *CA Cancer J. Clin.* **2020**, *70*, 7–30. [CrossRef]
4. Sung, H.; Ferlay, J.; Siegel, R.L.; Laversanne, M.; Soerjomataram, I.; Jemal, A.; Bray, F. Global Cancer Statistics 2020: GLOBOCAN Estimates of Incidence and Mortality Worldwide for 36 Cancers in 185 Countries. *CA Cancer J. Clin.* **2021**, *71*, 209–249. [CrossRef] [PubMed]
5. Dhamija, E.; Paul, S.B.; Kedia, S. Non-alcoholic fatty liver disease associated with hepatocellular carcinoma: An increasing concern. *Indian J. Med. Res.* **2019**, *149*, 9–17. [CrossRef] [PubMed]
6. Oda, K.; Uto, H.; Mawatari, S.; Ido, A. Clinical features of hepatocellular carcinoma associated with nonalcoholic fatty liver disease: A review of human studies. *Clin. J. Gastroenterol.* **2015**, *8*, 1–9. [CrossRef]
7. Sanyal, A.J.; Yoon, S.K.; Lencioni, R. The etiology of hepatocellular carcinoma and consequences for treatment. *Oncologist* **2010**, *15* (Suppl. S4), 14–22. [CrossRef]
8. Younossi, Z.M.; Henry, L. Epidemiology of non-alcoholic fatty liver disease and hepatocellular carcinoma. *JHEP Rep* **2021**, *3*, 100305. [CrossRef]
9. Samant, H.; Amiri, H.S.; Zibari, G.B. Addressing the worldwide hepatocellular carcinoma: Epidemiology, prevention and management. *J. Gastrointest. Oncol.* **2021**, *12*, S361–S373. [CrossRef]
10. Furuta, K.; Guo, Q.; Hirsova, P.; Ibrahim, S.H. Emerging Roles of Liver Sinusoidal Endothelial Cells in Nonalcoholic Steatohepatitis. *Biology* **2020**, *9*, 395. [CrossRef]
11. LaBrecque, D.R.; Abbas, Z.; Anania, F.; Ferenci, P.; Khan, A.G.; Goh, K.L.; Hamid, S.S.; Isakov, V.; Lizarzabal, M.; Peñaranda, M.M.; et al. World Gastroenterology Organisation global guidelines: Nonalcoholic fatty liver disease and nonalcoholic steatohepatitis. *J. Clin. Gastroenterol.* **2014**, *48*, 467–473. [CrossRef] [PubMed]
12. Brazdziute, E.; Laurinavicius, A. Digital pathology evaluation of complement C4d component deposition in the kidney allograft biopsies is a useful tool to improve reproducibility of the scoring. *Diagn. Pathol.* **2011**, *6* (Suppl. S1), S5. [CrossRef] [PubMed]
13. Wong, S.W.; Ting, Y.W.; Chan, W.K. Epidemiology of non-alcoholic fatty liver disease-related hepatocellular carcinoma and its implications. *JGH Open* **2018**, *2*, 235–241. [CrossRef]
14. Liu, K.; Zhang, X.; Xu, W.; Chen, J.; Yu, J.; Gamble, J.R.; McCaughan, G.W. Targeting the vasculature in hepatocellular carcinoma treatment: Starving versus normalizing blood supply. *Clin. Transl. Gastroenterol.* **2017**, *8*, e98. [CrossRef] [PubMed]
15. Runge, A.; Hu, J.; Wieland, M.; Bergeest, J.P.; Mogler, C.; Neumann, A.; Geraud, C.; Arnold, B.; Rohr, K.; Komljenovic, D.; et al. An inducible hepatocellular carcinoma model for preclinical evaluation of antiangiogenic therapy in adult mice. *Cancer Res* **2014**, *74*, 4157–4169. [CrossRef]
16. Zhang, Q.; Wu, J.; Bai, X.; Liang, T. Evaluation of Intra-Tumoral Vascularization in Hepatocellular Carcinomas. *Front. Med.* **2020**, *7*, 584250. [CrossRef]
17. Sugimachi, K.; Tanaka, S.; Terashi, T.; Taguchi, K.; Rikimaru, T.; Sugimachi, K. The mechanisms of angiogenesis in hepatocellular carcinoma: Angiogenic switch during tumor progression. *Surgery* **2002**, *131*, S135–S141. [CrossRef]
18. Naumov, G.N.; Akslen, L.A.; Folkman, J. Role of angiogenesis in human tumor dormancy: Animal models of the angiogenic switch. *Cell Cycle* **2006**, *5*, 1779–1787. [CrossRef]
19. Ma, M.; Hua, S.; Li, G.; Wang, S.; Cheng, X.; He, S.; Wu, P.; Chen, X. Prolyl hydroxylase domain protein 3 and asparaginyl hydroxylase factor inhibiting HIF-1 levels are predictive of tumoral behavior and prognosis in hepatocellular carcinoma. *Oncotarget* **2017**, *8*, 12983–13002. [CrossRef]

20. Wada, H.; Nagano, H.; Yamamoto, H.; Yang, Y.; Kondo, M.; Ota, H.; Nakamura, M.; Yoshioka, S.; Kato, H.; Damdinsuren, B.; et al. Expression pattern of angiogenic factors and prognosis after hepatic resection in hepatocellular carcinoma: Importance of angiopoietin-2 and hypoxia-induced factor-1 alpha. *Liver Int.* **2006**, *26*, 414–423. [CrossRef]
21. Koch, P.S.; Lee, K.H.; Goerdt, S.; Augustin, H.G. Angiodiversity and organotypic functions of sinusoidal endothelial cells. *Angiogenesis* **2021**, *24*, 289–310. [CrossRef]
22. Rafii, S.; Butler, J.M.; Ding, B.S. Angiocrine functions of organ-specific endothelial cells. *Nature* **2016**, *529*, 316–325. [CrossRef] [PubMed]
23. Haratake, J.; Scheuer, P.J. An immunohistochemical and ultrastructural study of the sinusoids of hepatocellular carcinoma. *Cancer* **1990**, *65*, 1985–1993. [CrossRef]
24. De Minicis, S.; Kisseleva, T.; Francis, H.; Baroni, G.S.; Benedetti, A.; Brenner, D.; Alvaro, D.; Alpini, G.; Marzioni, M. Liver carcinogenesis: Rodent models of hepatocarcinoma and cholangiocarcinoma. *Dig. Liver Dis.* **2013**, *45*, 450–459. [CrossRef] [PubMed]
25. Ekin, U.; Yuzugullu, H.; Ozen, C.; Korhan, P.; Bagirsakci, E.; Yilmaz, F.; Yuzugullu, O.G.; Uzuner, H.; Alotaibi, H.; Kirmizibayrak, P.B.; et al. Evaluation of ATAD2 as a Potential Target in Hepatocellular Carcinoma. *J. Gastrointest. Cancer* **2021**, *52*, 1356–1369. [CrossRef]
26. Masuzaki, R.; Kanda, T.; Sasaki, R.; Matsumoto, N.; Nirei, K.; Ogawa, M.; Karp, S.J.; Moriyama, M.; Kogure, H. Suppressors of Cytokine Signaling and Hepatocellular Carcinoma. *Cancers* **2022**, *14*. [CrossRef]
27. He, L.; Tian, D.A.; Li, P.Y.; He, X.X. Mouse models of liver cancer: Progress and recommendations. *Oncotarget* **2015**, *6*, 23306–23322. [CrossRef]
28. Steiger, K.; Gross, N.; Widholz, S.A.; Rad, R.; Weichert, W.; Mogler, C. Genetically Engineered Mouse Models of Liver Tumorigenesis Reveal a Wide Histological Spectrum of Neoplastic and Non-Neoplastic Liver Lesions. *Cancers* **2020**, *12*. [CrossRef]
29. Thoolen, B.; Maronpot, R.R.; Harada, T.; Nyska, A.; Rousseaux, C.; Nolte, T.; Malarkey, D.E.; Kaufmann, W.; Kuttler, K.; Deschl, U.; et al. Proliferative and nonproliferative lesions of the rat and mouse hepatobiliary system. *Toxicol. Pathol.* **2010**, *38*, 5S–81S. [CrossRef]
30. Thoolen, B.; Ten Kate, F.J.; van Diest, P.J.; Malarkey, D.E.; Elmore, S.A.; Maronpot, R.R. Comparative histomorphological review of rat and human hepatocellular proliferative lesions. *J. Toxicol. Pathol.* **2012**, *25*, 189–199. [CrossRef]
31. Yamamoto, T.; Kaneda, K.; Hirohashi, K.; Kinoshita, H.; Sakurai, M. Sinusoidal capillarization and arterial blood supply continuously proceed with the advance of the stages of hepatocarcinogenesis in the rat. *Jpn. J. Cancer Res.* **1996**, *87*, 442–450. [CrossRef] [PubMed]
32. El-Kharrag, R.; Owen, R.; Boison, D. Adenosine Kinase Deficiency Increases Susceptibility to a Carcinogen. *J. Caffeine Adenosine Res.* **2019**, *9*, 4–11. [CrossRef] [PubMed]
33. Zhou, L.; Wang, Q.L.; Mao, L.H.; Chen, S.Y.; Yang, Z.H.; Liu, X.; Gao, Y.H.; Li, X.Q.; Zhou, Z.H.; He, S. Hepatocyte-Specific Knock-Out of Nfib Aggravates Hepatocellular Tumorigenesis via Enhancing Urea Cycle. *Front. Mol. Biosci.* **2022**, *9*, 875324. [CrossRef]
34. Roncalli, M.; Roz, E.; Coggi, G.; Di Rocco, M.G.; Bossi, P.; Minola, E.; Gambacorta, M.; Borzio, M. The vascular profile of regenerative and dysplastic nodules of the cirrhotic liver: Implications for diagnosis and classification. *Hepatology* **1999**, *30*, 1174–1178. [CrossRef] [PubMed]
35. Kin, M.; Torimura, T.; Ueno, T.; Inuzuka, S.; Tanikawa, K. Sinusoidal capillarization in small hepatocellular carcinoma. *Pathol. Int.* **1994**, *44*, 771–778. [CrossRef]
36. Geraud, C.; Mogler, C.; Runge, A.; Evdokimov, K.; Lu, S.; Schledzewski, K.; Arnold, B.; Hammerling, G.; Koch, P.S.; Breuhahn, K.; et al. Endothelial transdifferentiation in hepatocellular carcinoma: Loss of Stabilin-2 expression in peri-tumourous liver correlates with increased survival. *Liver Int.* **2013**, *33*, 1428–1440. [CrossRef] [PubMed]
37. Ballke, S.; Heid, I.; Mogler, C.; Braren, R.; Schwaiger, M.; Weichert, W.; Steiger, K. Correlation of in vivo imaging to morphomolecular pathology in translational research: Challenge accepted. *EJNMMI Res.* **2021**, *11*, 83. [CrossRef]
38. Steiger, K.; Ballke, S.; Yen, H.Y.; Seelbach, O.; Alkhamas, A.; Boxberg, M.; Schwamborn, K.; Knolle, P.A.; Weichert, W.; Mogler, C. Histopathological research laboratories in translational research: Conception and integration into the infrastructure of pathological institutes. *Pathologe* **2019**, *40*, 172–178. [CrossRef]
39. D'Souza, J.C.; Sultan, L.R.; Hunt, S.J.; Gade, T.P.; Karmacharya, M.B.; Schultz, S.M.; Brice, A.K.; Wood, A.K.W.; Sehgal, C.M. Microbubble-enhanced ultrasound for the antivascular treatment and monitoring of hepatocellular carcinoma. *Nanotheranostics* **2019**, *3*, 331–341. [CrossRef]
40. Böhm, J.; Muenzner, J.K.; Caliskan, A.; Ndreshkjana, B.; Erlenbach-Wünsch, K.; Merkel, S.; Croner, R.; Rau, T.T.; Geppert, C.I.; Hartmann, A.; et al. Loss of enhancer of zeste homologue 2 (EZH2) at tumor invasion front is correlated with higher aggressiveness in colorectal cancer cells. *J. Cancer Res. Clin. Oncol.* **2019**, *145*, 2227–2240. [CrossRef]
41. Bankhead, P.; Loughrey, M.B.; Fernandez, J.A.; Dombrowski, Y.; McArt, D.G.; Dunne, P.D.; McQuaid, S.; Gray, R.T.; Murray, L.J.; Coleman, H.G.; et al. QuPath: Open source software for digital pathology image analysis. *Sci. Rep.* **2017**, *7*, 16878. [CrossRef] [PubMed]
42. Maronpot, R.R. Biological Basis of Differential Susceptibility to Hepatocarcinogenesis among Mouse Strains. *J. Toxicol. Pathol.* **2009**, *22*, 11–33. [CrossRef] [PubMed]

43. Blidisel, A.; Marcovici, I.; Coricovac, D.; Hut, F.; Dehelean, C.A.; Cretu, O.M. Experimental Models of Hepatocellular Carcinoma—A Preclinical Perspective. *Cancers* **2021**, *13*, 3651. [CrossRef] [PubMed]
44. Murakami, K.; Kasajima, A.; Kawagishi, N.; Ohuchi, N.; Sasano, H. Microvessel density in hepatocellular carcinoma: Prognostic significance and review of the previous published work. *Hepatol. Res.* **2015**, *45*, 1185–1194. [CrossRef]
45. Tanaka, S.; Sugimachi, K.; Yamashita, Y.; Shirabe, K.; Shimada, M.; Wands, J.R.; Sugimachi, K. Angiogenic switch as a molecular target of malignant tumors. *J. Gastroenterol.* **2003**, *38* (Suppl. S15), 93–97.
46. Nagtegaal, I.D.; Odze, R.D.; Klimstra, D.; Paradis, V.; Rugge, M.; Schirmacher, P.; Washington, K.M.; Carneiro, F.; Cree, I.A.; WHO Classification of Tumours Editorial Board. The 2019 WHO classification of tumours of the digestive system. *Histopathology* **2020**, *76*, 182–188. [CrossRef]
47. Du, Y.; Zhang, W.; Qiu, H.; Xiao, C.; Shi, J.; Reid, L.M.; He, Z. Mouse Models of Liver Parenchyma Injuries and Regeneration. *Front. Cell. Dev. Biol.* **2022**, *10*, 903740. [CrossRef]
48. Ding, B.S.; Cao, Z.; Lis, R.; Nolan, D.J.; Guo, P.; Simons, M.; Penfold, M.E.; Shido, K.; Rabbany, S.Y.; Rafii, S. Divergent angiocrine signals from vascular niche balance liver regeneration and fibrosis. *Nature* **2014**, *505*, 97–102. [CrossRef]
49. Ding, B.S.; Nolan, D.J.; Butler, J.M.; James, D.; Babazadeh, A.O.; Rosenwaks, Z.; Mittal, V.; Kobayashi, H.; Shido, K.; Lyden, D.; et al. Inductive angiocrine signals from sinusoidal endothelium are required for liver regeneration. *Nature* **2010**, *468*, 310–315. [CrossRef]
50. Hu, J.; Srivastava, K.; Wieland, M.; Runge, A.; Mogler, C.; Besemfelder, E.; Terhardt, D.; Vogel, M.J.; Cao, L.; Korn, C.; et al. Endothelial cell-derived angiopoietin-2 controls liver regeneration as a spatiotemporal rheostat. *Science* **2014**, *343*, 416–419. [CrossRef]
51. Mogler, C.; Wieland, M.; Konig, C.; Hu, J.; Runge, A.; Korn, C.; Besemfelder, E.; Breitkopf-Heinlein, K.; Komljenovic, D.; Dooley, S.; et al. Hepatic stellate cell-expressed endosialin balances fibrogenesis and hepatocyte proliferation during liver damage. *EMBO Mol. Med.* **2015**, *7*, 332–338. [CrossRef] [PubMed]
52. Miyao, M.; Kotani, H.; Ishida, T.; Kawai, C.; Manabe, S.; Abiru, H.; Tamaki, K. Pivotal role of liver sinusoidal endothelial cells in NAFLD/NASH progression. *Lab. Investig.* **2015**, *95*, 1130–1144. [CrossRef] [PubMed]
53. Katzenellenbogen, M.; Mizrahi, L.; Pappo, O.; Klopstock, N.; Olam, D.; Jacob-Hirsch, J.; Amariglio, N.; Rechavi, G.; Domany, E.; Galun, E.; et al. Molecular mechanisms of liver carcinogenesis in the mdr2-knockout mice. *Mol. Cancer. Res.* **2007**, *5*, 1159–1170. [CrossRef] [PubMed]
54. Katzenellenbogen, M.; Pappo, O.; Barash, H.; Klopstock, N.; Mizrahi, L.; Olam, D.; Jacob-Hirsch, J.; Amariglio, N.; Rechavi, G.; Mitchell, L.A.; et al. Multiple adaptive mechanisms to chronic liver disease revealed at early stages of liver carcinogenesis in the Mdr2-knockout mice. *Cancer Res.* **2006**, *66*, 4001–4010. [CrossRef]

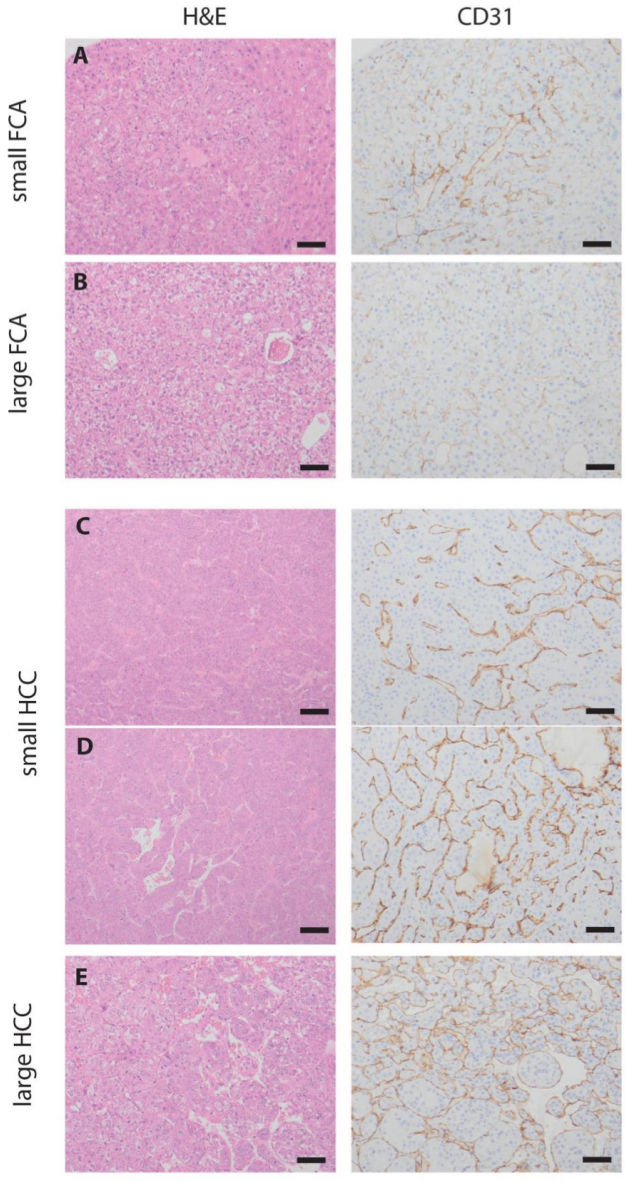
H&E
CD31
A
small FCA
B
large FCA
C
small HCC
D
E
large HCC

Scheme 1. Representative images of the H&E based vascular morphology in small and large Foci of cellular alteration (FCA). While FCA (A,B) present with a weak staining in CD31 showing narrow vessels with slight branching, HCC vasculature presented with stronger staining in CD31 highlighting different vascular pattern: elongated vessels with branching surrounding larger tumor clusters (C), with focal dilatation (D) or large dilated vessels in macrotrabecular HCC areas (E). Scale bar: 50 µm (magnification 20x).

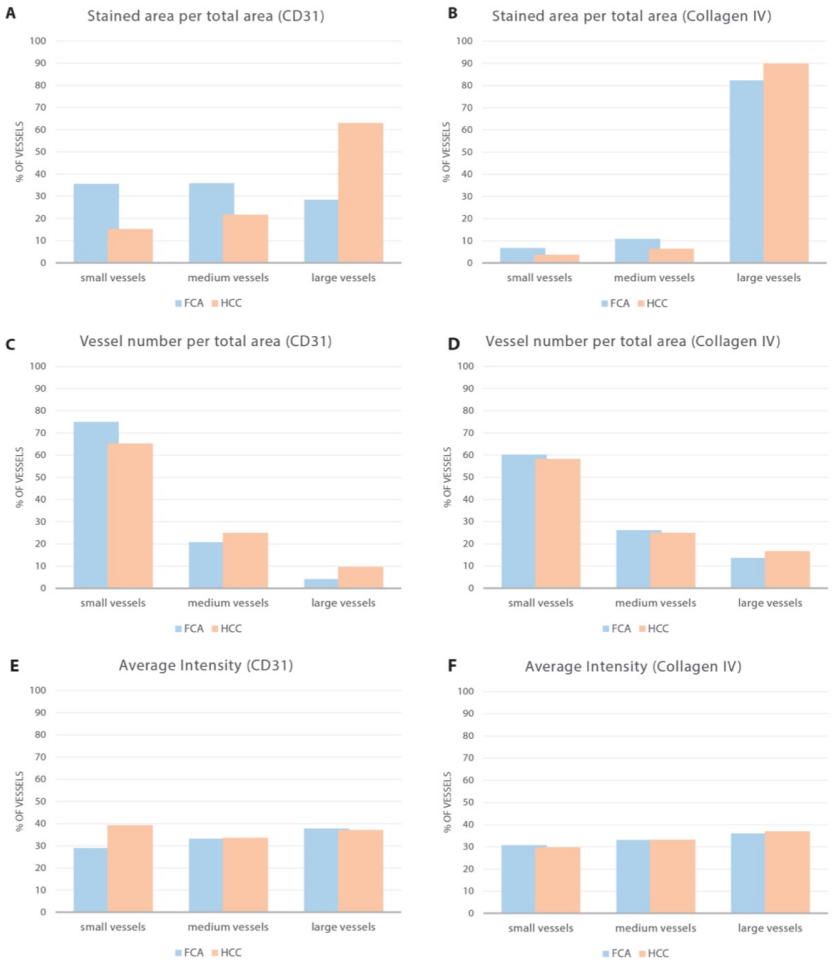

Scheme 2. The distribution of vessels according to size subgroups and investigated parameter: (**A**) & (**B**): stained area per total area (left panel: CD31, right panel Collagen IV). (**C**) & (**D**): vessel number per total area (left panel: CD31, right panel Collagen IV). (**E**) & (**F**): average staining intensity (left panel: CD31, right panel Collagen IV). **A, C, E**: CD31; **B, D, F**: Collagen IV.

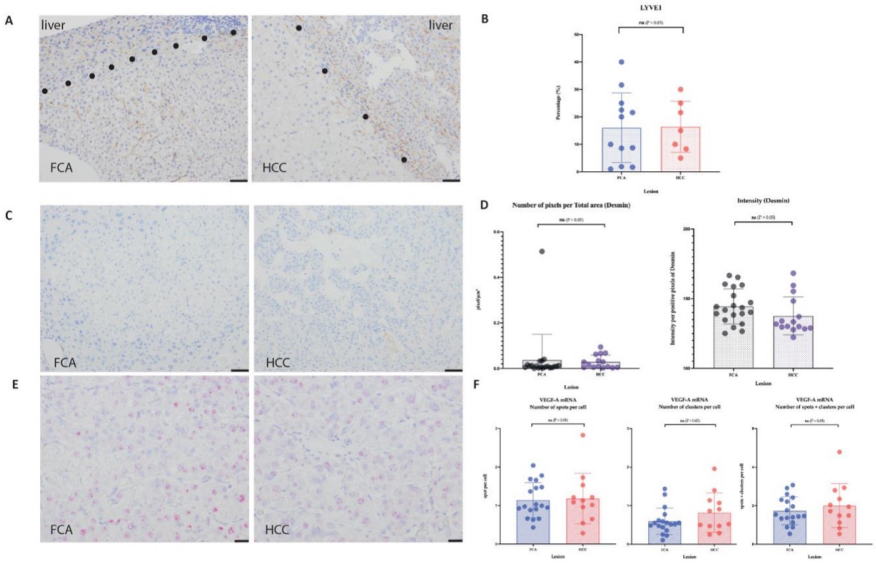

Scheme 3. Analysis of vessels per lesion for expression of LYVE, Desmin and VEGF mRNA. (A) Immunostainings of LYVE in FCA and HCC (A) showing a weak staining equal or less compared to sinusoidal expression of surrounding liver. (B) Semi-quantative analysis of percentage of LYVE positive vessels in FCA and HCC. (**C**) Immunostainings of Desmin in FCA and HCC, (**D**) number of Desmin positive pixel/total area (left panel) and intensity of Desmin/positive pixel (right panel). (**E**) mRNA in situ hybridization of VEGF-A in FCA and HCC, (**F**) Number of VEGF positive spots and clusters per cell (left panel), Number of VEGF positive spots per cell (center), (**J**) Number of VEGF positive clusters per cell (right panel). Error bars indicate mean and standard deviation for each lesion. P-Values: Not statistically significant (ns) P value > 0.05, for statistical significance accepted P value ≤ 0.05. *P value ≤ 0.05, **P value ≤ 0.01, ***P value ≤ 0.001, ****P value ≤ 0.0001. Scale bars: A, C: 50µm (20x magnification), E: 20µm (40x magnification).